

# Refrigeration Systems for Achieving Cryogenic Temperatures

Ronald G. Ross, Jr.

Jet Propulsion Laboratory  
California Institute of Technology  
Pasadena, CA 91109

## 6.1 Introduction — Achieving Cryogenic Temperatures

A sort of workingman's definition of cryogenic temperatures is temperatures below around 123 K, which equals  $-150^{\circ}\text{C}$  or  $-238^{\circ}\text{F}$ . In this temperature range and below, a number of physical phenomena begin to change rapidly from room temperature behaviors, and new phenomena achieve greatly increased importance. Thus, study at cryogenics temperatures typically involves a whole set of new temperature-specific discipline skills, operational constraints, and testing methodologies. One of these special attributes of cryogenics is the science and engineering of achieving cryogenic temperatures, both in the laboratory as well as in a sustained "production" environment. The latter can extend from a hospital Magnetic Resonance Imaging (MRI) machine, to a long-wave instrument on a space telescope, to a night-vision scope on a military battlefield. A number of technologies can provide the cooling required for these and other applications; the choice generally depends on the desired temperature level, the amount of heat to be removed, the required operating life, and a number of operational interface issues such as ease of resupply, sensitivity to noise and vibration, available power, etc.

This chapter provides an overview of the common means of achieving cryogenic temperatures for useful exploitation, including both passive systems involving the use of liquid and frozen cryogenics, as well as active cryorefrigeration systems—commonly referred to as cryocoolers. Separate subsections articulate the basic operating principles and engineering aspects of the leading cryocooler types: Stirling, pulse-tube, Gifford-McMahon, Joule-Thomson and Brayton. Because this field is very extensive, the goal of the chapter is to provide an introductory description of the available technologies and to summarize the key decision factors and engineering considerations in the acquisition and use of cryogenic cooling systems.

After summarizing the details of the refrigeration systems themselves, the remaining 40% of the chapter is devoted to reviewing the critical aspects of cryogenic cooling system design and sizing—including load estimation and margin management—and cryocooler application and integration considerations. Key integration topics include thermal interfaces and heatsinking, structural support and mounting, vibration and Electromagnetic Interference (EMI) suppression, and interface issues with electrical power supplies. The final subsection touches on techniques for measuring the performance of cryogenic refrigeration systems.

## 6.2 Passive Cooling Systems — Liquid and Frozen Cryogenics, and Radiators in Space

For many years, the use of stored cryogen systems has provided a reliable and relatively simple method of cooling over a wide range of temperatures—from below 4 K for liquid helium, to 77 K for liquid nitrogen, up to 150 K for solid ammonia. These systems rely on the boiling or sublimation of the low-temperature fluid or solid cryogenics to provide cooling of the desired load. For solid-cryogenics, the temperature achieved may be modulated to a modest extent by varying the backpressure on the vented gas from atmospheric pressure down to a hard vacuum.

In most cases, stored-cryogen cooling technology is fairly well developed with proven design principals and many years of experience in the trade. The advantages of these systems are temperature stability, freedom from vibration and electromagnet interference, and negligible power requirements. The disadvantages are the systems' limited life or requirement for constant replenishment, the inability to smoothly control the cryogenic load over a broad range of temperatures, and the high weight and volume penalty normally associated with long-life, stand-alone systems.

In systems where the temperature stability and heat transfer associated with cooling with a liquid cryogen is advantageous, one can often extend the useful life of the cryogen or greatly minimize needs for replenishment by adding in a mechanical refrigerator with the cryogen dewar to either recondense the boiled off vapor and return it to the dewar, or to simply intercept a significant fraction of the parasitic thermal load entering the dewar.

The use of stored cryogens such as liquid nitrogen or liquid helium has often been the preferred method for cryogenic cooling of a wide variety of devices—from a laboratory apparatus to an MRI machine in a hospital setting. Cryogenic liquids can be used for cooling in a number of different states, including normal two-phase liquid-vapor (subcritical), low-pressure liquid-vapor (densified), and high-pressure, low-temperature single-phase (supercritical) states. Subcritical fluids such as low-pressure helium have long been the cooling means of choice for very-low-temperature (1.8 K) sensors for space astronomy missions.

Solid cryogens are mostly used below their triple point where sublimation occurs directly to the vapor state. They provide several advantages over liquid cryogens including elimination of phase-separation issues, providing higher density and heat capacity, and yielding more stable temperature control, which is desirable for many applications.

### 6.2.1 Available Temperatures from Various Cryogens

The detailed thermodynamic properties of common cryogens are available in the literature for those designing cryogenic systems. However, it is useful to provide a brief overview of the practical operating temperature ranges and properties of common cryogens, along with an introduction to the thermodynamic operating regimes for their solid, liquid, vapor, and gas states.

Figure 1 describes the operating temperatures attainable with ten common cryogens that can be used to directly cool cryogenic loads or other components. Each cryogen is represented by a bar that extends from its minimum operating temperature as a solid—based on sublimation at a vapor pres-

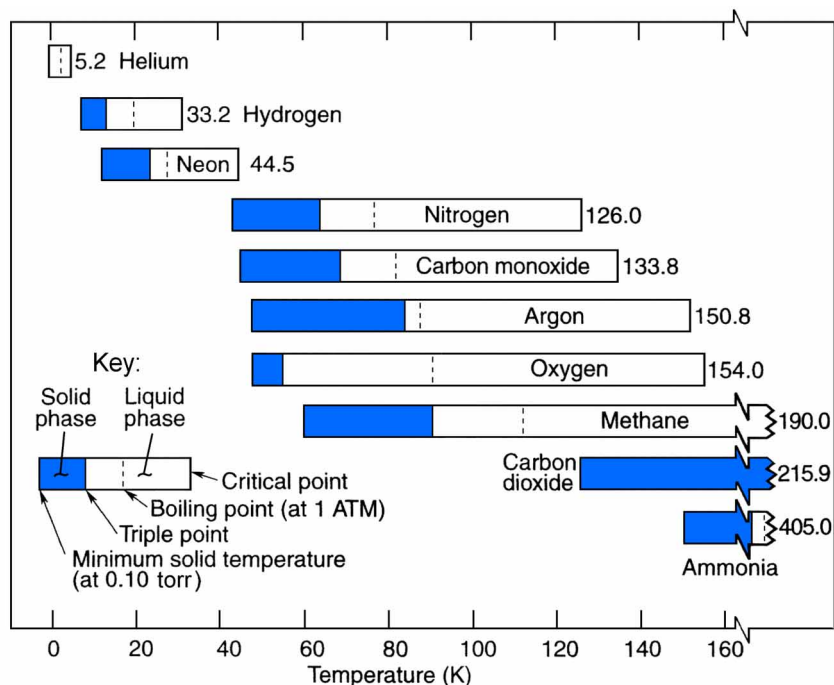


**Figure 1.** Operating temperature ranges for common expendable coolants.

sure of 0.10 torr—to its maximum operating temperature—its critical point, which is the maximum temperature at which a cryogen can exist as a two-phase liquid vapor. Within each bar, the region of solid phase is denoted by the shaded area defined at its maximum temperature by the cryogen's triple point, which is the maximum temperature at which a cryogen can exist as a solid. Above this, the cryogen's boiling point at a pressure of one atmosphere is noted by the dashed line. The use of 0.10 torr to define the lowest achievable temperature is for convenience, as the temperature can be lowered if the ability to pull a stronger vacuum is available.

### 6.2.2 Thermodynamic Principles of Cryogen Coolers

A modest familiarity with thermodynamics fundamentals is useful for understanding the limitations and constraints of stored-cryogen system operating states. Figure 2 expands on the key fluid parameters noted in Fig. 1 via an idealized temperature-entropy (T-S) diagram for a pure cryogenic fluid. Since entropy is defined as the heat transferred divided by the temperature at which the change occurs, the T-S chart is not only useful to visualize the boundaries between fluid states, but to also quantify the amount of heat transferred when a fluid undergoes a change of state.

Starting with the point *C*, the apex of the dome is called the critical point, and the conditions at that point are called the critical pressure, critical temperature, etc. When the fluid is at or above the critical temperature, it can never exist in the liquid state, but will remain as a single-phase, homogeneous gas. Fluids stored under these conditions are sometimes called cryo-gases.

The line described by curve *ABD* in Fig. 2 represents the path of a gas being cooled at constant atmospheric pressure. The horizontal line drawn at *C* represents the dividing line between a vapor and a gas. While they are technically in the same state, the points along the line *DE* represent a liquid and vapor mixture at constant temperature and pressure — point *D* being 100% saturated vapor while point *E* being 100% saturated liquid. As an example, for water, this *DE* line would be at 100°C, the boiling point of water at a pressure of one atmosphere. The change in energy from point *E* to *D* is the heat of vaporization. When a liquid is heated along this line, point *E* is also called the bubble point, because it is where the first vapor bubbles appear.

Further cooling of the liquid from *E* to *F* reduces the vapor pressure, and eventually the liquid freezes into a solid. Point *F* is defined as the triple point (or melting point), where the fluid exists as solid, vapor, and liquid. For water, this would be the temperature of an ice/water mixture, i.e. 0°C.

For a cryogen that is below the triple point temperature, such as point *G*, any addition of heat will cause the solid to sublime, as opposed to melting to a liquid. For the conditions of point *G*, the heat of sublimation is given by the change in energy from *G* to *H*.

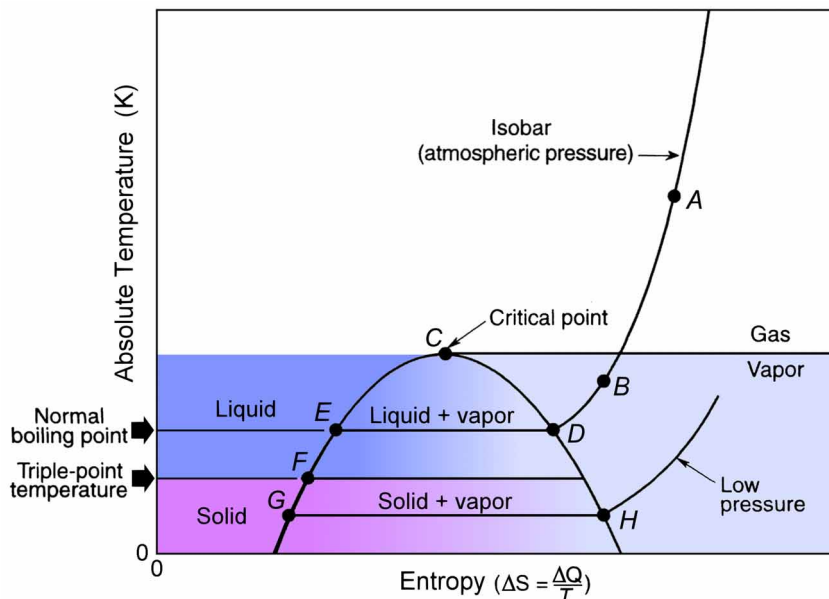


**Figure 2.** Idealized temperature-entropy diagram for a cryogenic fluid.

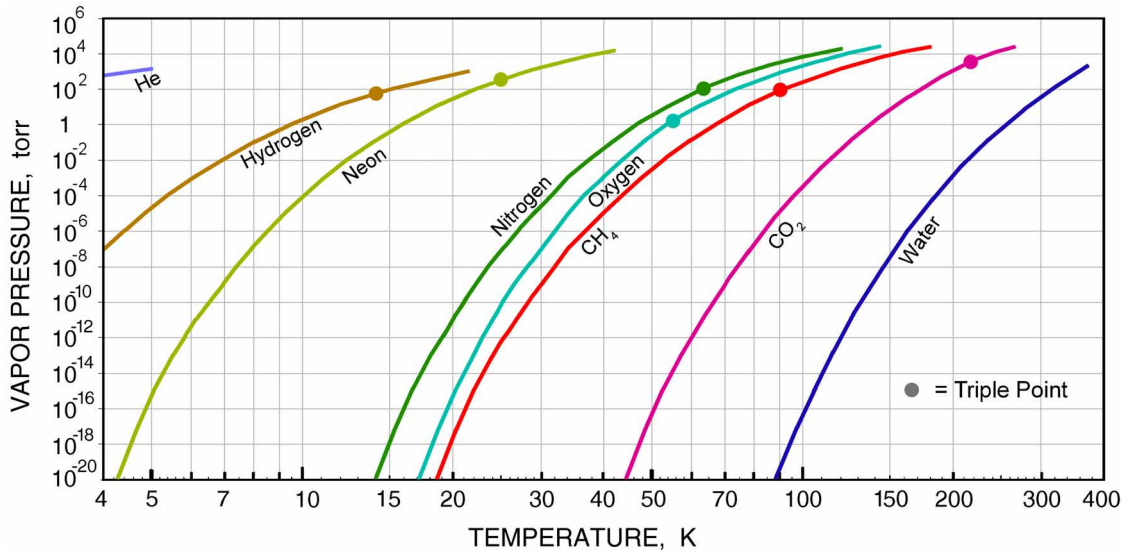


**Figure 3.** Boiling-point temperature of common gases as a function of external pressure.

Figure 3 expands on Fig. 2 by describing the dependence of boiling-point or sublimation temperature on external pressure for common cryogenics. Also noted is the triple point where the cryogen transitions to a solid. This plot also indicates the temperature and pressure where external contaminant gases, such as water vapor, will begin to condense on cryogenic surfaces such as low-emittance shields and MLI. Preventing such condensation is a critical issue for managing radiant parasitic loads on low-emittance shields and cryogenic surfaces. This topic of emittance degradation from contaminant films is covered later in this chapter in Section 6.4.3.5.

### 6.2.3 Cooling with Liquid Cryogenics

Over the years, many liquid cryogenic systems have been developed, fabricated, and operated in both ground environments and in space. They cover a wide range of cryogen fluids and construction features in terms of stored volume, pressure and temperature limitations, and relative efficiency in terms of the parasitic heat leaks. Many of these systems utilize liquid helium for achieving temperatures between 1.4 K and 4 K or liquid nitrogen for achieving temperatures around 77 K. To achieve temperatures below 4.2 K requires that liquid helium be stored under partial vacuum conditions. At pressures from 10 to 40 torr, temperatures in the range of 1.4 K to 1.8 K are achievable with liquid helium.

#### 6.2.3.1 Engineering Aspects of Liquid Cryogen Systems

**Typical Dewar Construction Features.** As illustrated in Fig. 4, liquid cryogen systems typically involve a nested storage tank concept whereby the inner tank, which holds the liquid cryogen, is suspended inside an outer vacuum shell with low-conductivity structural supports. These structural supports are typically made of low-conductivity tubes, struts or tension bands in order to achieve high structural efficiency and minimum conductivity between the two tanks. The gap between the two tanks is then evacuated and filled with Multilayer Insulation (MLI). In addition, a high efficiency dewar may also contain one or more strategically placed vapor-cooled shields (VCS) that are cooled by the evaporating cryogen as it vents from the inner tank.

The goal of the gap construction is to prevent gaseous conduction and radiation between the outer and inner tank and to achieve maximum thermal benefit from the evaporating cryogen. Although the heat of vaporization of the cryogen is the primary cooling force in the system, there is also considerable benefit associated with extracting the available heat from the vapor as it rises up in temperature from the cryogen temperature to the external vent temperature. This is accomplished by piping the venting gas through the vapor cooled shields, which serve to intercept much of the radiant energy coming through the MLI layers from the outer tank. The VCS can also be attached to the support struts or plumbing to further reduce conductive heat leaks.

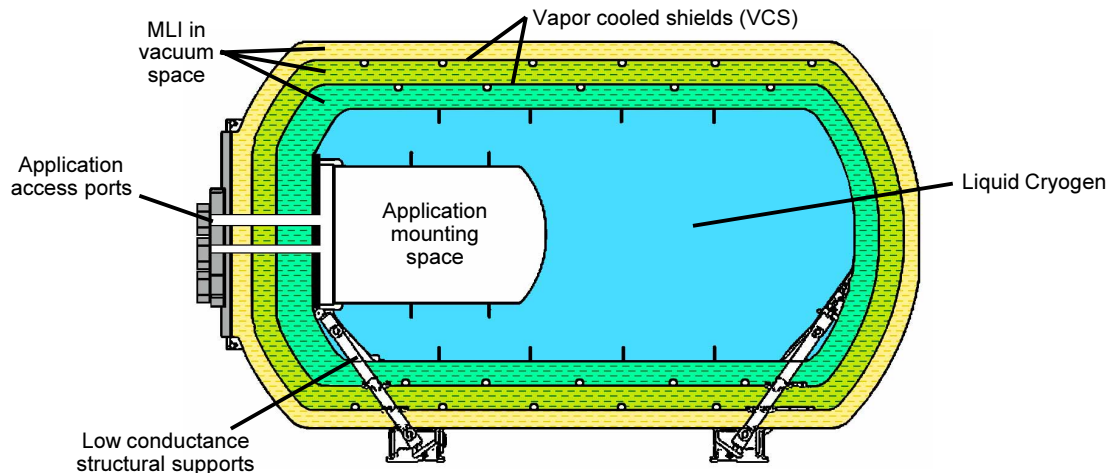


**Figure 4.** Example liquid cryogen dewar construction features.

An extensive summary of the construction features for representative stored cryogen tanks fabricated for space applications—and in some cases airborne use—has been assembled by Donabedian and is available in the *Spacecraft Thermal Control Handbook, Vol II: Cryogenics* [Donabedian, 2003b] and in Chapter 15 of the earlier *Infrared Handbook* [Donabedian, 1993]. Those reviews include tanks built for a variety of uses, fluids, and pressures, and contains designs for both subcritical and supercritical cryogen storage. As part of that work, a general performance, figure-of-merit database was also developed to serve as a convenient means of comparing and evaluating the performance of the various stored cryogen systems. The figure of merit is defined as the net heat leakage of the fluid ( $Q$ ) divided by the surface area of the pressure vessel ( $A$ ) in units of  $W/m^2$ . This  $Q/A$  parameter varies from as high as 0.1 to as low as  $0.003 W/m^2$  depending on the temperature and properties of the fluid stored, the tank design, and the external temperature.

**Multilayer Insulation (MLI).** High quality multilayer insulation (MLI) has been found to play a particularly critical role in achieving high-efficiency stored cryogen systems, and as a result, has been a focus for much research over the years within the cryogenic community. Lockheed-Martin Palo Alto, in particular, spent years testing and optimizing MLI for space cryogen dewars and has assembled a substantial data base on performance attributes, lessons learned and preferred practices (see for example [Johnson 1974], [Nast, 1993]).

Because MLI is also a key element of solid cryogen systems and cryocooler-cooled systems, a separate subsection of this chapter (section 6.4.3) has been devoted to a detailed summary of cryogenic MLI performance attributes and measured data. Its particular focus is on the use of MLI at cryogenic temperatures, which places greatly increased emphasis on the conduction properties of MLI.

**Porous Plugs.** For liquid helium systems, when the temperature is dropped below about 2 K, a point referred to as the lambda point, liquid helium undergoes a phase transition and becomes a "super fluid" with very special properties. These properties include: infinite thermal conductivity, zero viscosity and zero entropy. The substance, which looks like a normal liquid, will flow without friction along any surface and circulate over obstructions and through pores in containers which attempt to hold it. The porous plug was invented to contain super fluid helium in a cryogen dewar while allowing for evaporative cooling. Its micron-level pore sizes are required to separate the liquid and vapor phases to ensure that liquid does not escape before its heat of vaporization can be utilized. Selzer, et al. provide a summary of the physics behind the porous plug's operation as part of their paper on its original development at Stanford University in 1970 [Selzer, et al., 1970].

**Zero Boil-off (ZBO) Systems.** In the last 10 years or so, the concept of zero boil-off (ZBO) systems utilizing mechanical refrigerators combined with high-efficiency cryogenic tanks has been pursued to provide long-term storage of cryogenic fluids while minimizing storage volume and refrigerator power. These ZBO systems are being used for many ground-based systems and are being examined to provide liquid oxygen, methane, or hydrogen for future space planetary-mission

### 6.2.3.2 Liquid Cryogen Cooler Development History and Availability

As noted earlier, liquid cryogenic systems have been developed, fabricated, and operated for many years, in both ground environments and in space [Ross, 2007]. They cover a wide range of cryogen fluids and construction features in terms of temperatures, stored volume, and thermal isolation systems. Many present-day systems are used for cooling superconductor electronics and magnetics in applications such as Magnetic Resonance Imaging (MRI) systems and for cooling spacecraft instruments utilizing liquid helium to achieve temperatures below 2 K. Although not really a "cooling" application, much of the same technology is also used in liquid cryogen "storage" systems for liquid helium, hydrogen, oxygen, and nitrogen.

A number of manufacturers provide generic liquid cryogen dewars for laboratory and commercial applications. In space most dewars have been custom built for particular missions by contractors such as Lockheed Martin in Palo Alto, CA and Ball Aerospace and Technology Corp. (BATC) in Boulder, CO.

The tanks developed for NASA's Gemini and Apollo programs for storage of supercritical oxygen and hydrogen for their 7- to 14-day missions were the earliest space-qualified tanks for operation in near-zero-gravity environments. More advanced and larger tanks were developed by the Beech Aircraft Corp. Boulder Division (now BATC) for longer life. They were designed for general-purpose storage of LO<sub>2</sub>, LH<sub>2</sub>, LN<sub>2</sub>, and LHe for extended periods.

Nearly all actual liquid cryogen cooling applications in space have involved the use of super fluid helium to achieve temperatures below 2 K for cooling long-wavelength infrared sensors in space telescopes. The first of these was the IRAS dewar in 1983, followed by COBE in 1989, Spitzer in 2003, GPB in 2004, and XRS in 2005. For most other temperatures, space cryogen-cooled missions used solid cryogenes, which are discussed next. A summary of the history of cryogen systems used in space is provided by Ross [Ross, 2007].

### 6.2.4 Cooling with Solid Cryogenes

A second efficient way to use stored cryogenes is in the frozen state. As indicated in Fig. 5, the normal operating regime of a solid cryogen cooler is below its triple-point temperature. In this region, the addition of heat causes conversion of the solid directly into vapor through the process of sublimation, bypassing the liquid state. Operating below the triple point also eliminates the problems of fluid management and phase separation associated with fluid systems. From an efficiency

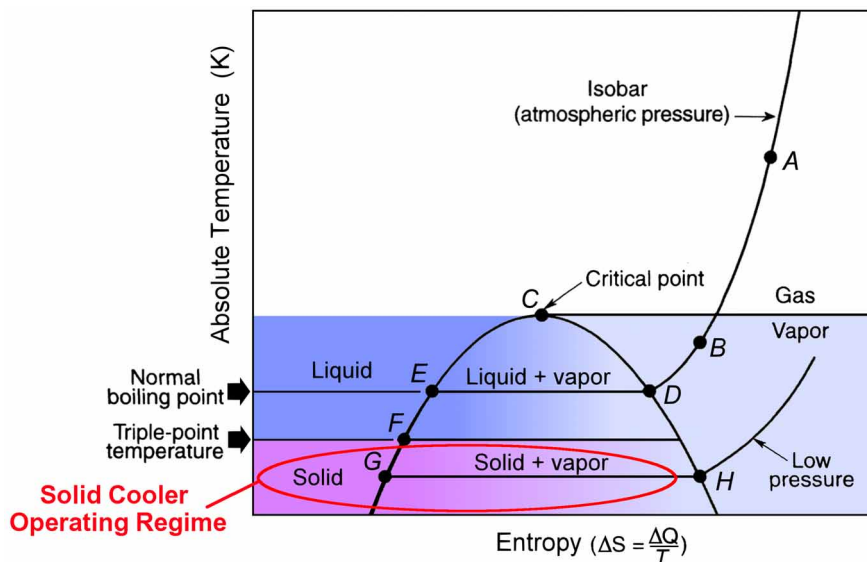


Figure 5. Solid cryogen operating regime; heat of sublimation =  $T \times (S_H - S_G)$ .

**Table 1.** Thermal Properties of Selected Solid Cryogenes

Cryogen	Heat of Sublimation (J/g)	Density of Solid at Melting Point (kg/m <sup>3</sup> )	Temperature Range (K)	
			0.1 Torr	Triple Point
Ammonia (NH <sub>3</sub> )	1719	822	150	195
Carbon dioxide (CO <sub>2</sub> )	574	1562	125	216
Methane (CH <sub>4</sub> )	569	498	60	90
Oxygen (O <sub>2</sub> )	227	1302	48	55
Argon (A)	186	1714	48	84
Carbon monoxide (CO)	293	929	46	68
Nitrogen (N <sub>2</sub> )	225	1022	43	63
Neon(Ne)	106	1439	14	25
Hydrogen (H <sub>2</sub> )	508	80.4	8	14

point-of-view, working with the solid phase provides greater density (and thus lower storage volume) and higher heat content per unit mass of cryogen. Other advantages of a solid cooler are relative simplicity, absence of moving parts, absence of noise and vibration, excellent temperature stability, and no power requirements.

The primary limitations or disadvantages include a limited number of suitable cryogenes, very large mass and volume required for large heat loads or long design lives, the need for very significant ground servicing facilities and manpower support, and safety implications associated with venting toxic or flammable vapors or having a vent become clogged—causing an explosion.

For space applications, the overboard vent of a solid cooler must also be designed to maintain the necessary pressure level on the cryogen and to not create unacceptable torques on the spacecraft. If the vent rate is significant, the gas may have to be vented along an axis passing directly through the center of gravity of the satellite and/or thrust compensation devices must be used to prevent attitude disturbances. Sustaining the desired operating temperature also requires that the back pressure on the sublimating cryogen be maintained at the fixed value associated with the design temperature.

This important interrelationship between the temperature and pressure of a frozen cryogen is presented in the vapor pressure-temperature plot presented earlier as Fig. 3. As noted, the sublimation temperature is strongly dependent on the vapor pressure maintained above the solid. Thus, given a fixed back pressure, a solid cryogen can be designed to maintain a very stable temperature.

#### **6.2.4.1 Thermodynamics of Solid Cryogenes**

Table 1 tabulates the key thermophysical properties of a number of cryogenes traditionally used in solid coolers, including their operating temperature range. The cryogenes are listed in descending order of minimum practical operating temperature (the table's fourth column) based on a reasonably achievable back pressure of 0.1 torr.

As was shown in Fig. 3 the minimum operating temperature depends on the minimum back pressure that can be sustained during cooler operation. If the heat load is small enough and the applied vacuum is high enough, then lower pressures, and thus lower temperatures, can be attained. The maximum temperature (the fifth column) is the highest temperature at which the solid phase can exist, which is its triple-point temperature. By proper design of the back pressure imposed by the vent gas system, any temperature between these two extremes can be achieved. The operating temperature range of a solid cooler is thus much wider than the range for a stored liquid cryogen cooler.

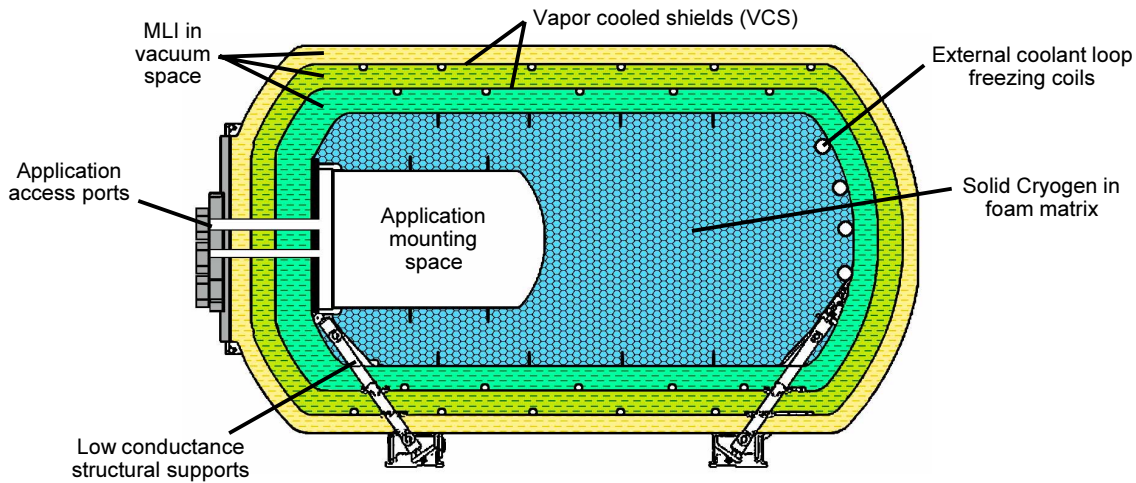


**Figure 6.** Example solid cryogen dewar construction features.

#### 6.2.4.2 Engineering Aspects of Solid Cryogen Coolers

**Solid Cryogen Dewar Construction Features.** As illustrated in Fig. 6, solid cryogen dewar systems are fundamentally similar to liquid cryogen dewars in their structural support and thermal insulation systems. Both include a nested storage tank concept whereby the inner tank, which holds the solid cryogen, is suspended inside an outer vacuum shell with low-conductivity structural supports. As with liquid cryogen dewars, these structural supports are typically made using low-conductivity tubes, struts or tension bands in order to achieve high structural efficiency and minimum conductivity between the two tanks. The gap between the two tanks is evacuated and filled with Multilayer Insulation (MLI), and for high efficiency dewars, one or more vapor-cooled shields (VCS) may be strategically placed inside the gap.

As with liquid cryogen dewars, the goal of the gap construction is to prevent gaseous conduction and radiation between the outer and inner tank and to achieve maximum thermal benefit from the evaporating cryogen. Although the heat of sublimation of the solid cryogen is the primary cooling force in the system, there is also considerable benefit associated with extracting the available heat from the vapor as it rises up in temperature from the cryogen temperature to the external vent temperature. This is accomplished by piping the venting gas through the vapor cooled shields, which can serve to intercept much of the radiant and conducted heat coming through the MLI layers from the outer tank. The VCS can also be attached to the support struts or plumbing to further reduce conductive heat leaks.

Two key differences between liquid and solid-cryogen dewars are the need for a thermally conductive matrix and freezing coils in a solid cryogen dewar. Because the solid cryogen evaporates selectively near the interface with the cryogenic load, it tends to withdraw away from this critical thermal interface as it is depleted and requires a means to keep it thermally connected to the load. This is accomplished by filling the cryogen tank with a high-conductivity open-cell metallic matrix or foam to provide a known thermal bridge to the load interface during all stages of evaporation of the solid cryogen.

The second addition to a solid cryogen dewar is a means to freeze the cryogen in place within the foam-filled dewar. This is accomplished by providing a cooling coil within the dewar that can be connected to an external coolant source sufficiently cold to freeze the cryogen. A second use of the cooling coil can be to keep the cryogen frozen during system integration and test periods.

This process of freezing the cryogen, or precooling it to temperatures well below its freezing point, requires great care and experience to avoid damaging the dewar. Like water ice—the frozen state of the cryogen often has a different density, and thus occupies a different volume than the liquid state. In the solid state, it is also likely to have a different coefficient of thermal expansion (CTE) than the metallic dewar. If not fully accommodated in the dewar design and filling procedure, these expansions or contractions of the cryogen can lead to rupturing portions of the dewar.

A compounding issue with solid cryogenics is their ability to relocate themselves within a dewar by evaporative transport from warmer regions to cooler regions; this involves the physics of cryopumping and can lead to a solid cryogen filling in the space critically needed for expansion during a subsequent warm-up operation. A very traumatic failure of the NICMOS solid nitrogen dewar occurred due to this cause during preparation for use on the Hubble Space Telescope [Miller, 1998a; Miller, 1998b].

#### **6.2.4.3 Solid Cryogen Cooler Development History and Availability**

The first operational long-life solid cooler used in space was a single-stage carbon dioxide system developed by Lockheed Martin and launched aboard an Air Force satellite (STP-72-1) on October 20, 1972 [Nast and Murray, 1976]. Since that time nearly a dozen cooler designs, both single- and two-stage, have been used to cool sensors to temperatures over a range of 10 to 65 K, with operational lifetimes from 10 months to 2.5 years.

Two-stage designs have been used several times to optimize the overall cooler performance and minimize cooler mass by using a high-temperature cryogen such as carbon dioxide or ammonia (both of which have higher operating temperatures and high heat content) to provide a shield for cryogenics that have lower operating temperatures, such as hydrogen, neon, and methane. In some cases, methane has been used as the shield cryogen for low-heat-content cryogenics like neon.

With the rapid development of long-life mechanical refrigerators and the relatively high cost of designing and servicing solid coolers, mechanical cryocoolers have increasingly become the cooler of choice for space missions that historically would have used solid cryogen coolers. An overview of the history of cryogenic coolers in space is provided by Ross [Ross, 2007].

#### **6.2.5 Radiation to Deep Space**

For spaceborne applications, cryogenic temperatures as low as 40 to 60 K can also be achieved using very carefully designed radiant cooler systems radiating into deep space. Although the effective radiation temperature in space is approximately 3 K, achieving these 40 to 60 K temperatures is generally limited to sophisticated cryoradiators on spacecraft well separated from the much warmer environment of Earth orbit. In Earth orbit, practical cryoradiator temperatures are closer to 80 K and above.

When striving for cryogenic temperatures above these levels, radiant cooling to deep space can provide an effective and cost effective means of cooling, although even then, elaborate shields from the sun and Earth, and from the warm environment of the supporting spacecraft are required.

The advantage of cryoradiators is relatively stable long-term performance without the need for power, or concerns about mechanical wearout, electronics failures, or depletion of a stored cryogen supply. Countering this attractiveness is the relatively challenging design associated with achieving sufficiently low parasitic thermal loads and maintaining sufficient structural robustness to survive the launch loading environment. To achieve useful performance, constraints are also typically required on the spacecraft's geometric configuration and orbital attitudes.

As with nearly all cryogenic applications there is a strong competition between structural robustness and thermal isolation (minimum thermal conductivity). This invariably leads to highly optimized structural/thermal designs often involving mechanical mechanisms for latching or unlatching supplementary structural supports used only to survive launch. Added to this is the difficulty of isolating from direct solar and Earth reflected solar (albedo) radiation, which typically requires Earth and sun shades; these too can often end up with mechanically deployed mechanisms. Lastly, isolating the radiator and cold plumbing from the warm spacecraft requires careful application of low-emittance surfaces and cryo multilayer-insulation (cryo MLI). At cryogenic temperatures, such surfaces and MLI can perform much more poorly than they do in room-temperature applications, so these contribute to additional engineering challenges in the design process.

The bottom line is that a significant number of cryo radiators have been successfully used in space since the early 1970s [Nast and Murray, 1976], but a modest fraction of these have had significant schedule and cost growths associated with meeting the design challenges; and, each

design tends to be a new custom design for each new spacecraft and mission. For higher temperatures, like the 150 K to 170 K temperatures needed for space optics, design criticality is much less severe, and cold radiators in this temperature range—just above cryogenic temperatures—have provided very effective long-term cooling of space instruments. See, for example, the 12-year space radiator performance on the Atmospheric Infrared Sounder (AIRS) instrument [Ross, 2014].

Crawford [Crawford, 2003] and Donabedian [Donabedian, 2003c] provide excellent reviews of the more detailed design principals developed for space cryo radiators over the past 40 years. Donabedian also presents comparative performance data for nearly two dozen flight designs. Their chapters in the *Spacecraft Thermal Control Handbook, Vol II: Cryogenics* are an excellent starting point for those wishing to more carefully examine the design options for space cryo radiators.

### 6.3 Active Refrigeration Systems—Stirling, Pulse Tube, GM, JT and Brayton

For cryogenic applications where stored cryogenics like liquid nitrogen and liquid helium are not readily available or are inconvenient to use, mechanical refrigerators, or cryocoolers, are often the preferred design solution. The primary considerations that differentiate mechanical refrigerators from stored cryogen cooling systems are the issues of cryogen storage, resupply and safety for cryogen systems and the requirement for electrical power and a means of heat rejection for cryocoolers. Because cryocoolers, or cryorefrigerators, are typically driven by electrical powered compressors, means must be available to provide both the electrical power and the means to reject the resulting heat dissipation. The power dissipation issue is particularly important because the resulting heat reject temperature strongly effects the thermodynamic efficiency of the cryocooler. A second aspect of the electrically driven compressor is the strong likelihood of measurable levels of equipment vibration, EMI, and audible noise that may interact negatively with the intended cryogenic application. Achieving low levels of vibration and noise has been an important focus in the cryocooler development industry, and is an important distinguishing attribute of certain cryocooler types and constructions. Another key advantage of a cryocooler is the ability of a single unit to provide cooling over a broad range of temperatures, many with closed-loop temperature control.

Some of the most important applications for cryocoolers include achieving high vacuum levels with cryopumps in semiconductor processing facilities, cooling infrared detectors and superconducting devices in a broad range of military, space, and laboratory instruments, and reliquefying cryogenics to provide a zero-boil-off recapture of the cryogen in systems using liquid helium or nitrogen. Key decision factors include the cooling system operational cost, complexity and reliability/maintainability.

To meet these broad needs, a wide range of cryocoolers has been developed, and these coolers use a number of different thermodynamic cycles. In general, the size (cooling capacity) and available cooling temperature range of mechanical cryocoolers span many orders of magnitude—from room temperature down to 1 K and below, and from microwatts to kilowatts of cooling power. The most common mechanical refrigeration cycles include Stirling, Pulse Tube, Gifford McMahon (GM), Joule-Thomson (JT), and reverse-Brayton cycles. The attributes of each of these types of coolers are discussed in the subsections that follow, including a brief description of their thermodynamic cycle, their operational features, representative performance, and general commercial availability.

In addition to these five cooler types, there are a number of lesser known cycles such as adiabatic demagnetization and the dilution cycle that are used primarily for achieving ultra-low temperatures below 1 K. The reader is referred to the literature on subKelvin coolers for further information on these specialty cooler types.

To achieve the lowest temperatures, typically 30 K and below, cryocoolers generally employ two or more linked stages, where an upper stage (higher temperature) cooler is used to provide a low-temperature heat rejection path for a lower-temperature stage. Although many multiple stage coolers employ the same thermodynamic cycle for each of the linked stages, there is sometimes an advantage to linking different types of coolers using different thermodynamic cycles. These are generally referred to as hybrid coolers and include combinations such as Stirling, Pulse Tube, or

GM upper stage with a Joule-Thomson bottom stage. Such a cooler can take advantage of the high efficiency of the Stirling cycle for higher-temperature precooling and also capture the remote-coldhead low-vibration attributes of a JT system for the final interface with the application load.

### 6.3.1 Cryocooler Cycle Types and Efficiency Measures

#### 6.3.1.1 Cryocooler Classifications and Practical Systems

All mechanical refrigerators generate cooling by basically expanding a gas from a high pressure to a low pressure. The primary distinguishing feature between cycles is how the compression is accomplished, what pressure-ratio is used, what method of expansion is used to achieve the cold temperature, how well and where heat is rejected, and how well thermodynamic efficiency is maintained using heat exchangers, regenerators, and recuperators.

Probably the most fundamental distinction between cryocooler types is the nature of the refrigerant flow within the cryocooler: either alternating flow (AC systems) or continuous flow (DC systems). This distinction is also denoted as *regenerative systems* versus *recuperative systems* based on the type of heat recovery heat exchanger that is applicable: regenerators for an alternating flow (AC system), or recuperators for a continuous flow (DC system).

In an AC-type cooler system, a regenerative heat exchanger stores and releases energy to the alternating refrigerant stream using a regenerator made of, for example, fine mesh screens or densely packed particles with good specific heat properties. In a DC-type system, a recuperative heat exchanger exchanges energy between two opposing streams of flowing gas or liquid using a counter-flow heat exchanger referred to as a recuperator. Of the common cooler types, Stirling, pulse tube, and Gifford McMahon use regenerative (AC flow) cycles, while Joule-Thomson and turbo-Brayton systems use recuperative (DC) flows. A key distinguishing feature of such systems is that the compressor generally must be quite close to the coldend expander in a regenerative AC-flow cooler, and can be very remote (many meters away) for a recuperative DC-flow cooler. This has important implications on managing the compressor's heat dissipation and possible vibration and noise in close proximity to the cryogenic load. One exception is the Gifford-McMahon cooler; it uses a regenerative refrigeration cycle, but uses a constant flow DC compressor that can be remotely located. To do this a GM cooler chops the DC flow into an AC flow within the coldhead itself, remote from the GM compressor.

#### 6.3.1.2 The Carnot Cycle and Efficiency References for Cryocoolers

As background before delving into the details of the various cryo refrigerator types, it is useful to touch briefly on the standard measure of cryocooler efficiency: the percent of Carnot Coefficient of Performance. The coefficient of refrigeration performance (COP) for any refrigerator is defined as the ratio of the extracted heat to the applied work, i.e.

$$\text{COP}_{\text{Cooler}} = \frac{\text{cooling power}}{\text{input power}} \quad (1)$$

Next, let's examine the Carnot-cycle refrigerator, which has the highest efficiency of any refrigeration cycle, and thus serves as a reference for all other refrigeration cycles. As shown in Fig. 7 (a temperature-entropy (T-S) diagram of the cycle), the cycle consists of gas compression on the right, constant-temperature heat-rejection at the top, an expansion phase on the left, and constant temperature heat absorption on the bottom. Heat absorbed during the process corresponds to the line with endpoints 1 and 4 (the refrigeration), while the heat rejected to the environment during the process (work done plus heat absorbed) is the line 2 to 3. Note that the compression and the expansion are both done isothermally (at constant temperature), while the expansion and the compression processes are done isentropically (i.e., with no heat transfer).

Applying Eq. (1) to the Carnot cycle in Fig. 7, we find that the ratio of cooling power (heat absorbed) to input power (heat rejected minus cooling power) is purely a function of the cold and hot temperature. Thus the COP of the Carnot-cycle refrigerator is uniquely defined in terms of the

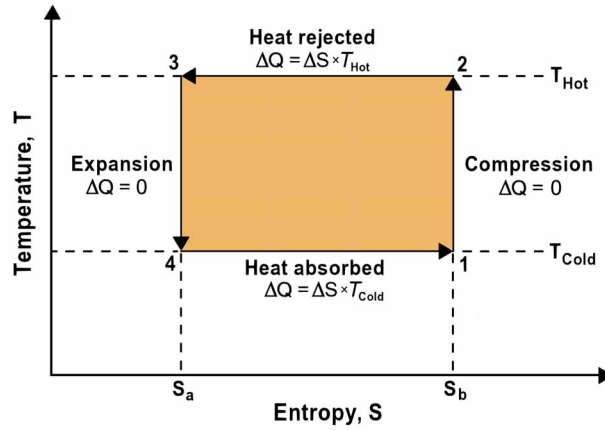


Figure 7. The Carnot refrigeration cycle.

coldtip temperature ( $T_{\text{cold}}$ ) and heatsink temperature ( $T_{\text{hot}}$ ) as:

$$\text{COP}_{\text{Carnot}} = T_{\text{cold}} / (T_{\text{hot}} - T_{\text{cold}}) \quad (2)$$

**Cryocooler Efficiency as Percent of Carnot.** An important figure-of-merit for cryocoolers is the thermodynamic COP of the refrigerator expressed as a percentage of the ideal Carnot COP. This efficiency measure is applicable to all the various cryocooler cycles discussed in the remaining subsections of this chapter and is thus defined as

$$\% \text{Carnot COP} = 100 \times \frac{\text{COP}_{\text{Cooler}}}{\text{COP}_{\text{Carnot}}} = 100 \times \frac{(\text{Cooling power @ } T_{\text{cold}}) (T_{\text{hot}} - T_{\text{cold}})}{\text{Input electrical power} \times (T_{\text{cold}})} \quad (3)$$

Notice that the percent Carnot COP is strongly dependent on both the hot and cold operating temperatures. Thus, when comparing the efficiency of various cooler candidates it is important to use common reference temperatures (both hot and cold) for the comparison. Figure 8 provides such a comparison assembled by Radebaugh, based on the reported performance of a broad number of cryocoolers with data available in the 2004 timeframe. This particular comparison is made for cryocooler operation at 80 K with a 300 K reject temperature [Radebaugh, 2004].

From the plot, the relative efficiency trends of the various cryocooler types are evident, as well as their typical range of available cooling powers at 80 K and their required input powers. These trends will be one of the key factors that influences the applications most appropriate for each cryocooler type as they are discussed later in this chapter.

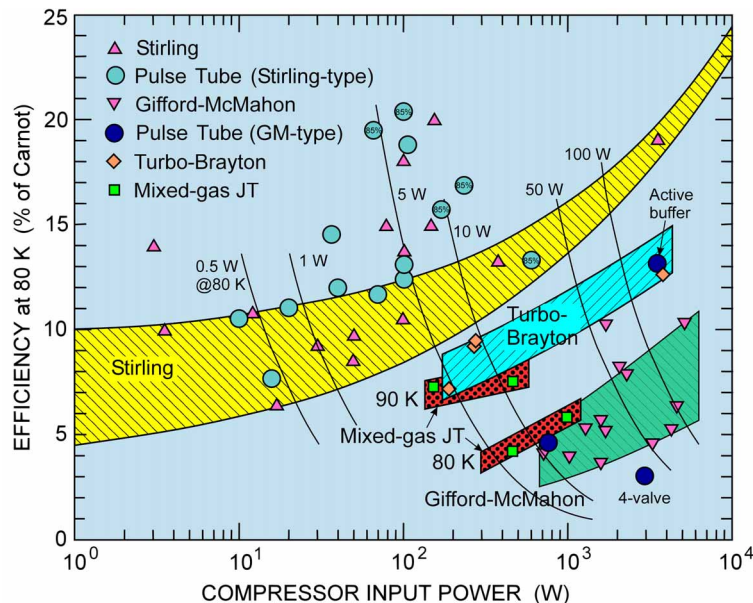


Figure 8. Efficiency for 80 K cooling for various measured cryocoolers of different types and input powers [Radebaugh, 2004].

**Dissecting Cryocooler Efficiency.** To provide visibility into the principal parameters controlling cryocooler efficiency, it is sometimes useful to separate the overall efficiency or COP of a cryocooler, Eq. (1), into its two main components: the thermodynamic efficiency of the compressor/expander combination, and the efficiency of the compressor drive motor. Cryocooler compressor motor efficiency is often found to be around 80%, or even less, and can represent a sizable fraction of the inefficiency of a cryocooler. Thus, it can be useful to break it out separately in understanding overall cryocooler efficiency.

Compressor/expander thermodynamic COP, which is a measure of the ability of the cooler to convert work done on the gas into net cooling power to the load, is thus defined as

$$\text{COP}_{\text{Thermodynamic}} = \frac{\text{cooling power}}{(\text{input PV work})} \approx \frac{\text{cooling power}}{(\text{input electrical power} - i^2R)} \quad (4)$$

In this expression, the work done on the gas is referred to as the Pressure-Volume work or PV-work and is often approximated as the compressor input electrical power minus the drive-motor  $i^2R$  losses. This is a relatively good approximation because the other compressor loss mechanisms such as windage, mechanical friction, and eddy current forces, are minor loss terms in a good compressor compared to its  $i^2R$  losses.

Similarly, because  $i^2R$  losses are generally the dominant loss term in a good motor, cooler motor efficiency can be usefully estimated as

$$\text{Motor efficiency} = (\text{input power} - i^2R)/(\text{input power}) \quad (5)$$

There are four principal contributors to high  $i^2R$  losses: 1) low magnetic flux density in the motor's magnet circuit, which requires greater current to generate a given drive force, 2) higher coil resistance for a given number of coil turns, 3) higher operating temperature of the coil and magnet, and 4) excessive capacitive or inductive circulating currents that contribute to  $i^2R$  losses, but do no useful work. Eliminating circulating currents is the same as requiring that the motor have a near unity power factor, where power factor is defined as the cosine of the phase angle between the input drive voltage and the input drive current. The power factor is also the input power consumed divided by the product of the true rms voltage times the true rms current. In calculating the  $i^2R$  losses, a common practice is to estimate the coil resistance based on the temperature of the compressor motor casing using the measured temperature dependence of the resistivity of copper.

### 6.3.2 Stirling and Pulse Tube Cryocoolers

Stirling coolers (both mechanical displacer and pulse tube-based) are one of the most widely used cryorefrigerator types for small remote and aerospace applications. Here small size & mass and high thermodynamic efficiency are paramount. These applications are often remote from available utility-supplied power, and are often mass and space constrained. Classic examples of Stirling applications include remote cell phone towers, military infrared vision sensors, and spacecraft-instrument infrared and gamma-ray sensors. However, the development of large commercial-scale Stirling-type pulse tube coolers has recently increased, aimed at efficiency and reliability improvements for large cost-sensitive continuous cooling applications such as cooling high-temperature superconductors, liquid oxygen/nitrogen production, as well as LNG production and LNG storage tank boil-off prevention. For these large coolers with multi-kilowatt input powers, efficiencies as high as 22% of Carnot have been achieved based on net useful cooling capacity on the order of 650 watts at 77 K and 8.5 kW total electrical power to the cryocooler.

#### 6.3.2.1 Stirling Thermodynamic Cycle & Operational Features

Stirling-cycle coolers tend to come in two flavors: those using a mechanical-displacer to effect the thermodynamic cycle, and those based on a pneumatic Pulse Tube (PT) circuit to achieve the thermodynamic cycle. Both use an oscillating-flow compressor to generate the AC flow needed by the cold head. However, the pulse tube version replaces the mechanical displacer of the classic Stirling cycle with a pneumatic (no moving part) expander to achieve the desired mass flow/gas

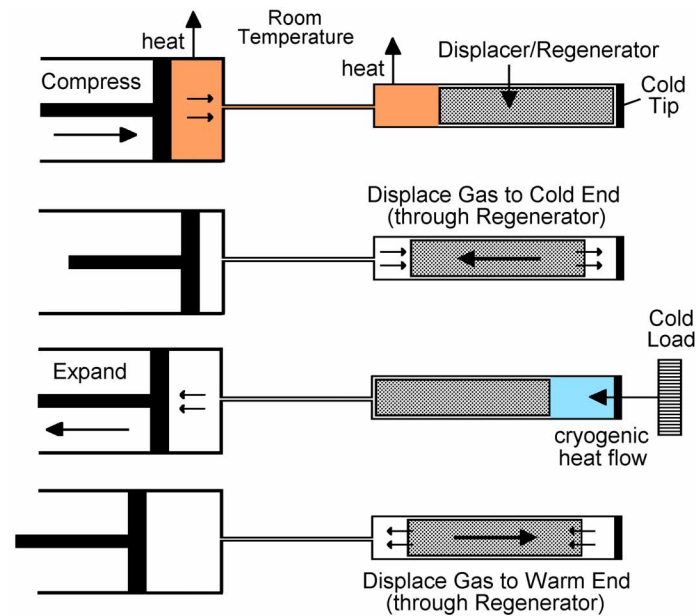


**Figure 9.** Schematic of Stirling cooler refrigeration cycle.

pressure phase relationship needed for high thermodynamic efficiency. The benefit of the PT version is lower expander vibration and elimination of complexity and possible mechanical wear associated with the moving displacer. These days, most of the industry is moving to the use of pulse tube expanders.

Because of the direct coupling between the compressor drive frequency and the expander drive frequency, most Stirling-based coolers operate at between 30 Hz and 70 Hz using helium in the 10 to 35 bar pressure range as the refrigerant gas. This relatively high AC frequency is an advantage for cooling in the temperature range above 80 K, but serves as a disadvantage for obtaining high efficiency at very low operating temperatures (below 20 K), where the reduced specific heat of regenerator materials drastically limits heat storage between cycle phases.

Figure 9 schematically illustrates the thermodynamic cycles of the mechanical Stirling-cycle cryocooler. Generally, for the mechanical-displacer Stirling cycle the regenerator and the displacer are combined in one single unit as noted.

The cycle can be roughly divided into four steps, as follows:

- The cycle starts with the compressor compressing the gas in the expander cold finger. Because the gas is heated by compression, the displacer is used to position the expander's gas pocket at the warm end of the cold finger which is coupled to a heatsink to dissipate the generated heat.
- At the completion of the compression phase, the displacer moves to the left to reposition the expander's gas pocket to the cold end of the cold finger to ready it for the upcoming expansion phase. During this part of the cycle, the gas passes through the regenerator entering the regenerator at ambient temperature  $T_{\text{High}}$  and leaving it with temperature  $T_{\text{Low}}$ . Thus, the heat storage feature of the regenerator smooths out the cyclic temperature of the gas in the two ends of the expander cold finger.
- Next, the compressor enters its expansion phase, thus expanding and cooling the gas in the expander's coldfinger—adjacent to the cryocooler's cold load. This is where the useful cooling power is produced.
- In the final portion of the cycle, the displacer moves to the right to reposition the expander's gas pocket to the hot end of the coldfinger to ready it for the upcoming compression phase. During this part of the cycle, the gas again passes through the regenerator entering the regenerator at the cold temperature  $T_{\text{Cold}}$  and leaving it with temperature  $T_{\text{Hot}}$ . Thus, the heat storage feature of the regenerator again smooths out the cyclic temperature of the gas as it flows between the two ends of the expander cold finger.

### 6.3.2.2 Pulse Tube Stirling Cycle

In contrast to the mechanical driven displacer of the classic Stirling cycle, the pulse tube version of the cooler uses a tuned pneumatic circuit with no moving parts to accomplish the gas position management functions accomplished by the conventional Stirling mechanical displacer.

The key elements of the pulse tube tuned circuit are analogous to the principal elements of an electrical Resistance-Inductance-Capacitance (RLC) phase shifting network. In the pulse tube the mechanical analogs are the reservoir volume, which provides the capacitance function, and an inertance tube, whose flow resistance provides the resistance function. The inductance or inertia function comes from the inertia of the gas flowing in the inertance tube, thus its name. The design objective of the circuit is to achieve an optimum phase shift ( $\sim 70$  degrees) between the mass flow through the regenerator and the instantaneous pressure from the compressor. This is accomplished by carefully tuning the pulse tube cold head's RLC parameters: the length and diameter of the inertance tube and volume of the reservoir.

The gas displacing function of the expander is carried out by the pulse tube itself. In addition to being the name of this type of expander, it is the name given to a short hollow tube between the inertance tube circuit and the regenerator. The objective of the hollow pulse tube is to isolate the cold end of the regenerator from the hot gases returning from the inertance tube circuit. It does this by achieving a careful stratification of temperatures along its length and having sufficient volume such that the gas at the hot (inertance) end of the pulse tube never reaches the cold-load interface end during each pressure/expansion cycle. In order to maintain this strict stratification of temperatures, the pulse tube design must carefully prevent any kind of gas mixing in the pulse tube due to turbulent flow or gravity caused convection.

The four cyclic phases of the pulse tube cooler are illustrated in Fig. 10. In this figure the displacer function of the pulse tube is noted by a virtual-displacer which represents the cold and hot boundaries of the stratified gas plug that oscillates back and forth in the pulse tube during the cooler's operation.

- As with the conventional Stirling cycle, the cycle starts with the compressor compressing the gas in the expander cold finger. Because the gas is heated by compression, the pulse tube's pneumatic circuit is used to position the expander's gas at the warm end of the regenerator which is coupled to a heatsink to dissipate the generated heat.
- At the compression phase ends, the pulse tube's pneumatic circuit repositions the expander's gas to the cold end of the regenerator to ready it for the upcoming expansion phase. During this part of the cycle, the gas passes through the regenerator to dampen out the cyclic temperature variations and preserve the temperatures at the two ends of the regenerator.

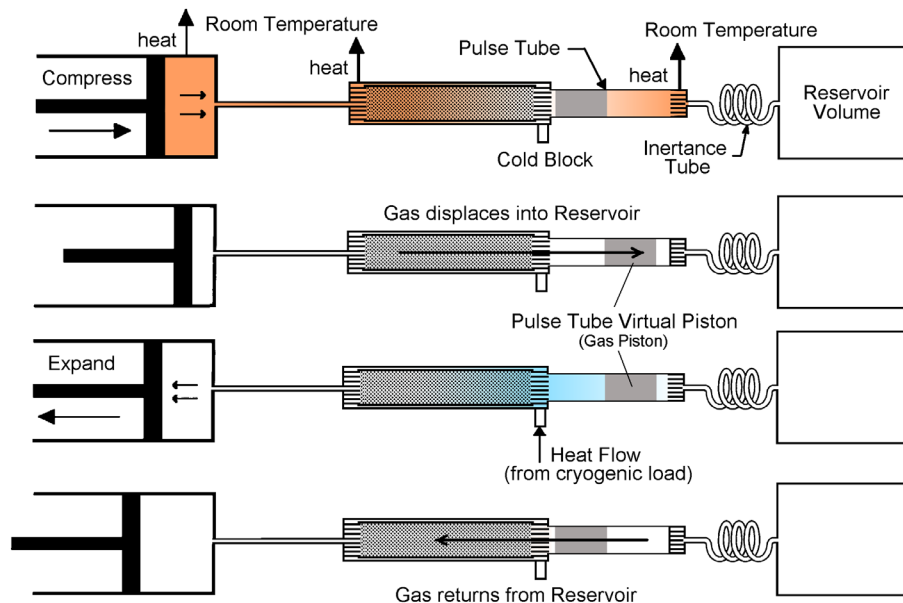


**Figure 10.** Schematic of pulse tube cooler refrigeration cycle.

- Next, the compressor enters its expansion phase, thus expanding and cooling the gas in the expander's coldfinger—adjacent to the cryocooler's cold load interface. This is where the useful cooling power is produced.
- In the final portion of the cycle, the pulse tube's pneumatic circuit repositions the expander's gas to the hot end of the regenerator to ready it for the upcoming compression phase. During this part of the cycle, the gas again passes through the regenerator to dampen out the cyclic temperature variations and preserve the temperatures at the two ends of the regenerator.

### 6.3.2.2 Engineering Aspects of Stirling and Pulse Tube Cryocoolers

Supporting the requirement for an alternating fluid flow with a frequency of from 30 to 70 Hz, Stirling cooler compressors are invariably piston-type compressors driven either by a rotating crank shaft like a car engine, or by a linear voice-coil motor, like a HiFi loud speaker.

**Rotary Crank Compressor.** The advantage of the rotary-crankshaft design is that the displacer can also be driven off the same crank shaft as the piston, thus achieving both gas compression and displacer control with the needed phase relationship between them from the same drive motor. The key disadvantage of the rotary crank design is the life issues associated with piston, displacer and bearing wear, and contamination of the helium working fluid by outgassing products of the required bearing lubricants. Note that a rotary compressor is essentially a constant-stroke variable-frequency compressor, the frequency being determined by the motor drive speed (rpm). A miniature Ricor K508 rotary-drive Stirling cooler is pictured in Fig. 11.

**Linear Compressors.** Over the past 25 years, the vast majority of Stirling coolers have migrated over to the linear compressor configuration to achieve higher-reliability, longer-life designs. An example is the DRS (formerly Texas Instruments) 1.75W at 80 K dual piston linear drive Stirling cooler shown in Fig. 12. This design uses a variable stroke and constant drive frequency, where the linear piston's mechanical resonant frequency is closely aligned with the drive frequency to achieve high drive motor efficiency. Maintaining a close match minimizes the required drive current and results in the drive current being closely in phase with the drive voltage. This minimizes circulating reactive currents that add to the  $i^2R$  losses, but do not contribute to work done by the motor.

The primary determiners of the compressor resonant frequency are the moving mass of the compressor piston assembly and the elastic spring constant of the combination of the gas under compression by the piston and the piston suspension springs. The resonant frequency is tuned to the desired value by adjusting these parameters.

To minimize exported vibration caused by the internal moving piston mass, most Stirling compressors are manufactured as a balanced head-to-head pair with two pistons moving in opposition into a common compression chamber. In this way, the momentum of the two pistons is cancelled out to a high degree, leaving a very quiet and relatively vibration-free compressor.

Although early linear compressor designs avoided the bearing wear and lubricant-caused issues of rotary Stirling coolers, they still contained rubbing pistons and displacers, which limited their useful lives to around 10,000 hours.

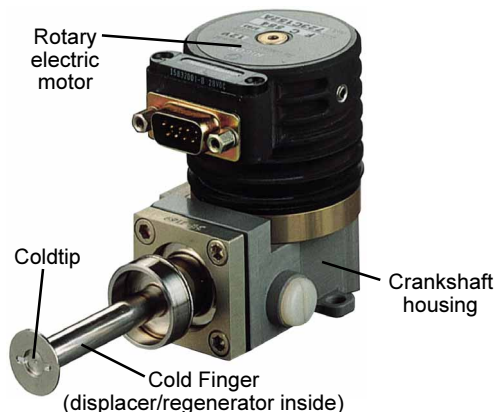


**Figure 11.** Miniature Ricor K508 rotary Stirling cooler (500 mW at 80 K).

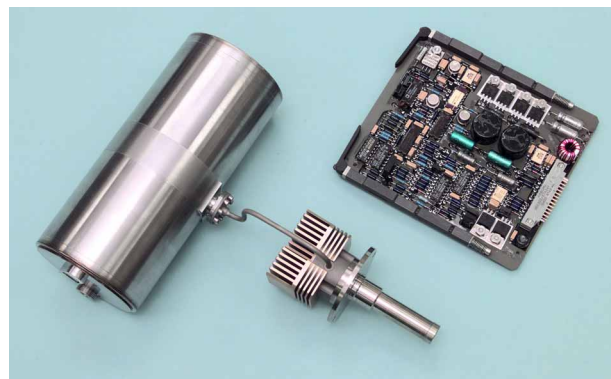


**Figure 12.** 1.75 W at 80 K DRS linear-motor dual-piston Stirling cooler.

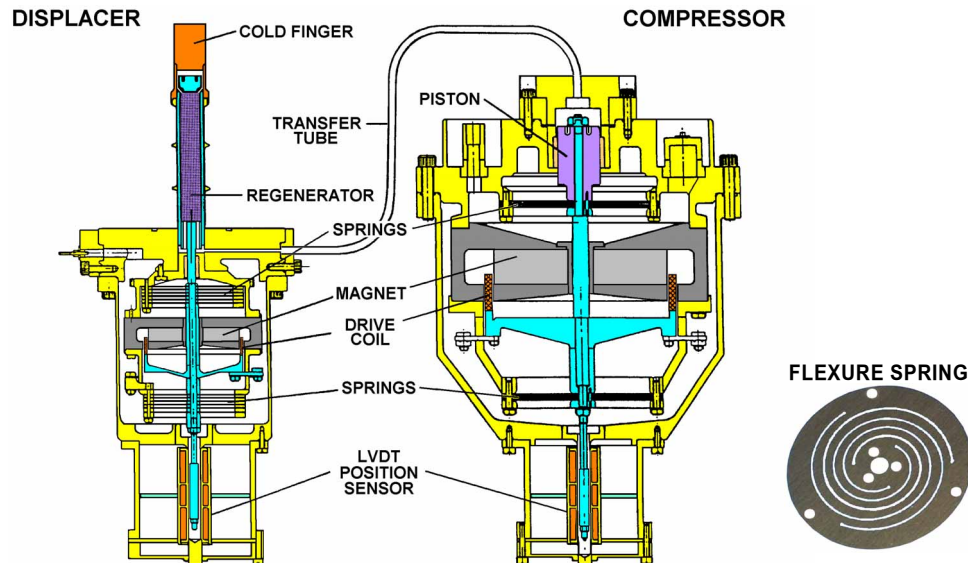


**Fig. 13** Construction features of the 1980s Oxford Stirling cooler which incorporates a flexure bearing supported linear-drive compressor and a flexure bearing supported linear-driven active displacer.

**The Oxford Compressor Design.** In the mid-1980s, Steve Werrett, Gordon Davey and their associates at Oxford University in England attempted to greatly extend the life of a linear Stirling cooler by supporting both the compressor piston and the displacer-regenerator/piston on linear flexure bearings [Werrett, et al., 1986; and Bradshaw, et al., 1986]. These were designed to prevent piston and displacer contact with the cylinder wall while maintaining a tight ( $\sim 0.0003$ " ) clearance between the piston and cylinder to achieve good compression efficiency. Figure 13 illustrates the mechanical features of the original 1980s Oxford cooler, including its spiral flexure spring design. This design was highly successful and was launched into space to support 80 K cooling of the Improved Stratospheric and Mesospheric Sounder (ISAMS) instrument on board NASA's Upper Atmospheric Research Satellite (UARS) in September 1991 [Ross, 2007].

Based on the demonstrated long life and mechanical simplicity of its flexure bearing design, the Oxford cooler concept was quickly adopted world wide by nearly all the leading manufacturers of long-life Stirling coolers. Since then, Oxford-style flexure supports have been adopted into all sizes of Stirling coolers from the lowest cost "tactical coolers" used in short life military applications, to large-scale multi-kilowatt machines targeted at liquefaction of natural gas.

**Mechanical Displacer.** The classic mechanical Stirling-cycle expander combines a regenerator with a mechanical piston displacer, often integrated into a single regenerator/displacer unit as shown in Fig. 13. For rotary-crank driven coolers, such as that in Fig. 11, the regenerator/displacer is driven off the crank shaft, offset from the piston position by around 70 degrees. For linear compressors with mechanical displacers, such as that shown in Fig. 12, the displacer is generally a passive resonant system like the compressor, but tuned to have its phase shifted from that of the compressor by that needed for good Stirling-cycle efficiency.

With the introduction of the long-life Oxford cooler design in the late 1980s, a greater degree of control over piston/displacer phasing was introduced by embedding a second linear motor in the displacer as shown in Fig. 13. This displacer motor was then used to provide precise stroke and phase control to the displacer via closed-loop drive electronics. However, the downside of this high-efficiency, long-life design was that the displacer and electronics complexity, mass, and cost increased substantially.

**Pulse Tube Expander.** The first pulse tube research dates from the 1960s with the work of Gifford and Longworth [Gifford and Longworth, 1965] and progressed rather slowly over the next 20 years [Radebaugh, et al., 1986]. However, in the early 1990's, research with pulse-tube expanders for Stirling cryocoolers made a giant leap forward in terms of efficiency. This was brought about by the introduction of the inertance tube, first introduced by TRW (now Northrop Grumman Aerospace Systems—NGAS) into cryocoolers being developed for space applications.

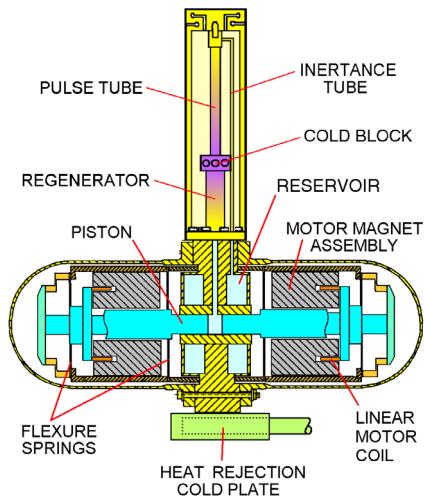


**Figure 14.** Schematic of dual-piston, linear-motor pulse tube cooler.



**Figure 15.** NGAS dual-piston, linear-motor HEC pulse tube cooler [Raab and Tward, 2010].

This technology allowed substantially improved Stirling-cycle tuning over that achievable with the use of the existing orifice pulse tube. As noted earlier, the inertance tube introduced the ability to provide 3-parameter Resistance/Inductance/Capacitance (RLC-type) tuning, and thus achieved the more extensive phase-angle control required for high cryocooler efficiency. Since the late 1990s, pulse tube expanders have been adopted worldwide as a leading expander type for Stirling cycle coolers. Figures 14 and 15 illustrate the features and appearance of a typical single-stage pulse tube cooler utilizing an integral head-to-head Oxford-style linear compressor. Pulse tube coldheads are also being adapted for use on Gifford-McMahon coolers, as described in Section 6.3.3.

**Drive Electronics.** A second area of advanced development first introduced by the Oxford cooler and its space-cooler derivatives is advanced solid-state drive electronics for precise control of cooler operation. For Stirling coolers with mechanical displacers this typically involves precise control of compressor and displacer stroke amplitude and the phase between them; with pulse tube coolers, only compressor stroke needs to be controlled. Taking advantage of the precise control of compressor stroke, many electronics expand this capability to also provide closed-loop control of the coldtip temperature and active nulling of vibration harmonics in the drive axis [Harvey, et al., 2004]. A representative set of modern pulse tube drive electronics is pictured in Fig. 16.

In addition to controlling and managing the power interface, many advanced electronics also provide a digital interface for remote programming of the cooler and feedback of cryocooler-related digital data such as coldtip temperature, stroke level, and vibration level.

A common electrical interface issue with linear-drive coolers is the feedback of large ripple currents at twice the cooler drive frequency into the power supply bus. This and other electrical and mechanical interface considerations are discussed later in this chapter in Sections 6.5.2 and 6.5.3.



**Figure 16.** NGAS HEC dual-piston, linear-motor pulse tube cooler drive electronics [Harvey, et al., 2004].

### 6.3.2.3 Stirling and Pulse Tube Cooler Development History and Availability

Small Stirling cycle cryocoolers (such as those shown in Figs. 11 and 12) were first used in military/space applications in the early 1970s and first launched into space in 1975 [Ross, 2007]. Since that time, they have become the workhorse of the military and space industry. Starting in the mid 1990s high efficiency pulse tube coolers (such as that shown in Fig. 15) emerged and have all but replaced the mechanical displacers of earlier generations of Stirling-cycle refrigerators [Raab and Tward, 2010].

Presently there are a number of active manufacturers of Stirling and pulse tube cryocoolers located all over the world: in the US, Europe, Israel and Asia. Starting originally with modest size units with a cooling capacity of around 1W at 80 K, the recent stable of available Stirling-cycle coolers ranges from palm-size units weighing just a few ounces and providing a cooling capacity of 500 mW at 80 K, to units that weigh 350 lbs and provide 650 W of cooling at 80 K. As shown in Table 2 Stirling and pulse tube cryocoolers have developed an enviable record in space applications over the last 20 years, with some units having demonstrated lives of greater than 139,000 hours (over 15 years) of continuous 24/7 operation [Ross, 2007].

**Table 2.** Space Stirling and Pulse Tube Cryocooler Flight Operating Experience as of Oct 2013

Cooler / Mission	Hours/Unit	Comments
<b>Ball Aerospace (BATC) Stirling</b>		
HIRDLS (60K 1-stage Stirling)	80,000	Turn on 8/04, Ongoing, No degradation
TIRS cooler (35K two-stage Stirling)	7,000	Turn on 3/6/13, Ongoing, No degradation
<b>Fujitsu Stirling</b> (ASTER 80K TIR system)	119,400	Turn on 3/00, Ongoing, No degradation
<b>Mitsubishi Stirling</b> (ASTER 77K SWIR system)	115,200	Turn on 3/00, Ongoing, Load off at 71,000 h
<b>NGAS (TRW) Coolers</b>		
CX (150K Mini PT (2 units))	139,000	Turn on 2/98, Ongoing, No degradation
HTSSE-2 (80K mini Stirling)	24,000	3/99 thru 3/02, Mission End, No degrad.
MTI (60K 6020 10cc PT)	119,000	Turn on 3/00, Ongoing, No degradation
Hyperion (110K Mini PT)	111,000	Turn on 12/00, Ongoing, No degradation
SABER (75K Mini PT)	107,000	Turn on 1/02, Ongoing, No degradation
AIRS (55K 10cc PT (2 units))	99,000	Turn on 6/02, Ongoing, No degradation
TES (60K 10cc PT (2 units))	80,000	Turn on 8/04, Ongoing, No degradation
JAMI (65K HEC PT (2 units))	72,000	Turn on 4/05, Ongoing, No degradation
GOSAT/IBUKI (60K HEC PT )	40,700	Turn on 2/09, Ongoing, No degradation
STSS (Mini PT (4 units))	30,200	Turn on 4/10, Ongoing, No degradation
<b>Oxford/BAe/MMS/Astrium Stirling</b>		
ISAMS (80 K Oxford/RAL)	15,800	10/91 thru 7/92, Instrument failed
HTSSE-2 (80K BAe)	24,000	3/99 thru 3/02, Mission End, No degrad.
MOPITT (50-80K BAe (2 units))	114,000	Turn on 3/00, lost one disp. at 10,300 h
ODIN (50-80K Astrium (1 unit))	110,000	Turn on 3/01, Ongoing, No degradation
AATSR on ERS-1 (50-80K Astrium (2 units))	88,200	3/02 to 4/12, No Degrad, Satellite failed
MIPAS on ERS-1 (50-80K Astrium (2 units))	88,200	3/02 to 4/12, No Degrad, Satellite failed
INTEGRAL (50-80K Astrium (4 units))	96,100	Turn on 10/02, Ongoing, No degradation
Helios 2A (50-80K Astrium (2 units))	74,000	Turn on 4/05, Ongoing, No degradation
Helios 2B (50-80K Astrium (2 units))	30,200	Turn on 4/10, Ongoing, No degradation
<b>Raytheon ISSC Stirling</b> (STSS (2 units))	30,200	Turn on 4/10, Ongoing, No degradation
<b>Rutherford Appleton Lab (RAL)</b>		
ATSR 1 on ERS-1 (80K Integral Stirling)	75,300	7/91 thru 3/00, Satellite failed
ATSR 2 on ERS-2 (80K Integral Stirling)	112,000	4/95 thru 2/08, Instrument failed
Planck (4K JT)	38,500	5/09 thru 10/13, Mission End, No Degrad.
<b>Sumitomo Stirling Coolers</b>		
Suzaku (100K 1-stg)	59,300	7/05 thru 4/12, Mission End, No degradation
Akari (20K 2-stg (2 units))	39,000	2/06 to 11/11 EOM, 1 Degr., 2nd failed at 13 kh
Kaguya GRS (70K 1-stg)	14,600	10/07- 6/09, Mission End, No degradation
JEM/SMILES on ISS (4.5K JT)	4,500	Turn on 10/09, Could not restart at 4,500 h
<b>Sunpower Stirling</b> (75K RHESSI)	102,000	Turn on 2/02, Ongoing, Modest degradation

### 6.3.3 Gifford-McMahon (GM) and GM/Pulse Cryocoolers

Gifford-McMahon (GM) cryocoolers (with both mechanical displacer and pulse tube coldheads) are one of the most widely used coolers for commercial and laboratory use where low cost and operational convenience is important, and lots of electrical power is widely available. The GM cycle is very similar to the Stirling cycle in that its expander is based on an AC oscillating flow, typically using helium in the 10 to 30 bar range as the refrigerant gas with a working frequency of 1 to 2.4 Hz.

The one significant difference between Stirling-type coolers and GM coolers is that the GM cooler uses a low-cost high-availability DC flow compressor (typically acquired from a commercial air conditioning application) to provide the primary gas-compression function. The alternating flow needed by the GM expander is then provided by a rotary valve mounted on the GM cooler's cold head assembly. This valve chops the DC flow into an AC flow by alternately connecting the expander to the high- and low-pressure sides of the compressor at the required oscillatory frequency of 1 to 2 Hz. This low frequency is particularly useful for obtaining improved efficiency at very low operating temperatures where the reduced specific heat of regenerator materials limits heat storage between cycle phases. The required phase relationship between refrigerant pressure and mass flow is achieved by synchronizing the rotary valve with the motor- or pneumatic-driven motion of the displacer. Because the compressor is a DC-flow device, it can be located remote from the actual cryogenic application, connected only by high-pressure hoses. However, the GM compressor must also use a highly efficient oil separator and a high-quality gas purification trap to prevent compressor oil vapor from reaching the expander.

#### 6.3.3.1 GM Thermodynamic Cycle & Operational Features

Gifford-McMahon cryocoolers tend to come in two flavors, those based on the historic GM motor-driven mechanical-displacer expander, and those based on the more recently developed Pulse Tube (PT) expander. Both use the same DC-flow compressor and rotary valve to generate the AC flow needed by the cold head. However, the pulse tube version replaces the motor-driven mechanical displacer of the GM cycle with a pneumatic (no moving part) expander to achieve the desired mass flow/pressure phase relationship needed for high thermodynamic efficiency. The benefit of the PT version is lower vibration and elimination of mechanical wear in the moving displacer.

Figure 17 schematically illustrates the thermodynamic cycle of the mechanically driven GM refrigerator. Generally, for the mechanical GM cycle the regenerator and the displacer are combined into one displacer/regenerator unit as noted. The cooling cycle for a GM-pulse tube type cooler is essentially identical, except that the phasing of the gas flow in the cold finger is controlled by the pulse tube's tuned pneumatic circuit instead of by the motion of the mechanical displacer.

The GM cooling cycle can be divided into four steps as follows:

- The cycle starts with the rotary valve connecting the expander to the high-pressure room-temperature gas from the compressor. This fills the expander's gas pocket, which has been previously positioned at the warm end of the cold finger, with high pressure gas
- At the completion of the high-pressure filling phase, the displacer moves to the left to reposition the expander's gas pocket to the cold end of the cold finger to ready it for the upcoming expansion phase. During this part of the cycle, the gas passes through the regenerator entering the regenerator at ambient temperature  $T_{\text{Ambient}}$  and leaving it with temperature  $T_{\text{Low}}$ . Thus, the heat storage feature of the regenerator retains the temperature gradient between the warm and cold ends of the cold finger and smooths out the cyclic temperature variation of the gas.
- Next, the rotary valve connects the low pressure suction from the compressor return to the expander, thus expanding and cooling the gas in the expander's coldfinger tip—adjacent to the cryocooler's cold load. This is where the useful cooling power is produced.
- In the final portion of the cycle, the displacer moves to the right to reposition the expander's gas pocket to the room temperature end of the coldfinger to ready it for the upcoming high high-pressure gas filling phase. Again, during this part of the cycle, the gas passes through

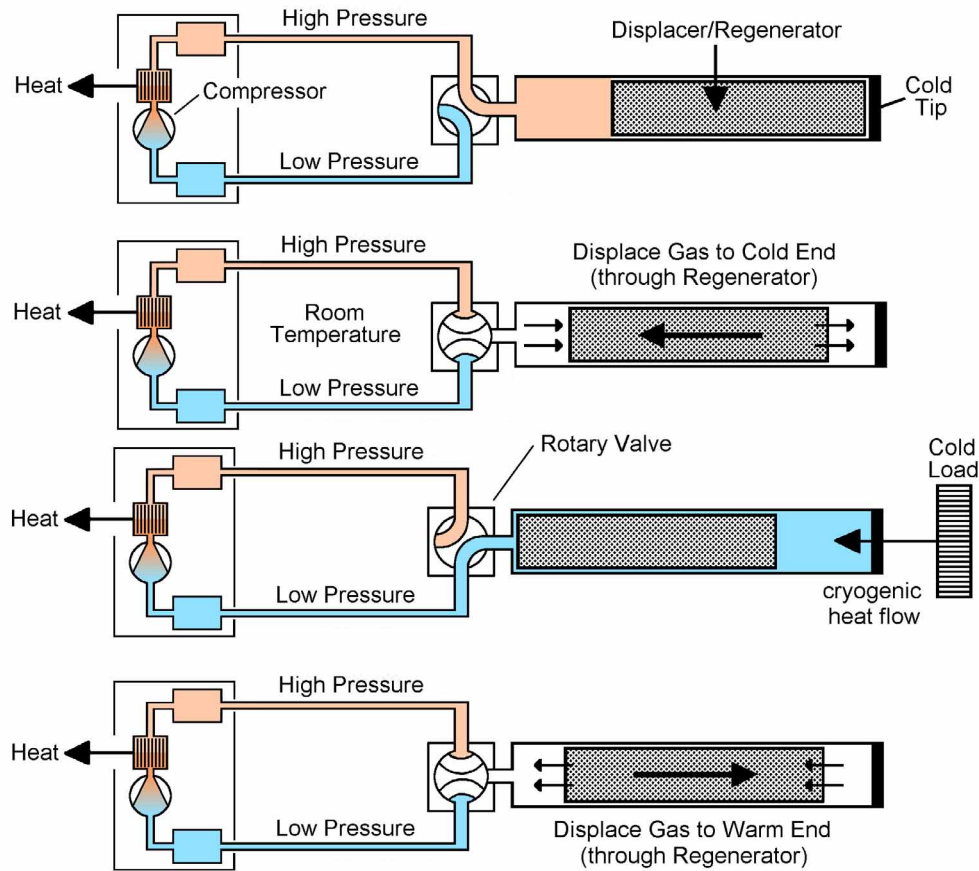


**Figure 17.** Schematic of Gifford McMahon refrigeration cycle.

the regenerator, and the heat storage feature of the regenerator smooths out the cyclic temperature of the gas as it flows between the two ends of the regenerator.

### 6.3.3.2 Engineering Aspects of Gifford-McMahon Cryocoolers

**Compressor.** A key engineering attribute of the GM process is the use of readily available, mature, DC-flow air conditioning compressors for the compression part of the cycle. This allows GM coolers to directly benefit from the years of reliability development and cost reduction of these OEM compressors. In addition, the DC-flow nature of these compressors allows them to be remotely located (up to 10s of feet) from the application cold load — a big advantage in many applications. The one downside is probably that these compressors are almost all sized for large loads and draw input powers from 1 to 14 kW. Thus, they have serious electrical power and heat dissipation requirements — typically requiring 220 to 440 volt electrical supplies and facility-based chilled water for cooling. In summary, GM machines are generally associated with modest to large loads in institutional settings, and are not particularly well suited to small, compact or portable applications.

**Cold Head.** Having the GM coldhead operational frequency decoupled from the compressor's drive frequency provides another big advantage for the GM cooler. This allows the cold head operational frequency to be optimized for maximum cold head performance without regard to the compressor's operation. The ability to select a low expander frequency of around 1 Hz greatly simplifies the design of the regenerator beds for low-temperature applications where the low specific heat of materials is a severe constraint. The low drive frequency allows the use of much larger regenerator particles (on the order of 0.25 mm diameter) which are much easier to package and contain in comparison to ~0.05 mm particles that would be required for say a 20 Hz Stirling-cycle coldhead.

The one disadvantage of the GM coldhead, particularly those with the classic mechanically driven displacer, is a modest (some would say high) level of mechanical vibration and audible noise



**Figure 18** Example GM cooler components: a) 200 W at 80 K Cryomech GM expander; b) 0.5 W at 4.2 K Cryomech two-stage GM pulse tube expander; c) Example Sumitomo GM compressor.

generated directly by the coldhead. However, the recent GM pulse tube coldheads are a big improvement in this regard, leaving the rotary valve as the only noise source in these units; and the rotary valve can be separated away from the cold head in some units to further reduce vibration [Wang, 2005; Xu, 2003].

### 6.3.3.3 GM Development Status and Typical Performance

Gifford-McMahon refrigerators have been the workhorse of the domestic cryogenic cooler industry for many years. Primary applications include cryopumping vacuum chambers used for semiconductor processing, cooling superconductor magnets such as in MRI machines in hospitals, and providing general purpose cooling in cryogenic laboratories. Another common use these days is in zero-boil-off systems where the GM cooler is used to reliquefy the evaporated gases from liquid nitrogen and liquid helium systems. Where the use of liquid nitrogen and liquid helium were once the preferred cooling means in the past, GM cryocoolers have replaced the stored cryogen systems in many places because of their ability to cool to a wide range of temperatures from 4 K to 150 K and at loads as large as 1.5 watt at 4.2 K and 600 watts at 80 K. Both single and two-stage machines are widely available (see Fig. 18), with two-stage machines offering simultaneous cooling of loads at two different temperatures. Leading suppliers of GM machines include Sumitomo Heavy Industries (SHI) in Japan and Cryomech and CTI-Cryodyne in the US. Figure 19 provides

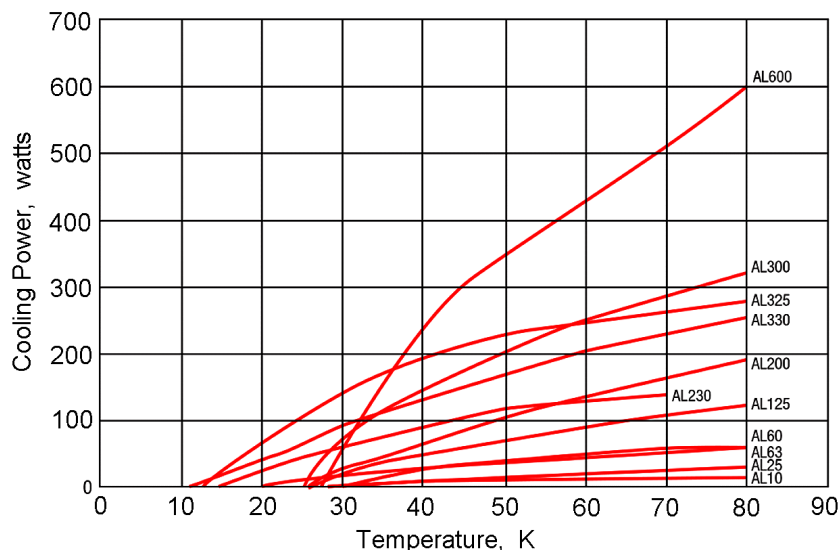


**Figure 19.** Representative cooling curves for the family of Cryomech GM refrigerators. Sumitomo has a similar family.

representative cooling curves for a variety of GM coolers manufactured by Cryomech. SHI and CTI have their own offerings. In addition, both Cryomech and SHI have units for substantial cooling down to 4.2 K [Wang, 2005; Wang & Gifford, 2003; Xu, 2003].

In general, GM cryocoolers have a good mean time to maintenance of around 10,000 hours or more, comparable to a commercial air conditioning system. This has been improved to 30,000 to 45,000 hours with some of the latest of pulse tube cold heads.

As shown earlier in Fig. 8, GM machines tend to be less efficient than Stirling coolers and tend to have large power draws (typically from 1 to 8 kW and often utilize 3-phase electricity at 200 to 440 volts). To manage the rejected heat from their large compressors, most provide facilities for water cooling via user-provided coolant water supplies. Smaller compressor units can also be acquired with interfaces for air cooling and utilizing 120 volt single-phase power.

### 6.3.4 Joule-Thomson Refrigeration Systems

Joule-Thomson (JT) based refrigeration systems are probably the most familiar type of refrigeration system to the general public. A variant of this cycle, referred to as the vapor compression or throttle cycle, is used in nearly all domestic refrigerators and freezers, and residential, commercial and automotive air conditioning systems. A second major use of the vapor compression cycle is the liquefaction of oxygen and nitrogen for industrial uses. However, today, the use of the JT or throttle cycle is not particularly common for general cryogenic cooling applications. Two specialized uses include the cooling of the small tip of cryogenic surgical probes and as a bottoming cycle for cooling focal planes to 4-6 K in vibration sensitive space-viewing instruments and telescopes. In years past, JT open-cycle blow-down systems were commonly used to cool infrared detectors in many tactical military applications [Longsworth and Steyert, 1988; Bonney and Longsworth, 1990]. However, such applications have greatly diminished in recent years, replaced mostly by small fast-cooldown tactical Stirling cryocoolers.

#### 6.3.4.1 JT Thermodynamic Cycle & Operational Features

Fundamentally, the Joule-Thomson (JT) cycle is a recuperative cycle that is built on a constant DC flow of high-pressure fluid that is expanded isenthalpically (no heat transfer) to a low pressure through a JT expansion valve [Maytal and Pfothenauer, 2012]. Except for the open-cycle, fast-cooldown military applications mentioned above, most JT cooling systems are closed-cycle systems, meaning that the fluid is circulated in a closed-cycle system as shown in Fig. 20.

Such systems incorporate a high pressure compressor to first pressurize the refrigerant stream to a relatively high pressure—much higher than that of a Stirling-cycle cooler, for example. Here, the heat of compression is extracted via heat exchange to an ambient-temperature heatsink. For the vapor compression or throttle-cycle version of the JT cycle, the refrigerant is chosen so that it is actually liquefied at this temperature and pressure; for the conventional JT cycle it is generally still a gas, but must be cooled below its inversion temperature before reaching the expansion valve.

To achieve maximum efficiency, the circulating refrigerant may be passed through a counter-

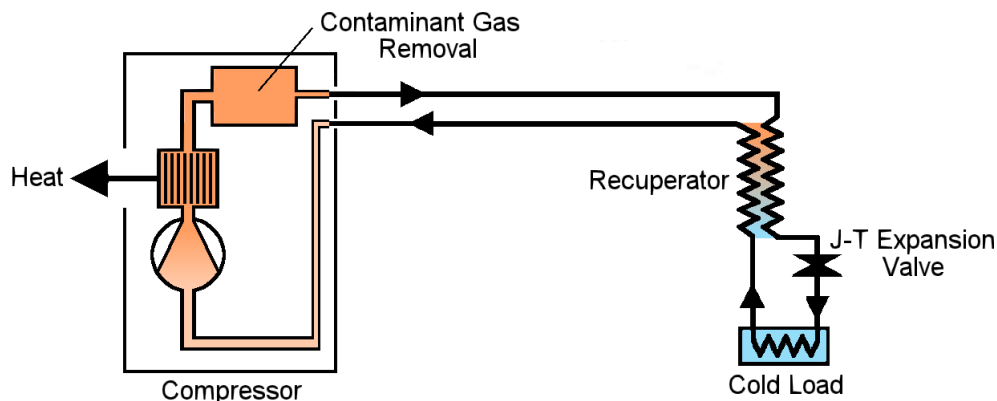


**Figure 20.** Basic mechanical setup of the closed JT cycle.

flow heat exchanger (recuperator) to utilize the remaining cooling capacity of the spent refrigerant to precool the refrigerant stream entering the JT valve. Typically, the vapor compression or throttle-cycle version of the JT cycle does not incorporate the recuperative heat exchanger.

The refrigerant is next expanded through the JT valve, or throttle valve in the case of a liquid, to where it is used to cool the refrigeration load. Depending on the refrigerant gas and pressures used, the resulting cold refrigerant can be a pure gas or a mixture of gas and liquid. After cooling the load, the refrigerant is circulated back to the compressor for repressurization. For the case where the refrigerant is a liquid following the expansion process, the liquid may be contained in a reservoir or "evaporator" where it is boiled off as it is used to cool the load.

#### 6.3.4.2 Basic Thermodynamics of the JT Cycle

A key feature of the Joule-Thomson effect is that it critically depends on gas properties that deviate from those of an ideal gas; in fact, an ideal gas exhibits no JT cooling effect when expanded. As a result, the JT cycle is highly dependent on the choice of refrigerants and the temperatures and pressures used. Table 3 tabulates some of the key properties of common gases used in cryogenic JT cooling systems. When using these gases, conditions close to gas liquefaction temperature typically lead to properties that deviate the most from ideal gas properties, and thus tend to be ideal for the maximum JT cooling effect. For refrigerators using a vapor-compression or throttle cycle, the fluid is kept very close to liquefaction and thus very non-ideal. Thus, those applications tend to have the highest efficiency.

From a physics point of view, as a non-ideal gas expands, the average distance between molecules grows. Because of the attractive part of the intermolecular force, expansion causes an increase in the potential energy of the gas. If no external work is extracted in the process and no heat is transferred (the isenthalpic JT process), the total energy of the gas remains the same because of the conservation of energy. The increase in potential energy thus implies a decrease in kinetic energy and therefore a decrease in temperature of the gas.

Unfortunately, a second mechanism has the opposite effect. During gas molecule collisions, kinetic energy is temporarily converted into potential energy (corresponding to the repulsive part of the intermolecular force). As the average intermolecular distance increases, there is a drop in the number of collisions per time unit, which causes a decrease in average potential energy. Again, total energy is conserved, so this leads to an increase in kinetic energy and an increase in gas temperature upon expansion.

Below what is referred to as a gas' inversion temperature (column 5 in Table 3) the former effect dominates, and JT expansion results in gas cooling; above the inversion temperature, the second process dominates, and JT expansion causes the gas to increase in temperature.

The rate of change of temperature for a change in pressure in a Joule-Thomson expansion process is referred to as the *JT coefficient* of a gas. It is commonly expressed in °C/bar or K/Pa and

**Table 3.** Fluid properties important to JT coolers.

Fluid	Normal Boiling Point (K)	Freezing Point (K)	Critical Point (K)	Max. Inversion Temp. (K)
Helium	4.2	1.8	5.2	39
Hydrogen	20.4	13.8	33.2	195
Neon	27.1	24.6	44.5	220
Nitrogen	77.4	63.3	126.2	608
Argon	87.3	83.8	150.7	763
Oxygen	90.2	54.4	154.6	758
Methane	111.7	90.7	190.6	980
Krypton	119.8	115.8	209.4	1054

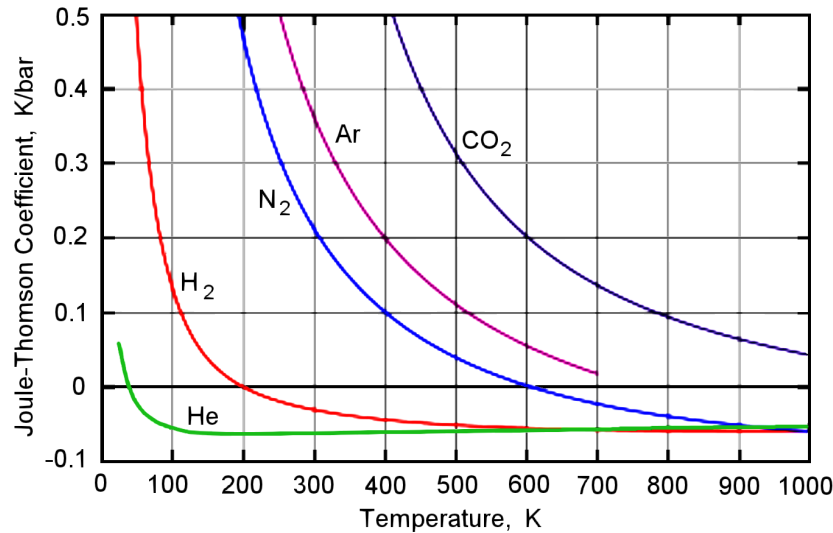


**Figure 21.** Joule-Thomson coefficients for various gases at atmospheric pressure.

depends critically on the type of gas and on the temperature of the gas before expansion. Its pressure dependence is usually only a few percent for pressures up to 100 bar. Figure 21 plots the JT coefficient for a number of common gases at atmospheric pressure. For positive JT cooling to take place, the JT coefficient must be positive; thus the zero crossings in the plot define the *inversion temperatures* of the displayed gases.

**Use of Mixed Gas Refrigerants.** When trying to achieve cryogenic temperatures between 80 K and 120 K with conventional gases such as Nitrogen one finds that the efficiency is quite low and the required pressure ratio for good efficiency is impractical to achieve with an inexpensive single-stage compressor. To combat these limitations, experimentation initiated in the 1970s examining the possibility of combining nitrogen with various hydrocarbon gases to yield a mixed gas with substantially improved JT properties that would allow efficient operation with a lower-pressure-ratio single-stage compressor. The primary challenges involved achieving throttle-cycle performance at the higher temperatures while achieving gas-liquid solubilities that prevented expansion valve plugging as the higher temperature constituents drop in temperature. Other constraints on the constituents include oil solubility and flammability. Progress on the development of mixed gases over the years has been quite successful and has led to a variety of proven mixed-gas refrigerants for various cryogenic temperature ranges [Boiarski, 1998; Arkhipov, et al., 1999][Bradley, et al., 2009].

One of the first commercial cryogenic JT coolers, called the Cryotiger, was developed by Ralph Longworth in 1994 [Longworth, et al., 1995; Longworth, 1997]. It married the use of a mixed-gas refrigerant with an inexpensive oil-lubricated compressor and Gifford-McMahon oil stripping technology to yield a low-cost, relatively long-life JT cryocooler for use in the range of 80 K.

#### 6.3.4.3 Engineering Aspects of JT Cycle Cryocoolers

**High-Pressure Piston Compressors.** Key engineering attributes of the JT process are the need for high pressure ratios, relatively low refrigerant mass flow rates, and needs to prevent blockage of the JT valve by refrigerant contaminants such as water ice or compressor lubricants. For ground-based systems, this typically leads to a high-pressure piston or scroll-type compressor with oil lubrication and the complimentary need to have the refrigerant compatible with the oil lubricant. For applications near room temperature (like domestic refrigeration and air conditioning) the compressor lubricant is allowed to flow freely around the JT circuit as it remains dissolved in the refrigerant. However, for cryogenic applications, the oil from a lubricated compressor must be stripped from the refrigerant stream before entering the expansion valve where it could freeze out and plug the valve. A similar need exists in the implementation of Gifford-McMahon compressors, and thus this technology has been well developed for a mean time between maintenance of 10,000 hours and more.

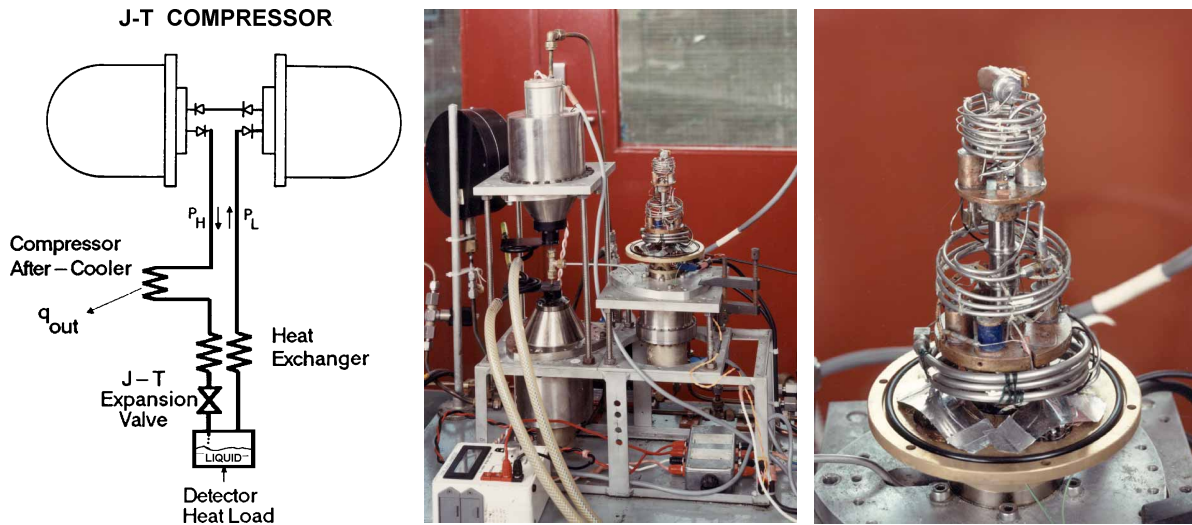


**Figure 22.** Oxford-compressor driven 4K JT cryocooler at Rutherford Appleton Labs in 1988.

**Oxford-based Linear-Motor Compressors.** For long-life applications, the desire for a lubricant-free JT compressor has led to the use of oil-free, linear-motor compressors based on the Oxford-cooler technology used in Stirling and PT coolers. Such compressors are fitted with reed valves to effect a DC flow, but the low piston forces available from such compressors severely limit the allowable JT pressure ratios available to around 3:1; at a cost of increased complexity, this can be overcome by using multiple compressor stages as required.

Initial research on Oxford-based JT compressors was conducted by Bradshaw and Orłowska at England's Rutherford Appleton Laboratory in the late 1980s [Bradshaw & Orłowska, 1991]. This technology, shown in Fig. 22, utilized a two-stage JT compressor with helium gas to achieve cooling at 4.2 K. When matured, this technology successfully flew on the European Planck mission launched in May 2009 [Bradshaw, et al., 1999]. More recently, the Oxford-JT-compressor technology is being used to provide 6 K cooling for the MIRI instrument on the James Webb Space Telescope. This application, scheduled to launch in 2018, uses a single-stage Oxford-style JT compressor with helium that is pre-cooled to ~18 K via a three-stage Oxford-style pulse tube refrigerator [Raab and Tward, 2010; Petach and Michaelian, 2014].

**Sorption Compressors.** Another compressor technology that is sometimes used in a JT cooler is a sorption compressor. Such a compressor uses a chemical or physical sorbent material to absorb a refrigerant at low pressure and temperature and then to desorb it at high pressure and high temperature...thus achieving the required compression. Microporous activated carbons, zeolites and silica gels are some typical physical sorbers, whereas metal-hydrides and oxides are well-known chemical sorbers for hydrogen and oxygen, respectively. Here, the driving force is thermal input, either from electrical heaters or other heat source. A sorption compressor cell basically consists of a container that is filled with the sorbent material that is fitted with a means of being heated and cooled (thermally cycled) while the gas flow to and from the system is controlled with check valves. As a result, a sorption compressor has no moving parts and generates no vibration that would disturb a sensitive application.

Sorption based cryogenic JT systems tend to be a speciality technology focused mainly at space observatory applications requiring extremely low levels of vibration. The Planck sorption cooler developed by NASA's Jet propulsion Laboratory for the European Planck mission is a prominent recent sorption cryocooler development [Wade, et al., 2000]. This system uses a metal-hydride compressor to compress hydrogen gas for cooling to 18 K. Another prominent research center for sorption cryocooler technology is the University of Twente in the Netherlands [ter Brake, et al., 2011].

**JT Blockage.** Experience has shown that water vapor is the most common cause of blockage of a JT valve, even with oil lubricated compressors. Generally, moisture concentration must be less

than around 2 ppm to achieve long blockage-free operational periods [Bonney and Longworth, 1990]. The probability of blockage tends to increase for smaller systems with low flow rates, as the orifices tend to be smaller and the gas spends a greater time cold prior to reaching the JT valve, thus producing larger ice crystals. The shape of the JT restrictor is also important. A large-ID capillary tube is least prone to plugging, followed by an equivalent round orifice. The annular gap of a needle valve is worst. Systems with high flow rates and relatively large JT restrictions tolerate much higher levels of contamination. For long-lifetime systems, often an in-line getter is incorporated in the system to maintain the necessary low level of contaminant gases to prevent JT blockage over long operating periods [Bradshaw, et al.,1999].

**Integration Features.** From an integration point-of-view, the DC-flow nature of a JT system makes it easy to provide cooling at relatively large distances (many meters) from the compressor, thus minimizing exposure of the cryogenic load to compressor-generated vibration and electromagnetic interference (EMI). The long flow path also allows flexibility in packaging and integration. Cooling can be distributed over large areas or multiple cold heads. For applications where saturated liquid is generated, the pooled liquid can provide temperature stability and load-leveling for varying heat loads.

**Hybrid Coolers.** One means of achieving higher efficiency or lower temperatures is to pre-cool the JT gas stream using a second cooler, either a second JT cooler (as with the Planck cryocooler system), or another active cooler such as a Stirling, pulse tube, or GM, as with the JWST/MIRI cooler [Petach and Michaelian, 2014]. This can significantly reduce the temperature range required for the JT working fluid and significantly (by a factor of 10) reduce the operating pressures required of the JT compressor. The disadvantage of using multiple coolers is a somewhat lower level of reliability that may result from increased system complexity.

#### 6.3.4.4 JT Cryocooler Development History and Availability

An important downside of JT cryo refrigerators is their relative scarcity. The 4 - 6 K hybrid JT bottoming-stage units developed for the Planck and JWST MIRI space applications are one-of-a-kind custom units costing millions of dollars each and are not easily transferrable to other applications. However, in the area of commercial hybrid 4 K JT coolers, Sumitomo acquired the cryocooler and cryopump business of the Daikin company in 2005. One of the cryocooler products acquired was the line of Gifford-McMahon (GM) refrigerators with a Joule-Thomson (JT) third stage. Designed primarily for radio telescope astronomers, these three-stage cryocoolers, an example of which is shown in Fig. 23, have high cooling powers of up to 5 watts at 4.3 K as well as very stable temperatures at the third stage.



**Figure 23.** Sumitomo hybrid Gifford-McMahon/JT coldhead for 4K cooling.



**Figure 24.** Cryotiger 70 K JT cryocooler

In terms of commercial units providing 80 K temperatures, the Cryotiger developed by Ralph Longsworth of APD Cryogenics in the 1995 timeframe is one of the few commercial units available [Longsworth, et al., 1995; Longsworth, 1997]. The latest reincarnation of this cooler is now being sold by Brooks as their Polycold PCC cooler. This unit (shown in Fig. 24) uses a separate GM-type compressor with a remote cold head to achieve cooling powers of around 5 watts at 70 K using a mixed-gas refrigerant.

Another application of custom JT coolers has been for cooling cryogenic medical catheters and cryosurgical probes. Here, the small size of a JT cold end can be successfully integrated into the medical probe's tip while the compressor unit is external, some distance away [Dobak, et al., 1998; Marquardt, et al., 1998; Longsworth, 2002;].

### 6.3.5 Brayton Refrigeration Systems

A reverse-Brayton cycle cryocooler is a second type of recuperative or DC-flow cryocooler. However, it differs considerably from the JT cycle by using a high-flowrate, low-pressure-ratio refrigerant stream to produce cooling. As a result, it generally uses an entirely different type of compressor, a high speed gas turbine which operates at speeds of 100,000 to 600,000 rpm. Positive displacement compressors and expanders could also meet the functional needs of the cycle; however their mass and vibration characteristics tend to make them less desirable.

As shown in Fig. 25 the reverse-Brayton cycle schematic looks very similar to that of the JT cycle, but with the JT expansion valve replaced with a gas turbine expander. This turbine expander both expands the gas and withdraws some work from the gas; this provides near isentropic expansion as opposed to the isenthalpic expansion (constant energy expansion) used in the JT cycle. Because of the use of the turbine compressor and expander, the cycle is also commonly referred to as the turbo-Brayton cycle.

Unfortunately, like the JT cycle, the turbo-Brayton cycle is not particularly common in general cryogenic cooling applications. Its key advantages, like the JT cycle, are very low generated vibration and the ability of the compressor to be remotely located from the cold load. The low-mass turbine rotors are the only moving parts in the system, and because they are precision balanced and operate at very high rotational speeds (1000 to 10,000 revolutions per second), the systems generate extremely low levels of vibration. With the use of non-wearing gas bearings, they also tend to have high reliability for long-life applications. This is achieved by avoiding the oil lubricated compressors and oil stripping issues associated with common JT and GM systems.

The primary disadvantage of the turbo-Brayton cycle is its manufacturing challenges which are driven by the need for a very high construction quality to achieve competitive efficiencies. Both the tiny turbines and the recuperator must be designed and fabricated to very exacting standards if high efficiency is to be realized. Because of the issues with achieving the build precision required with very small turbine parts and high-effectiveness recuperators, the technology tends to be better suited to larger applications requiring several watts of cooling and requiring the unique features of an ultra-low-vibration, long life refrigerator.

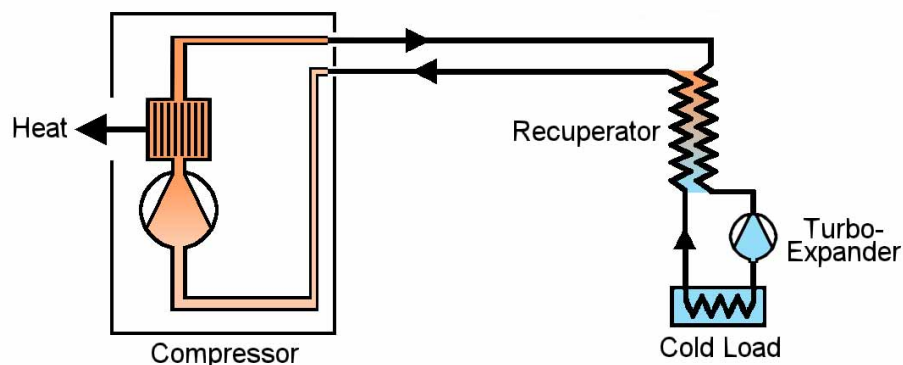


Figure 25. Turbo-Brayton cryocooler schematic.



**Figure 26.** Fully assembled turboalternator (left) and rotor assemblies (right) for 2 kW class turboalternator and 2 watt class turboalternator [Zagarola, et al., 2012].

Recent specialized uses of the turbo-Brayton technology include building a long-life, ultra-low-vibration cryocooler (the NICMOS cooler) for use on the Hubble Space Telescope, building a low vibration freezer for the International Space Station, and building helium liquefiers for large industrial-scale liquid helium applications.

#### 6.3.5.1 Engineering Aspects of Brayton Cycle Cryocoolers

Three factors influence the efficiency of a turbo-Brayton cryocooler: the speed of the compressor, the thermal effectiveness of the recuperator, and the precision of the small-scale turbine blades. A fourth key element of the cooler is the specialized electronics used to drive the compressor and control the cooler's operation.

**Compressor.** A typical turbo-Brayton compressor comprises a small-diameter, low-mass rotor with a centrifugal impeller at one end. This rotor is driven by a three-phase variable-frequency motor built into the assembly. Radial and longitudinal support for the rotor is commonly provided by self-acting gas bearings. The compressor assembly may also incorporate an integral heat exchanger to reject the heat of compression and motor losses to a suitable thermal interface

From a practical point-of-view, the pressure ratio that can be achieved depends primarily on the speed of the compressor. Mechanical features (centrifugal stresses, shaft dynamics, etc.) and gas properties (molecular weight, Mach number, etc.) constrain the maximum pressure ratio that can be achieved in a single compression stage to about 1.8 in neon and 1.26 in helium. Compression efficiency, on the other hand, is driven by the precision of the turbines and their internal losses, both of which result in an increasing proportion of losses as size is decreased.

**Expansion Turbine.** The expansion turbine provides the refrigeration to the cycle by expanding the gas from high pressure to low pressure; this reduces the temperature of the gas and also produces shaft work. This work may be used to drive a brake or an alternator; if the work is removed by a brake, the component is referred to as a turboexpander. If the work is converted to electric power, the component is a turboalternator.

To be reasonably efficient, the expansion turbines in small capacity machines must be extremely small as shown in Fig. 26. Rotational speeds are comparable to the turbo compressors, with speeds of 100,000 to 500,000 rpm. Self-acting gas bearings similarly provide radial and longitudinal support for the rotors, and the rotors must be balanced to a high degree of precision, resulting in vibration levels that are nearly undetectable.

**Recuperator.** The thermal effectiveness of the recuperator is also very critical to the refrigeration efficiency of the reverse-Brayton cycle. The recuperator's primary purpose is to efficiently precool the high-pressure gas flow between the compressor and the expansion turbine. Achieving the high thermal effectiveness values (greater than 0.99) that are typically needed to achieve competitive Brayton-cycle efficiencies requires very thoughtfully developed, highly optimized designs,

particularly given the low pressure-ratio and high flowrate of the reverse-Brayton cycle. The major contributor to ineffectiveness of the recuperator is generally the longitudinal heat conduction between its warm end and its cold end. Thus, a major consideration in the design of the devices is the reduction of axial conduction to the lowest practical value. Meeting these needs frequently results in the recuperator being the highest-mass device in the cooler system.

**Electronics.** The electronics of a turbo-Brayton cryocooler perform two functions. First, they convert power from the available power source to regulated, three-phase AC power at the multi-kilohertz drive frequency of the centrifugal compressor. To achieve high overall cryocooler electrical efficiency, a key driver on the power supply design is achieving high electronic conversion efficiency. A second key function of the cooler's electronics is to provide the control functions needed to operate the cooler system. A key one of these is to adjust the frequency of the compressor drive (i.e. the turbine speed) to increase or decrease the pressure ratio. This increases or decreases the available refrigeration to allow control of the cold-load temperature to correct for possible changes in the heat-rejection temperature or variations in the cold load.

Both of these processes (power conversion and control) tend to be highly specialized functions that lead to carefully optimized, highly customized electronics [Konkel and Bradley, 1999].

### **6.3.5.2 Turbo-Brayton Cryocooler Development History and Availability**

Turbo-Brayton cryogenic expanders have been under development for many years, starting in the late 1950s and early 1960s [Sixsmith, 1984]. In the early 1970s, under DoD sponsorship, large DoD contracts to General Electric and Garrett AiResearch were made to develop high capacity 12 K cryocoolers for military space reconnaissance applications [Ross, 2007]. The original system goal for the GE unit was for cooling loads of 1.5 W at 12 K plus 30 W at 60 K, with a 30,000 hour lifetime and a maximum power consumption of 4 kW [Sherman, 1982]. The Defense Advanced Research Project Agency (DARPA) initiated a follow-on turbo-Brayton program in 1978 with Garrett AiResearch [Harris, 1981]. This system was designed, fabricated and performance tested in the early 1980s. Although, it exhibited satisfactory operation, contamination and other issues prevented performance goals from ever being fully reached.

**Creare Coolers.** In the early 1980s Creare, Inc. in Hanover, NH began work on critical elements of smaller turbo-Brayton systems for both the DoD and NASA applications. These activities eventually led to the development of a successful engineering model cooler [Swift and Sixsmith, 1993; Dolan, et al., 1997] and to eventual selection of Creare to build a very low vibration turbo-Brayton cooler to cool the NICMOS instrument on the Hubble Space Telescope. This cooler was designed to replace the instrument's 65 K solid-nitrogen dewar, which was severely degraded during launch in 1997 [Miller, 1998b]. This NICMOS turbo-Brayton cooler, which was installed by astronauts on orbit in March 2002, worked exceptionally well providing around 7 watts of cooling at 77 K to the NICMOS instrument over the next 7 years [Swift, et al., 2008]. The cryocooler refrigerant gas in the NICMOS cooler is neon at a nominal pressure ratio of 1.6:1. The inlet pressure to the compressor is 1.5 atm and the compressor operates at variable speeds up to 440,000 rpm. Under these conditions, the input power to the compressor is 315 W at a rejection temperature of 280 K. [Swift, et al., 2008].

Since the NICMOS instrument development and launch, Creare has been developing a number of additional advanced turbo-Brayton technologies focused on future NASA and DoD cooler opportunities, both smaller than and larger than the NICMOS cooler [Zagarola, et al., 2012].

**Air Liquide.** In Europe, Air Liquide has developed, qualified, and delivered a reversed turbo-Brayton cooler for the  $-80^{\circ}\text{C}$  MELFI freezer on the International Space Station (ISS) in 2006 [Ravex, et al., 2005]. The MELFI cooler, like the Creare NICMOS cooler, is based on high-speed turbo machinery supported on gas bearings, and carrying the compressor and expander turbine wheels. For 840 W of electrical power the unit is designed to provide 60 W of cooling at 178 K, and for 1000 W input power to produce 90 W at 178 K. The mass is 8.5 kg.

Air Liquid, like Creare, is also actively expanding its base of turbo-Brayton technologies to support additional future missions on board scientific satellites. One key focus is on turbo machines for applications of around 110 mW in the 2 to 5 K temperature range.

## 6.4 Cryogenic Cooling System Design and Sizing

The intent in this section is to cover some important aspects of cryogenic cooling system design that are generic in nature, and thus applicable to any cooling means, passive or active. Section 6.5 will then expand on a number of cryocooler-specific considerations associated with integrating with active cryocoolers. In general, the cryogenic system design process includes a number of iterative steps:

- 1) Derive a strawman cryogenic system design including rough estimates of all key parameters such as geometric sizes, power dissipations and active cooling loads, and candidate cooling approaches.
- 2) Estimate the total cooling load over the system's total operating range and life including both active loads and passive parasitic loads
- 3) Acquire performance data for the candidate cooling approaches for the full range of projected cooling loads, cooling temperatures, and external environmental temperatures
- 4) Iterate the cryogenic load projections with the cooler performance projections to achieve a successful cooling system design
- 5) Validate the design with detailed calculations and engineering tests.

Unfortunately, for many cryogenic applications, parasitic loads, which typically carry large uncertainties, often represent 80% of the total load. Thus, it is best to apply large conservative margins for these poorly predictable loads during the design process and to implement a process to "burn down" the uncertainties as the design progresses toward the final implemented system. This process of resolving the uncertainties over time to lower the risk of poor system performance or the cost of excessive conservatism is a critical part of the cryogenic system design process.

### 6.4.1 Cryogenic Load Estimation and Management

Generally, one of the most important and difficult tasks in cryogenic system design is establishing what the expected cryogenic loads are going to be and what the primary drivers are in determining the loads. Knowing the load drivers allows emphasis to be focused on these specific areas of the design and to perhaps integrate in additional cooling stages to carry some of the loads at higher temperatures, or to refine specific load estimates or reduce them through experiments or technology developments. It is also important to recognize that the total range of loads that can be efficiently provided at a given temperature by a given cryogenic cooling system is generally not much greater than a factor of two. Therefore, in practical terms, the cooling system design must be matched to the load early in the design process with relatively good accuracy, that is, better than a factor of two. Achieving a proper match between system design and load, and maintaining the match over a multiyear project development cycle is an important integration challenge faced by cryogenic system engineers.

To estimate the cryogenic load it is essential to address a number of key issues. These include:

- 1) Accurately estimate the active part of the cryogenic load and the rough details of the overall cooling system configuration. By active loads we mean the loads other than parasitic conduction and radiation loads. An example would be direct electric power dissipation by focal planes, motors, electronics, etc at the cryogenic temperature. Other active loads would be the cryogenic load associated with liquefying gases or cooling a fluid as part of the cryogenic application.
- 2) Estimate any conduction loads associated with connecting the application to the outside world. Connection parasitics include conduction down electronic wires from outside the cryogenic application or conduction down tubing and pipes from the cryogenic stage to

outside the application. Wiring and harness loads can often be large contributors to the cryogenic load if very special low-conductance wiring is not employed.

- 3) With the proposed system configuration in mind, attempt to accurately estimate the total parasitic conduction loads associated with structurally supporting the application. These are often difficult to estimate without at least a conceptual structural design and estimates of any applied structural loads such as vibration and handling during transportation to the application site. Helpful tips on estimating structural conduction loads are presented below in Section 6.4.2.
- 4) As with the conduction parasitics, attempt to estimate the total parasitic radiation loads absorbed by the application from the external thermal environment. These are often the most challenging to accurately quantify, as radiation loads are a strong function of the surface emittance of application materials, and these emittances can have very large uncertainties and change over the life of an application. Background on the prediction of radiation loads and MLI performance is presented in Section 6.4.3.

### 6.4.2 Estimating Structural Support Thermal Conduction Loads

For structural support conduction there are four key issues: (1) achieving a high strength and low thermal conductivity structural support design using low conductivity, high strength materials such as stainless steel, titanium, fiberglass, and Kevlar, (2) supporting the assembly from an intermediate-temperature support to reduce the  $\Delta T$  across the support structure, (3) using vacuum insulation systems to avoid gaseous conduction loads, and (4) minimizing the mass and size of the assembly to reduce the structural loads that the supports must carry.

In a relatively mature design, the conduction loads can be computed with good accuracy based on the design details and the relatively well known conductivity properties of common cryogenic

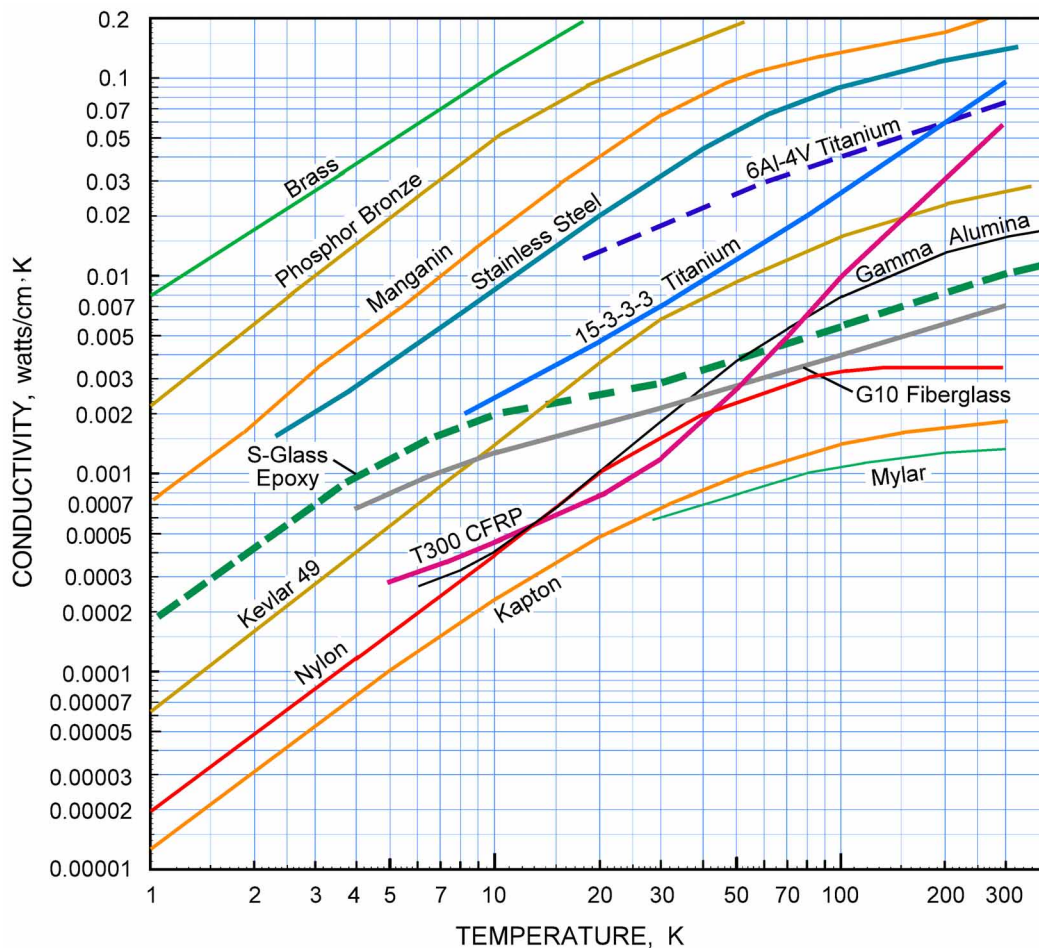


Figure 27. Thermal conductivity of common cryogenic structural materials as a function of temperature.

structural materials; representative properties of common low-conductance materials are shown in Figure 27. The most structurally and thermally efficient structural designs are generally ones that use structural members in pure axial tension and compression and minimize loads carried in bending.

#### 6.4.2.1 Load Estimating "Rule of Thumb"

Unfortunately, early in an application's conceptual design, details of the design don't yet exist, and what is needed are some generic "rules of thumb" for estimating overall support conductance in terms of the  $\Delta T$ s involved, the candidate structural materials, and the supported masses. Such a load estimating algorithm has been developed for space applications, based on examining a wide variety of flight-proven space-instrument designs with cryogenic structural supports [Ross, 2004]. The developed rules account for the known relationships between material conductivity and temperature, between launch acceleration level and assembly mass, between launch acceleration loads and required support-member cross-sections, and between support-member cross-section and conductive thermal load.

Although, these estimates were generated for space applications with typical launch loading environments, they should also be useful for estimating conductive loads for systems subject to common transportation loads, and may serve as useful bounds for stationary laboratory facilities, as often considerations of structural robustness may lead to similar design-load levels.

The general relationship derived for predicting cryogenic structural conduction loads is given by

$$Q \approx \bar{A} \kappa m^{0.66} \Delta T \quad (6)$$

where

- Q = Conductive load being estimated (watts)
- $\bar{A}$  = Empirical scaling factor = 0.02 (very efficient structures) to 0.27 (less-efficient)
- $\kappa$  = Average conductivity of support material in temperature range  $\Delta T$  (watts/cm $\cdot$ K)
- m = Mass of supported assembly (kg)
- $\Delta T$  = Differential temperature across support structure (K)

The empirically derived constant  $\bar{A}$  in Eq. (6) reflects how efficiently the structural materials are used in the design. Thus, a lower value ( $\bar{A}=0.02$ ) correlates with axially loaded structures using high strength materials such as a tension band system, while a higher value ( $\bar{A}=0.27$ ) is used for structures using members in bending, like a cantilever-type structure, or one using lower strength materials. Notice, that the range from 0.02 to 0.27 reflects an order of magnitude difference between the structural conduction loads of a highly efficient structural design and those of a satisfactory, but inefficient design.

#### 6.4.2.2 MLI and Gold Plating Lateral Conductivity

Because of the relatively high thermal conductance of MLI blankets when compared with low-conductivity structures, one needs to be particularly sensitive about allowing MLI to thermally bridge between two components or surfaces with substantially different temperatures. This is true for conduction through the thickness of an MLI blanket, and is even more true for heat transfer parallel to the blanket surface. The aluminized layers of MLI have quite high lateral conductivity and can seriously deteriorate the thermal resistance of low conductance structural supports upon which they might be wrapped. In a similar vane, gold plating to achieve a low emittance surface on a low conductance structural members can substantially deteriorate their thermal resistance.

#### 6.4.2.3 Vacuum Requirements to Minimize Gaseous Conduction

To achieve low thermal conduction loads it is invariably necessary to eliminate gaseous conduction and convection heat transfer from the ambient environment into the cold load. Thus, nearly all cryogenic applications incorporate vacuum insulation systems and must be mounted in vacuums that achieve levels of at least  $10^{-4}$  torr. For applications striving for very low conduction rates and elimination of condensation on cold low-emittance surfaces, much better vacuum levels are required.

Gaseous conduction ( $Q$ ) between surfaces surrounded by gas in the free-molecular regime is independent of the gap spacing, and linearly dependent on the temperature difference ( $\Delta T$ ) between the surfaces, on the pressure of the gas ( $P$ ), and on the surface area of the cold object ( $A$ ). Thus:

$$Q \propto A P \Delta T \quad (7)$$

Additional parameters that affect the proportionality relate to the specific heat transfer properties of different gases, which can vary somewhat with temperature. Useful estimates for gaseous conduction loads for various vacuum levels are presented later in Fig. 28 in Section 6.4.3. These are for free-molecular conduction through a He / H<sub>2</sub> mixture likely to exist at cryogenic temperatures and for representative temperature differences between surfaces. For more exact calculations for specific system designs, one should appeal to the equations governing thermal conduction through free-molecular gases as described in cryogenic heat transfer texts such as [Scott, 1988].

### 6.4.3 Estimating Thermal Radiation Loads

Estimating thermal radiation loads often poses the largest challenge to the cryogenic systems designer trying to predict cryogenic loads over multiyear operational periods. This is because radiation loads increase as the 4th power of the radiating temperature—making loads very sensitive to temperature predictions — and are also directly proportional to the surface emittance properties of cryogenic surfaces, which can vary by two orders of magnitude. Low emittance gold-plated and polished-aluminum surfaces and Multi Layer Insulation (MLI) have very low effective emittance values and are commonly used to minimize radiant heat transfer.

MLI is constructed of layers of aluminized Mylar or Kapton separated by low-conductance spacers or stippled surfaces that are designed to minimize heat conduction between adjacent shield layers. The spacer layers also have the important function of providing for the evacuation of residual gas from between the shield layers when vacuum is applied. Although the spacer features minimize the contact between the low-emittance shields, the result is still a relatively high degree of heat conduction through a typical MLI blanket when compared with low-power cryogenic loads.

A key difficulty in estimating thermal radiation loads is that the heat transfer properties of MLI are not easily addressed using analytical models because the effective emittance is strongly affected by a number of physical parameters such as contact pressure between the layers and the level of thermal conductance that results. To eliminate gaseous conduction and surface contamination, MLI and low-emittance shields must also be mounted in a low-pressure vacuum space.

#### 6.4.3.1 Radiation Heat Transfer in Cryogenic Applications

To help understand the behavior of radiation heat transfer in cryogenic applications, it is instructive to examine the heat transfer properties of various surfaces and MLI that have been measured in extensive studies conducted in support of the development of early spacecraft and ground cryogenic applications [Johnson, W.R., 1974; Kutzner, 1973]. Heat transfer measurements from these and other studies have been summarized by [Nast, 1993] and reduced by this author into a single plot (Fig. 28) so that comparisons and conclusions can be more readily drawn.

At the highest level, Fig. 28 plots total heat transfer between a hot enclosure of temperature ( $T_{Hot}$ ) and a cold surface that is enveloped by the hot enclosure. A central feature of the plot is the bold line labeled "SLI Radiation Heat Transfer." This line describes the radiation absorbed by a Single-layer Insulation (SLI) cold polished aluminum surface from a facing hot-side surface with temperature ( $T_{Hot}$ ) that has an emittance of unity (the typical case for a small cold object in a large hot enclosure); it is also assumed that the cold surface is cold enough that reradiation from this surface is negligible compared to the heat absorbed from the hot surface (the usual case).

The SLI bold line follows the relationship ( $P \propto T^{4.67}$ ), where the  $T^{4.67}$  term includes the classic ( $P \propto T^4$ ) relationship for radiation heat transfer plus the relationship between the emittance of aluminum and temperature ( $\epsilon \propto T^{0.67}$ ) as described in [Nast, 1993]. In reality, this "emittance" is actually the infrared absorptance of the cold surface to the wavelengths emitted by the hot surface. Since emittance equals absorptance at any given temperature, the IR absorptance of the cold surface is computed as the emittance of the cold surface at the hot-side temperature ( $T_{Hot}$ ).

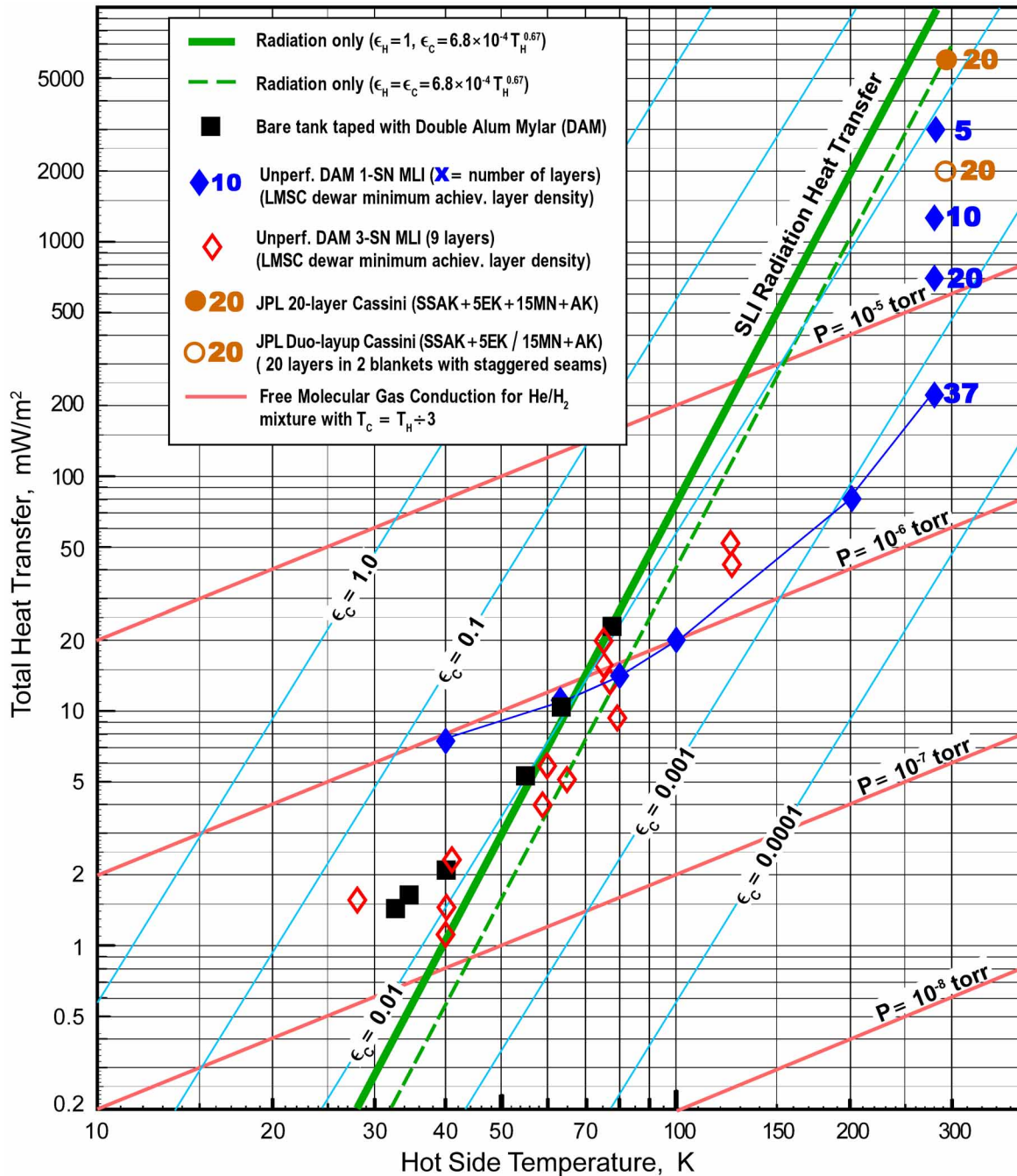


**Figure 28.** Radiation heat transfer to a cold polished aluminum body and through various MLI formulations as a function of hot-side temperature. Also shown are contours of constant emittance and background gas pressure.

The resulting  $P \propto T^{4.67}$  relationship for radiation heat transfer as a function of temperature is a fundamental part of the classic Lockheed MLI equation widely promoted in the literature. The position of the bold line in the plot corresponds to an emittance (infrared absorptance for room temperature radiation) of 0.031, the consensus value used for 300 K aluminum MLI surfaces. Lines of constant effective emittance are also drawn on the plot, roughly parallel to the bold line for SLI heat absorptance. The bold SLI line drops faster, reflecting the drop in emittance ( $\epsilon \propto T^{0.67}$ ) with temperature. The dashed line (parallel to the bold line) denotes the heat absorbed by the cold surface when the hot and cold surfaces are closely spaced, parallel, and both have the emittance of polished aluminum.

#### 6.4.3.2 Room-Temperature MLI Performance

Also plotted in Fig. 28 for  $T_{\text{Hot}} = 300$  K, are measured property data for a variety of room-

temperature MLI constructions. By room-temperature we mean MLI designed for a hot-side temperature near 300 K where heat fluxes are quite large. This is the typical MLI discussed in heat transfer texts and must be carefully distinguished from that used in cryogenic applications with much lower hot-side temperatures.

In general, MLI comes in two distinct designs, that designed to be self supporting and attached to the outside of an application, and that captured in the internal vacuum space of a dewar. For dewar MLI, the layers are individually stacked with minimal pressure pushing them together; this minimizes the thermal conduction through the MLI stack. In contrast, self-supporting, external MLI, which is usually sewn together, tends to have much higher conduction, and thus has substantially poorer performance than dewar MLI.

Plotted in Fig. 28 are measured heat transfer data for Lockheed's best (maximum loft) dewar MLI (solid diamonds) [Nast, 2003] and JPL's traditional sewn-through spacecraft MLI (solid circular bullet) [Lin, et al., 1995]. Note that the 20-layer JPL sewn-through MLI has 10x higher heat transfer than the 20-layer dewar MLI.

As one means of reducing the spacecraft MLI emittance, note that two sewn-through half-blankets with staggered seams (open circular bullet) provides a 3x improvement over a single sewn-through blanket with the same total number of layers [Lin, et al., 1995].

#### **6.4.3.3 MLI Performance at Cryogenic Temperatures**

Next, consider the MLI data in Fig. 28 for hot-side temperatures of 100 K and below. As the hot-side temperature decreases, the radiation heat transfer drops by  $T^{4.67}$  and the conduction term only drops linearly (proportional to  $T$ ). The net result is that conduction through MLI becomes a critical issue at cryogenic temperatures. This relatively high conductivity at cryogenic temperatures is compounded by any compressive pressure or blanket bending that squeezes the layers together.

For hot-side temperatures below around 100 K, most of the advantage of the multiple layers of even fluffy dewar MLI is lost (see plot data for the 37-layer Lockheed MLI). As a result, Lockheed formulated a special cryo-temperature dewar MLI for hot-side temperatures below 100 K (open diamonds). This MLI has only nine aluminized layers and uses three silk nets between each layer to further minimize the conduction between layers. However, even this cryo-MLI leads to only a marginal improvement over just a single low-emittance aluminized surface (black squares) below around 77 K. At the lowest hot-side temperatures, say below 50 K, MLI is often replaced by just bare low-emittance surfaces, as they exhibit comparable or better performance than even the best low-conductivity cryo MLI. If one has to use sewn-through construction for cryo-MLI for an external-surface application, the MLI is likely to act essentially as a single-layer shield (SLI) at cryo temperatures. Or, if the MLI doesn't maintain a smooth surface, its emittance can be much (10x) worse than that of a single well-polished low-emittance surface.

#### **6.4.3.4 Effect of Vacuum Pressure on MLI Conductance**

In viewing the measured data for the cryo-MLI in Fig. 28, it is seen that the data begin to diverge and rise above the bold SLI line for hot-side temperatures below about 50 K. When gas conduction effects are examined (see the heat transfer lines in Fig. 28 for various vacuum pressure levels), it is seen that these gas-conduction effects correlate quite well with the observed flattening of the measured MLI heat transfer. This suggests that gas conduction is beginning to dominate the heat transfer at these temperatures. In general, operational vacuum environments rarely achieve pressures much below  $10^{-6}$  to  $10^{-7}$  torr, and this pressure correlates quite well with gaseous-conduction heat transfer becoming comparable to and even exceeding radiation heat transfer at hot-side temperatures below 50 K.

#### **6.4.3.5 Effects of Contaminants on Emissivity**

The aluminum emittance properties detailed in Fig. 28, are for hyper-clean, smooth polished surfaces. When a surface becomes contaminated with an external high-emittance substance such as a thin film of water ice, the emittance of the surface increases rapidly. Figure 29 highlights the sensitivity of surface emissivity to the thickness of common contaminants [Viehmann, W. and

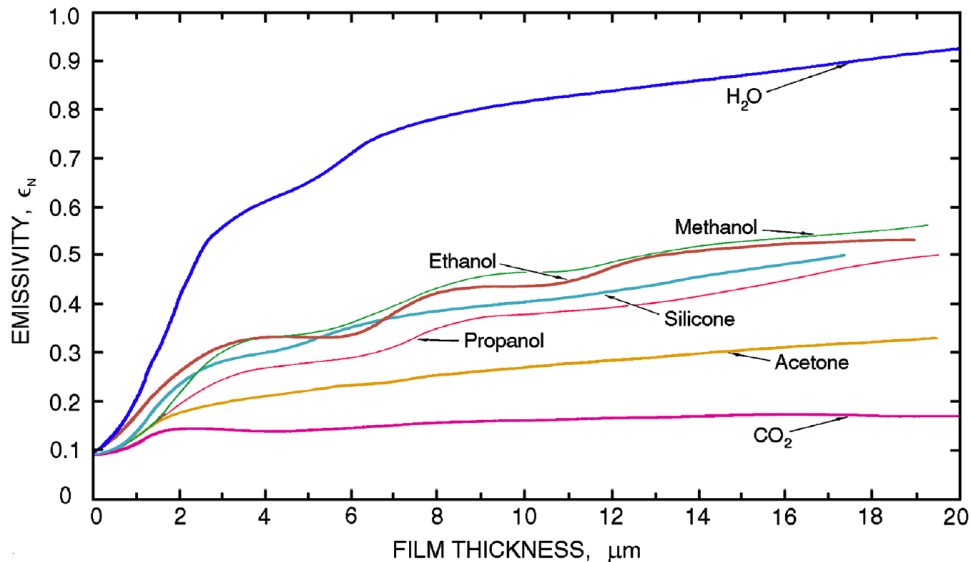


**Figure 29.** Emissivity of polished stainless steel to 300 K blackbody radiation versus film thickness.

Eubanks, 1972]. Note that just a one micrometer deposit of water ice will more than double the emittance (IR absorptance) of a low-emittance surface. Figure 3, presented earlier in this chapter, provides data on the allowable maximum pressure levels to prevent condensation of various common gases. Means of computing the rate of buildup of contaminant films are provided by [Ross, 2003a]. Such computations are useful to gage the required vacuum level for the interior of vacuum insulation systems and the expected rate at which radiation loads can be expected to build up.

One means of maintaining and improving the vacuum level achievable is to incorporate getters into the vacuum space. A wide variety of getter materials are available that can sorb all active gasses such as  $\text{H}_2$ ,  $\text{O}_2$ ,  $\text{H}_2\text{O}$ ,  $\text{CO}$ ,  $\text{CO}_2$  and  $\text{N}_2$  by a chemical reaction under vacuum [Saes, 2007]. Depending on the final application and the production processes, different getter metallic alloys and shapes have been developed. These are used to pump out residual gases that remain in, or develop in the vacuum space over time.

Once contaminated, the well-established approach to deal with radiation shield or MLI degradation is to periodically boil off the contaminants by heating the cryogenic surfaces to near room temperature. However, this deep thermal cycling can be very stressful to other cycled components. To minimize and limit the amount of decontamination cycling, it is prudent that the cryogenic system designer develop a robust system design that is able to accommodate predicted cryogenic load increases due to radiation property degradation over the life expectancy of the application as well as having margin for other degradation mechanisms.

#### 6.4.4 Coldlink Design and Integration Considerations

As part of the cryogenic system design process, there is another set of integration issues that are both thermal and structural. These relate to how the cryogenic cooling source is attached to the cold application. The mechanical attachment to the load is often referred to as the coldlink. This assembly is typically a highly optimized, multi-discipline, thermal-mechanical device designed to transmit heat efficiently at cryogenic temperatures, but to also carry out many other functions.

Important cold-link design considerations include:

- 1) Minimizing the  $\Delta T$  between the cryogenic load and the cryogen or cryocooler
- 2) Providing flexibility to accommodate differential motions between the cold load and the cooler cold-load interface
- 3) Minimizing parasitic conduction and radiative parasitics into the coldlink assembly including the effects of surface contamination of low-e surfaces

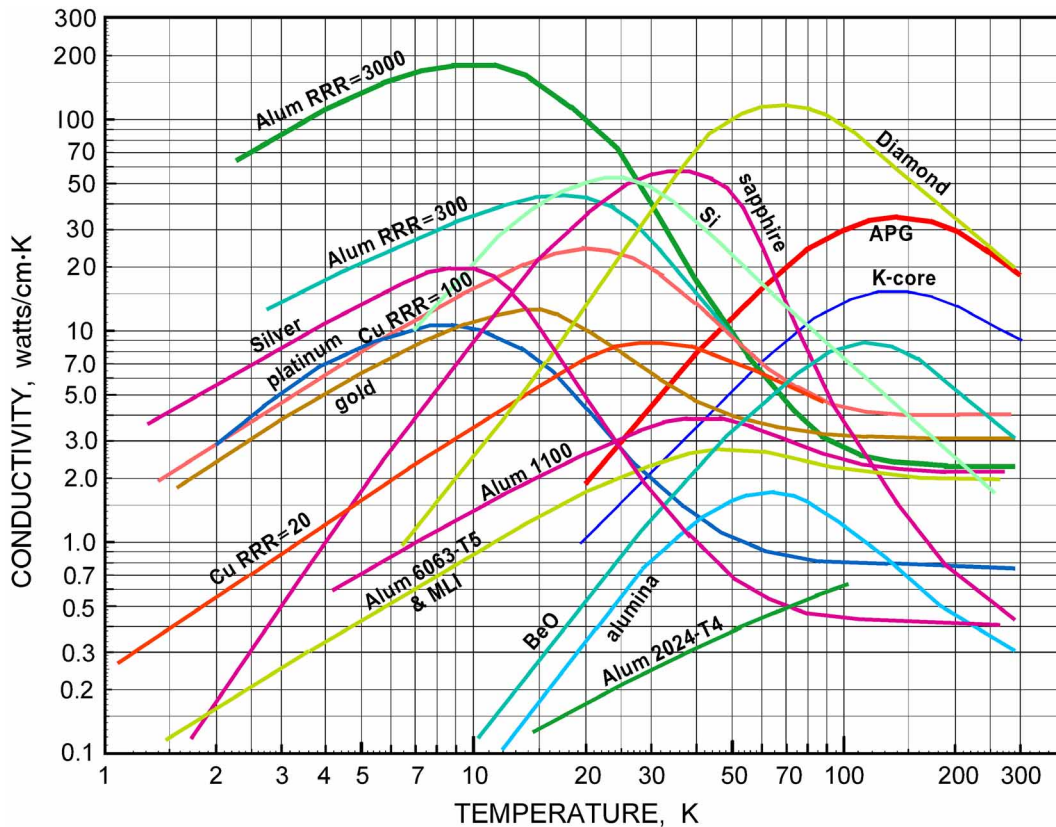


**Figure 30.** Thermal conductivity of common high-conductivity materials as a function of temperature.

- 4) Providing for easy attachment and removal of the load from the cooler, or vice versa
- 5) Providing for active temperature control of the cold load
- 6) Providing for measurement of the cryogenic load for system diagnostics

Although one's initial focus may be on the coldlink's thermal design issues, the structural issues associated with the coldlink are inseparable and must be fully integrated into the design so that a complete multi-discipline solution of the integrated problem is achieved.

#### 6.4.4.1 Coldlink Thermal Conductance

The primary requirement of any coldlink is to conduct heat between the cold load and the cryocooler interface with minimal thermal drop. One means of doing this is to utilize very high conductivity materials in the primary heat conduction path, especially materials that have improved thermal conductivities at cryogenic temperatures. Example materials include high-purity copper and aluminum, silver, and single-crystal materials like sapphire and silicon. As shown in Figure 30, the versions of aluminum and copper that exhibit very high conductivity are those that are exceptionally pure as reflected in the material's high Residual Resistivity Ratio (RRR). Common materials, such as OFHC copper and 1100 aluminum, have RRR values around 20; these have good conductivity, but not the exceptional conductivity of the hyperpure materials. A point to be drawn from these curves is that hyper pure and single-crystal materials can have very high cryogenic conductivities, but their conductivity is also likely to be extremely sensitive to small levels of impurity elements and crystalline imperfections, such as those acquired from cold working. Measuring the actual conductivity of any high-conductivity materials that are to be used is highly recommended.

As an example use of single-crystal sapphire to achieve exceptionally high conductivity, Fig. 31 shows the coldlink assembly of the AIRS instrument that conducts heat from the instrument's 58 K focal plane array to its pulse tube cryocoolers [Ross and Green, 1997]. An important point is that when using high-conductivity materials, one must pay particular attention to interface resistances that can often dominate the total thermal resistance of the coldlink assembly. These are the attach-



**Figure 31.** AIRS focal plane/cryocooler coldlink assembly with sapphire rod conductor.

**Table 4.** Breakdown of AIRS coldlink assembly thermal resistances

ITEM	Resistance (K/W)
Focal plane to Sapphire rod	1.57
Conduction down Sapphire rod	0.16
Sapphire rod to moly coupling	0.34
Resistance across shrink-fit joint	0.40
Resistance across flex braid	1.35
Coldblock contact resistance	0.30
<b>Total focal plane/pulse tube thermal resistance</b>	<b>4.12</b>

ment resistances between cooler and flex element, between the flex element and primary conductor, between the primary conductor and load, etc. As shown in Table 4, these various attachment resistances and flexbraid assembly greatly exceed the resistance of the sapphire rod in the AIRS coldlink.

#### **6.4.4.2 Providing Flexibility to Accommodate Differential Motions**

A prominent part of nearly all coldlinks is a flexbraid or S-link assembly such as that shown at the left end of the cold link in Fig. 31. Such a flexible coupling is invariably required to limit structural loads transmitted into the cryocooler or the cryogenic payload due to differential motions between the two. These differential motions can be caused by dimensional differences during assembly, by thermal contractions during cooldown, and by relative motions during transportation or launch. The level of flexibility required is specific to the payload and cooler design; however, typical devices achieve structural stiffnesses around 1 - 3 N/cm (0.5 - 1.5 lbs/in), and thermal resistances around 1 - 2 K/W [Sugimura et al.,1995; Williams et al., 1997; Arentz et al., 1995; Kawecki, 1995]. A common design requirement on the flexlink assembly is to maintain the sideloads on the cryocooler's coldfinger below the level that would cause excessive side deflection, or rubbing and wear of any internal moving elements. This is particularly true for Stirling and GM cryocoolers, which have a tight-tolerance moving displacer internal to the coldfinger.

#### **6.4.4.3 Minimizing Cold Link Support Conduction and Radiative Loads**

Minimizing parasitic conduction to the coldlink and radiative loads onto its surfaces, including the effects of surface contamination, are an important element of the design of the coldlink assembly. Candidate materials and a load estimation algorithm for achieving low conductance structural supports were highlighted in Section 6.4.2. However, a key point is minimizing the mass of the coldlink assembly as much as possible to reduce the structural loads that the supports must carry.

This is where the use of lightweight conductor materials such as aluminum and sapphire pays off.

Maintaining a low emissivity (low IR absorptivity) on the coldlink surfaces is another priority so as to reduce radiation parasitics. Polishing and gold plating cold link surfaces, such as the gold plated sapphire rod shown in Fig. 31, is very useful. Flexible elements typically create a greater challenge, as their multilayer makeup typically gives them a naturally high IR absorptivity. These are best wrapped with low-emissivity Single Layer Insulation (SLI) such as gold or aluminum vapor deposited on Kapton or Mylar.

#### **6.4.4.4 Providing for Easy Attachment and Removal of the Cold Load**

With many cryogenic applications, gaining access to fasteners to allow installation and removal of the load from the cooler can be a difficult design issue. This is often resolved by providing a no-fastener blind mating between the cooler and the cold load by including a shrink-fit joint in the coldlink assembly. For example, the joint can be composed of an outer ring made of a high coefficient of thermal expansion (CTE) material and a central low-CTE cylinder that is mounted to the mating half of the joint. The differential thermal expansion between the outer ring and the inner cylinder provides an easy slip fit between the two at room temperature, and then a low- $\Delta T$  rigid coupling at cryogenic temperatures. Work has been done over the years on pairs of materials that have the necessary high CTE difference and are resistant to cold welding between the mating elements. Classic material pairs include beryllium with copper and aluminum with molybdenum — as is used in the AIRS coupling shown in Fig. 31 [Ross and Green, 1997]. To get repeatable performance requires careful selection of the gap between the two materials, and a high-quality surface finish on the mating surfaces.

A second area of cold load attachment often involves the use of a soft metal gasket such as indium to improve interfacial conduction in a bolted joint. After a period of time, such a joint can become diffusion bonded to some extent and become very difficult to remove without exerting large forces. One means to allow large detachment forces to be applied in a way consistent with the fragility of many coldlink assemblies is to incorporate jack screws into the cold interface. Such screws allow one face to be carefully pried away from the other by tightening the jack screws.

#### **6.4.4.5 Providing for Active Temperature Control**

Many cryogenic applications require very tight regulation of the cold load temperature, often down to the milliKelvin level. To achieve very tight temperature regulation, one can couple the cold load to the cooler using a passive thermal filter involving combinations of thermal masses and thermal resistances. Another common approach is to provide active temperature control via a small heater on the cold load.

A third approach to coldload temperature control is to use the variable cooling capability of the mechanical cryocooler to control the temperature via closed loop control of the cryocoolers drive level. This latter approach has been used for many years in small tactical military Stirling coolers to provide rough ( $\pm 1$  K) control of coldtip temperature. In the 1990s this means of temperature control was expanded into space Stirling and pulse tube coolers to provide precise milliKelven control for space-instrument focal plane temperatures [Clappier and Kline-Schoder, 1994]. This form of control does not add to the coldend heat load, and is commonly available as a feature of many of today's Stirling and pulse tube cryocoolers.

#### **6.4.4.6 Providing Measurements for Troubleshooting**

Quantifying cryogenic system cooling performance during system-integration is an important aspect of system operation and troubleshooting. Invariably, during cooler operation, performance deviates from predictions due to a wide variety of reasons including manufacturing and thermal property variabilities and better definition of the actual application cryogenic loads.

To efficiently focus corrective actions, it is extremely useful to be able to quickly separate cryocooler performance issues from various load-related issues. One means of doing this is to provide a means of directly measuring the cryogenic load at the cooler attachment interface. This can often be done by adding a second temperature sensor to the opposite side of the flexlink ele-

ment from the cooler coldtip. When combined with the coldtip temperature sensor this allows the differential temperature drop across the flexible link to be used as a measure of the heat conduction through the flexlink. The flexlink element can be easily calibrated by using a resistive heater on the cryogenic load side of the interface during cooler ground characterization testing. Because the thermal conductivity of the flexlink will vary with temperature, the calibration needs to be mapped over the temperature range of interest.

## 6.5 Cryocooler Application & Integration Considerations

In the previous section (6.4), generic topics of cryogenic system integration were discussed. However, when a mechanical cryocooler is used as the primary cooling instrument, a number of additional cryocooler-specific integration considerations become important. These include things to do to best take advantage of cryocooler-unique capabilities, things to do to prolong the life and health of the cooler, and things to do to minimize the impact of less desirable cooler-generated environments.

Key cryocooler-specific integration topics include:

- 1) Providing for removal of the cryocooler's rejected heat with acceptable thermal gradients. This includes such things as understanding the amount and distribution of heat rejection between the compressor and expander heat rejection interfaces and understanding the dependence of cryocooler cooling performance on its heat sink temperature.
- 2) Providing structural support to hold and align the cryocooler in its intended application. The mounting structure must address both gravity mounting loads, differential expansion cool-down loads, and transportation loads if the application is to be transported to its final destination. The structural design must also limit the maximum static and dynamic displacements that will be transmitted into the cryocooler's coldend flexbraid assembly and prevent warping loads that would distort or destroy the tight clearances and alignments of the cryocooler's sensitive piston and/or displacer mechanisms
- 4) Managing cryocooler-generated vibration and minimizing any negative interactions between the cooler-generated vibration and the cryogenic application. This includes providing for the measurement of the cryocooler vibratory response either through the use of accelerometers or load cells; these measurements are often an integral part of a Stirling or pulse tube cooler's closed-loop vibration suppression system
- 5) Managing the electrical interfaces with the facility power source and managing the effects of any cryocooler-generated ripple-currents on the input power bus or radiated electromagnetic interference (EMI).

### 6.5.1 Cryocooler Thermal Interfaces and Heatsinking Considerations

Integrating cryocoolers into a cryogenic system involves four key heatsinking/thermal issues, plus some consideration of cryocooler internal parasitic loads and their sensitivity to gravity orientation:

#### 6.5.1.1 Managing Compressor and Expander Heat Rejection

By their nature, cryocooler compressors draw and thus must dissipate a significant amount of power — typically >100 watts for modest size units and kilowatts for larger machines. Since the efficiency of a cryocooler strongly depends on its heatsink temperature, a fundamental design trade-off involves increasing the thermal-system size, mass and complexity to avoid large temperature gradients that increase heatsink temperature and degrade refrigeration performance. Overall, the performance sensitivity closely follows the generic Carnot equation and results in the coldend rising approximately 1 K in temperature for each 5 K rise in the cryocooler heatsink temperature [Ross and Johnson, 1998].

Most cryocoolers prefer to operate in the -20°C to +40°C temperature range, with non-operating temperatures in the range -40°C to 60°C. This temperature range is limited by constraints imposed by the cooler's precision mechanisms, electronics components, and internal construction materials. Often a heatsink temperature around 0°C is considered ideal, but such a low tempera-

ture is often not feasible from a system mass/temperature trade-off point-of-view. In the end, most cryocooler systems end up requiring a very robust heat-rejection system to achieve the necessary temperature control and heatsink temperatures of around 20°C. As a result, a key lesson learned is to address the heat rejection system early and thoroughly during the cryogenic system thermal design.

### **6.5.1.2 Spatial Distribution of Rejected Heat**

Given the strong sensitivity to heatsink temperature, understanding where the heat is dissipated is critical to the heatsink design process. Generally, the primary source of the power that must be rejected by a cryocooler comes from the electrical power input to its compressor. In addition, there is a small amount of heat that is absorbed from the cryogenic load. However, for regenerative cryocoolers (e.g., pulse tube and Stirling coolers) a significant fraction (25% to 50%) of the power input to the compressor is rejected at the hot end of the expander rather than at the compressor. The division of heat between the compressor and expander is also influenced by the relative temperatures of the two. If the compressor and expander are run at different temperatures, heat dissipation will shift toward the colder of the two [Kotsubo, et al., 1992; Johnson and Ross, 1994].

GM, JT and Brayton cryocoolers, on the other hand, tend to dissipate all their heat at the compressor. In summary, for sizing heat-rejection systems and calculating thermal gradients between the sensitive cooler stages and external heatsink temperatures it is critical to know how much heat is rejected and at what location.

### **6.5.1.3 Implications of Heatsink Temperature on Coldend Temperature Fluctuations**

Because of the fundamental Carnot equation that governs the efficiency of cryocoolers, changing the heat sink temperature directly impacts the cooler thermal efficiency. The net result is that changes in cryocooler heatsink temperature due to any cause are likely to directly reflect into changes of the cooler's coldend temperature...and thus to fluctuations in the cryogenic load temperature. Common causes of heatsink temperature variability include compressor cooling-loop control cycling, room temperature variations, orbital heating variations in space, and changes in the power dissipated by the cryocooler. For a typical Stirling-cycle cryocooler, each 5 K change in the cryocooler heatsink temperature will result in the cold load changing approximately 1 K in temperature [Ross and Johnson, 1998].

The bottom line is that tightly controlling heatsink temperature has a large benefit in helping to minimize cryocooler coldtip temperature fluctuations and easing the problem of achieving precise control of the cold load temperature via closed-loop cryocooler stroke control or an independent heater on the cold load.

### **6.5.1.4 Implications of Cryocooler Temperature Control on Thermal Runaway**

The strong dependency of cooler performance on heatsink temperature also raises the possibility of thermal runaway under unfavorable heatsinking conditions. Common heat rejection temperature control modes include constant reject temperature (generally maintained via closed-loop temperature control), heat rejection temperature rising linearly with power dissipation (typical of conduction/convection to a constant temperature heatsink), and heat rejection temperature dependent on the fourth root of power dissipation (typical for radiation to deep space). Any mode other than constant heatsink temperature can significantly alter the performance attributes of the cooler and can raise the possibility of thermal runaway, whereby increased input power required at elevated heatsink temperatures further increases the heatsink temperature in an unstable spiral until maximum cryocooler stroke is exceeded. A good overview and analysis of the thermal stability of various heat rejection modes is described by Ross and Johnson [Ross and Johnson, 1998]. As described, operational stability limits are most in danger of being exceeded at high operating powers and the lowest operating temperatures for a given cooler.

In summary, to understand the system-level thermal implications of the cryocooler's operation it is necessary to analyze not just the cryocooler by itself, but the complete cryocooler system

including its heat rejection system. In general, the safest cooling system is one that guarantees a roughly constant heat rejection temperature independent of compressor power dissipation.

### 6.5.1.5 Cold Finger Off-State Conduction

Parasitic conduction down the coldfinger of Stirling, pulse tube and GM refrigerators can become an important design consideration in systems that incorporate non-operating standby coolers of these types for added redundancy. This is because the parasitic heat load placed on operating coolers by a non-operating cooler can be a substantial fraction (30 to 50%) of the available cooling power of such coolers. Data on representative off-state conduction and means of measuring it are provided using both the transient warm-up rate method [Orlowska and Davey, 1987; Kotsubo et al, 1991] and by measuring the actual conductance in a cryogenic conductance measurement facility [Kotsubo et al, 1991]. In general, the second technique is the more accurate, as it assures true equilibrium thermal gradients within the off-cooler coldfinger and regenerator.

### 6.5.1.6 Pulse Tube Sensitivity to Gravity Orientation

For pulse tube cryocoolers, the off-state conduction can additionally have a strong dependence on gravity orientation. This is caused by convection heat transfer occurring in the pulse tube when the cold end of the pulse tube becomes level with or higher than its hot end. Figure 32 provides example data for the AIRS pulse tube measured at JPL [Ross, 2003b]. Note that the off-state conduction is a near-constant 0.5 watts when the hot end of the pulse tube is pointed up, but abruptly increases to very high levels as a horizontal attitude is reached. When the hot end is pointed down, convection-caused loads increase to over 3 watts.

Pulse tube convection also affects the cooling performance of operational pulse tube refrigerators by adding a gravity-dependent convection load onto the operating cooler. This convection loading tends to be quite dependent on the diameter/length aspect ratio of the pulse tube itself and varies with angle similar to that shown in Figure 32. For very long and slim pulse tubes the gravity affect is minimal, whereas short, squat pulse tubes can have an appreciable gravity sensitivity. Even for sensitive pulse tubes, their performance is minimally affected as long as the warm end of the pulse tube is 10 degrees or more above horizontal. Typical gravity-sensitivity data for operational pulse tubes is provided by [Ross, Johnson and Rodriguez, 2004].

## 6.5.2 Cryocooler Structural Mounting Considerations

From an engineering perspective, most cryocoolers are sensitive mechanical mechanisms that invariably demand a very well engineered thermal-mechanical attachment if optimum system per-

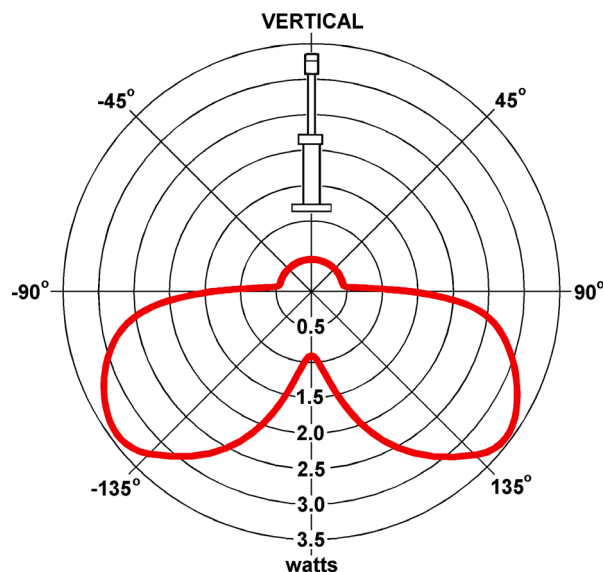


**Figure 32.** Thermal conductance of the AIRS pulse tube as a function of angle with respect to gravity.

formance and long life are to be achieved. For cases where the cold head is separate from the compressor, there will be a separate set of thermal-mechanical interfaces for the expander.

Key considerations that influence the cryocooler mechanical interface design include the following somewhat diverse items:

### 6.5.2.1 Surviving Transportation and Launch Acceleration Levels

Typical qualification-level random vibration environments for cryocoolers are around  $0.1 \text{ g}^2/\text{Hz}$  from 100 to 500 Hz, although for some applications the level can be as high as  $0.3 \text{ g}^2/\text{Hz}$ . In general, cryocooler compressors and displacer "bodies" have little difficulty meeting such vibration environments.

However, a classic problem with cryocoolers is the fragility of the coldfinger to vibration loads. This is because the structural robustness of the coldfinger is in direct competition with minimizing thermal parasitic loading from conduction down the coldfinger. The result is a highly optimized coldfinger structural design that may require some sort of auxiliary vibration restraint or added damping to survive high vibration levels. The resulting force levels are magnified by the attachment of a typical coldload interface mass, which is often in the range of 50 to 100 g.

There are two common means of limiting vibration loads on the coldfinger: coldfinger bumper assemblies and add-on damper assemblies.

**Coldfinger Bumper Assemblies.** A coldfinger bumper assembly, such as that shown in Fig. 33a, is a separate structural support designed to limit the maximum dynamic deflection of the coldfinger during high vibration levels. To avoid imparting a static deflection or parasitic thermal conduction path to the coldfinger, the redundant structure provides bumpers that are separated away from the coldfinger by a very small gap, typically a few thousandths of an inch. The gap is sized by the maximum deflection that can be withstood by the particular coldfinger without risking damage during exposure to high vibration levels. Because the bumper assembly has to be in close proximity to the coldfinger, it invariably must become an integral part of the coldlink and cryogenic thermal insulation implementation.

**Coldfinger Damper Assemblies.** As an alternative to the coldfinger bumper assembly, one can limit the dynamic response of the coldfinger to high vibration inputs by adding damping to its motion. One significant source of damping is just the flexbraid or S-link assembly itself. These assemblies provide a modest degree of damping ( $Q \approx 20$ ) due to the internal rubbing that occurs between the assembly's many wires and foils. Often this is enough to allow the coldfinger to survive the required vibration levels. However, development testing should be conducted with the selected flex-element to confirm the design's robustness prior to committing to the final hardware implementation. A second means of adding damping is to attach a separate particle damper such as that shown in Fig. 33b to the coldfingers cold stage [Fowler, et al., 2001]. Such dampers have the advantage of being tolerant to cryogenic temperatures and imparting no significant thermal loads on the system—just a minimal increase in cold surface area.

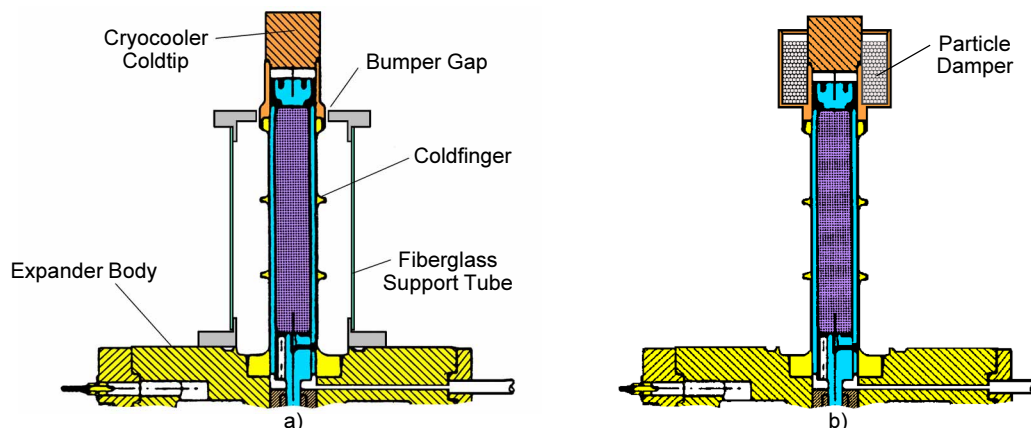


**Figure 33.** Example means of adding robustness to vibration loading: a) coldfinger bumper assembly, b) coldfinger damper assembly.

### 6.5.2.2 *Piston Sensitivity to Low Frequency Excitation*

Most application structures have their resonant frequencies above 100 Hz as part of achieving sufficient stiffness to satisfy typical handling and alignment demands. In sharp contrast, most Stirling and pulse tube cryocoolers have their fundamental drive frequency tuned in the range of 30 to 70 Hz, and commonly have highly resonant piston and balancer vibration modes as low as 20 to 30 Hz when not operating. A particularly sensitive vibration mode is the in-phase piston response of a dual-piston linear compressor when it is unpowered. In this mode the two pistons travel in the same direction at the same time and do no gas compression. This mode has a strong coupling to low frequency excitation and has a high amplification factor ( $Q \approx 30$ ). The key issue is whether the excited motions during low frequency excitation will cause the cooler piston, displacer, or balance motor assemblies to hit their end stops and possibly damage the internal parts or knock the cooler out of alignment.

During the cryosystem design process with such hardware it is important that these cryocooler low-frequency vibration modes be specifically addressed to insure that the cooler hardware will safely withstand the vibration and transportation environments of the intended application. For cryocoolers intended to be launched into space, it is common to introduce special launch-vibration latches for cryocooler internal drive assemblies. For assemblies with motor drives, a favored means of introducing launch restraint is to short the drive motor coils during launch. Alternatively, some space systems power the coolers during launch and use closed-loop piston servo control to maintain the pistons in a centered position.

In circumstances where motor shorting is not an option, such as with Stirling coolers with unpowered mechanical displacers or balancers, the cooler system design needs to be thoroughly qualified for the low-frequency vibration environment anticipated. Chapter 11, Section 5 of the *Spacecraft Thermal Control Handbook, Vol. II: Cryogenics* presents a detailed discussion of Stirling cryocooler low-frequency vibration modes and means of predicting the expected damping level, with or without motor shorting [Ross, 2003d].

### 6.5.2.3 *Minimizing Cryocooler Warping Loads*

One of the greatest challenges facing the designers of cryocoolers is achieving long life. A key issue is the possibility of internal gaseous contamination from lubricants and wear products associated with bearings or rubbing surfaces. To address the related issues, there has been an unwritten rule that a multi-year-life cryocooler must avoid rubbing surfaces, and maintain a tolerance to small particulate contamination as well. The flexure bearings and piston clearance seals incorporated into the Oxford-style Stirling cryocooler design concept are examples of the application of this rule. To maintain their tight non-contacting piston seals, linear compressors of this type face the challenge of maintaining tight manufacturing and assembly tolerances and a high degree of cooler dimensional stability in all operational environments.

Another important lesson learned in early cooler applications is how difficult it can be to structurally attach to a cryocooler's housing and heat-transfer interface without warping the cooler sufficiently to violate its tight internal running clearances. The act of just bolting a cooler into its support structure can be sufficient to cause rubbing of pistons and displacers in an early Oxford-style Stirling cooler. The culprit is redundant load paths or non-flat mounting surfaces that apply static warping loads into the cooler body. The radial running clearances of the compressor piston and moving displacer of the typical space cryocooler are around 0.0003". Thus, only a very small permanent deflection of the compressor or displacer structure may be required to cause rubbing and accelerated wear of the compressor piston and/or displacer. With such coolers, one needs to be particularly sensitive about these issues and check at the time of system integration that running clearances have not been violated by warpage associated with the cooler's structural/thermal attachment, or by excessive coldfinger side loads.

### 6.5.2.4 *Managing Cryocooler-Generated Vibration*

As shown in Fig. 34, cryocoolers that incorporate low frequency compressors, such as Stirling, pulse tube and GM coolers, can generate significant vibratory forces at their drive frequency and at

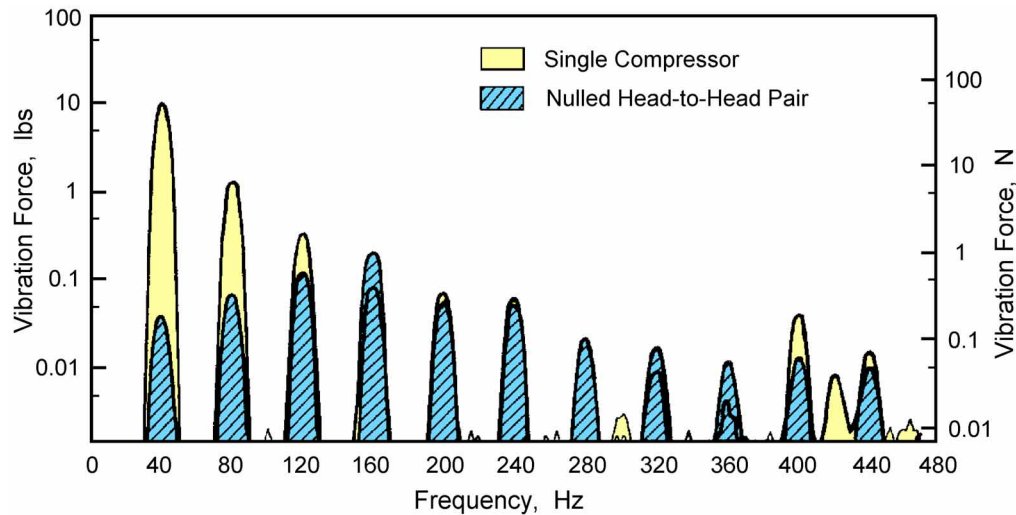


**Figure 34.** Example on-axis vibration force generated by an Oxford-style linear compressor operating at 40 Hz with and without using a second piston for head-to-head cancellation.

every multiple of that frequency. The key sensitivity is the extent to which the cooler vibration excites mechanical system resonances that degrade application performance with respect to parameters like optical resolution, pointing accuracy, or electronic noise. The lowest vibration levels are achieved with cryocoolers, such as turbo-Brayton or sorption JT, which do not incorporate low-frequency compressors.

In characterizing cooler-generated vibration, a useful parameter is the peak vibratory force imparted by the cooler into its supports when rigidly mounted. This force is the reaction force to moving masses within the cooler that undergo peak accelerations during various phases of the cooler's operational cycle. The accelerations can be from controlled motion such as the reciprocating motion of the compressor pistons, or natural vibratory resonances of the cooler's elastic structural elements. The example vibration spectra shown in Figure 34 is for a representative Oxford-style linear compressor — both from a single compressor and from a balanced pair of compressors. Notice that the force levels from a balanced pair are relatively constant over the first several harmonics. Similar force levels are found for a single compressor that is balanced using an active or passive counter-balancer.

Although the level of vibratory force that is acceptable is a strong function of the specific application, a value on the order of 0.2 N (0.05 lbs) is fairly representative of that to be expected from typical coolers with two-piston, head-to-head designs. Although the levels shown in Fig. 34 are for the piston-stroke axis, the measured levels in cross-axes can be very similar in magnitude due to internal resonances within the cooler. An extensive summary of cryocooler vibration characteristics and control methods is presented by [Mon, et al., 1995; and Ross, 2003c].

To achieve further reductions in the on-axis vibration levels, higher-end Stirling and pulse tube cryocoolers, such as those used for space applications, generally incorporate some level of active vibration suppression based on piston stroke control and closed-loop monitoring on the generated vibration. Such systems use active feedback to selectively null each of the first several harmonics in the drive axis by tailoring the electrical input to the individual linear drive motors.

A final category of cooler generated vibration is oscillatory motion of the coldblock itself caused by a combination of pressure-driven elongation of the coldfinger at the drive frequency combined with some lateral vibration in response to higher frequency cooler harmonics. These levels can be similar to the levels generated by a well balanced compressor [Collins, et al., 1995].

**Providing for Vibration Measurement.** Many space Stirling and pulse tube cryocoolers utilize a closed-loop vibration suppression system to balance the vibratory forces generated by the opposing pistons. Because such a system requires a feedback signal proportional to the unbalanced vibration, either an accelerometer mounted on or near the cryocooler body, or a load cell mounted between the cryocooler and its support structure is required. Both types of feedback transducers have been used successfully. However, an accelerometer typically places fewer requirements on

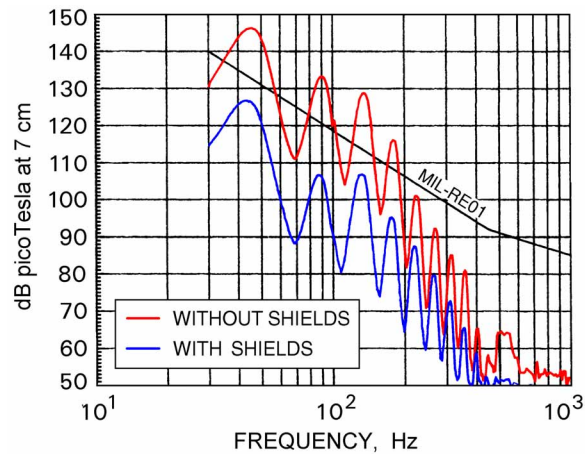


**Figure 35.** AC magnetic field emissions measured for the AIRS mechanical cooler with and without the addition of the flight mu-metal shields (versus MIL-STD 461C RE01 requirements).

the cryocooler thermal/mechanical integration, and has been found to provide adequate sensitivity to allow effective nulling over the full range of cooler drive harmonics.

If a load-cell type vibration transducer is used, it must be integrated into the cooler's structural load path so that it shares a portion of the coolers generated vibration forces. At the same time it must be robust enough to survive launch loading levels, and must not lead to a significant thermal impedance in the cryocooler's heat-rejection path.

#### 6.5.2.5 Shielding Cryocooler Compressor Magnetic Fields

In another area of integration sensitivity, Stirling and pulse tube cryocoolers invariably result in the compressors being mounted in close proximity to the cold load. This raises the possibility of negative interactions with the compressor's electromagnetic fields, which are maximum at the cooler's 30-70 Hz drive frequency. Substantial data have been gathered over the years on the EMI signatures of space-rated Stirling and pulse tube cryocoolers with respect to their ability to meet the AC magnetic field emissions requirements of the MILSTD-461C RE01 test specification (see for example [Johnson, et al., 1995 and Johnson, et al., 1999]).

Although the cooler magnetic fields have been found to cause no negative interactions with most applications, means have also been developed to greatly suppress the fields using mu-metal shielding attached to the cooler body. Figure 35 highlights the magnetic field reductions achieved by Johnson, et al. using add-on mu-metal shields on the AIRS cryocoolers [Johnson, et al., 1999]. A finding from these efforts is that the shields work well if they fully surround the compressor motors, but they need to be separated just enough so that they don't saturate and lose effectiveness. Their close proximity generally causes them to interface directly with the cryocooler support structure and thus become an integral part of the overall cooler structural integration task.

The key point is for the system integrator to be aware of the sensitivities in this area and to do diligence in terms of exploring compatibilities and corrective actions prior to finalizing the application's structural/thermal design.

#### 6.5.2.6 Providing for an External Vacuum Environment

Although the cryogenic application itself invariably requires a vacuum environment to be fully operational, an issue that often arises during system integration and testing is the desire to run key portions of the integrated cryocooler plus payload outside of its formal application vacuum chamber where access for measurements and troubleshooting is greatly improved. Providing for this external operational capability is often a useful part of the overall system design effort and may involve such things as the design of temporary vacuum bonnets or purge gas enclosures that allow the cooler to be turned on and run during various short-term tests.

Although a separate temporary vacuum enclosure is generally preferred if the payload design allows it, the purge solution is a viable alternative. However, a purge solution generally does not

allow normal operation due to the heavy convection loading caused by the purge gas—typically a zero-moisture purge source such as LN<sub>2</sub> boil off.

### 6.5.3 *Managing Cryocooler Electrical Functions and Interfaces*

In addition to providing power to drive the cryocooler, cryocooler electronics are often tasked to provide a number of related functional capabilities such as closed-loop temperature control of the cryogenic stage, closed-loop vibration control, and acquisition and conversion of cooler performance data into digital form with engineering units. Incorporating these diverse functions into the electronics can result in embedded processors, digital logic, sensitive analog circuits, and digital communication interfaces in addition to the needed power-drive circuitry. See, for example, [Harvey, et al., 2004].

In addition, the cooler drive motors and electronics themselves generally generate electromagnetic signatures or electromagnetic interference (EMI) that can adversely interact with the cryogenic application's performance. Understanding and accommodating these diverse functions and their interfaces is important to successfully integrating an active cryocooler into a cryogenic system design.

#### 6.5.3.1 *Power Subsystem Considerations*

The fundamental task of the cooler electronics power subsystem is to provide and control the power required by the cooler's drive motors. This includes accepting power from the facility power source and converting it into the form (voltage, current, frequency, phasing, etc) needed to drive the cooler's motors and control their operation. The power source may be a DC source, such as a 28-volt spacecraft, or an AC source (single or 3-phase) such as a commercial laboratory or production facility. Adapting the source power to the cooler's needs often involves such things as pulse width modulated (PWM) power amplifier stages, DC/DC converter circuitry, and inverters to generate AC drive waveforms at the cryocooler's drive frequency.

Additional features of the power drive circuitry can include such things as providing full voltage isolation from the power source to eliminate ground loops and noise, and providing high levels of suppression of conducted and radiated EMI from the power amplifier stages. The level of incorporation of EMI suppression and bus isolation are topics that need to be carefully examined and thoughtfully specified by the cooler integrator.

**Power System EMI Considerations.** Of the many issues involved in the design of cryocooler electronics, the power subsystem interface is one area in particular that has been a challenging area for many Stirling-cooler systems. The issue here is meeting power system requirements on allowable conducted emissions, particularly low frequency ripple currents and maximum allowable in-rush currents at turn-on [Johnson, et al., 1995]. Low-frequency linear drive compressors, such as those used with Stirling and pulse tube cryocoolers, introduce large pulsating currents onto the power bus at twice the cooler operating frequency. Unfortunately, filtering these currents can require massive filters, and not filtering them can result in unacceptable impacts on power system regulation. This has resulted in Stirling coolers connected to DC power systems having to add expensive auxiliary ripple-current filters [Johnson, et al., 1999].

A number of the latest high-end Stirling and pulse tube cryocooler electronics have introduced active ripple-current filtering as a cooler-electronics function [Harvey, et al., 2004]. This solves the problem with minimal mass and efficiency impact. However, excessive ripple currents remain an issue for many Stirling and pulse tube cooler electronics and must be carefully addressed by the cooler integrator.

Other power-system EMI issues that have been somewhat difficult to meet, but are more traditional in scope, include application requirements on high frequency conducted and radiated emissions from electronics enclosures and cabling. These can have negative interactions with such things as wireless communication applications. The key point is to be aware of the sensitivities in this area and to do diligence in terms of exploring compatibilities and corrective actions prior to finalizing the application's system design. Example high-frequency EMI measurements are available in the cooler literature, e.g. [Johnson, et al., 1995 and Johnson, et al., 1999].

**Incorporation of Caging Relays.** Sometimes embedded within the power drive electronics are caging relays meant to short the drive coils of linear motors to prevent excessive motion or possible damage during such things as peak spacecraft launch loads [Harvey, et al., 2004]. Embedding shorting relays within the drive electronics can simplify the overall cryocooler system design by adding this functionality within the existing electronic packaging, cable routing, and communication interfaces, thus eliminating the need for development of separate hardware to carry out this function.

### **6.5.3.2 Digital Control and Communication Considerations**

In addition to powering the cryocooler's drive motors, the cooler electronics are commonly tasked with a number of operational control functions that are generally managed by an integrated digital controller or microprocessor. Such functions include controlling compressor drive power or piston-stroke level, providing closed-loop temperature control, providing closed-loop vibration control, and providing measurement of cooler control parameters such as coldtip temperature, compressor piston stroke level, and measured vibration level [Harvey, et al., 2004]. Additional functions include monitoring cooler health and safety parameters such as cooler maximum temperatures, excessive current levels, and excessive piston stroke levels.

**Communication Interfaces.** The electrical interface to the electronics from the host application generally consists of a serial command and telemetry link. Commands are used to set operating modes and such things as compressor stroke or speed, desired coldtip temperature, etc. Commands also request telemetry data, and, if required, diagnostic fault conditions or alarms set by the drive electronics. Communication interfaces and protocol are a topic that need to be carefully examined and thoughtfully specified by the cooler integrator.

### **6.5.3.3 Electronics Environmental and EEE Parts Considerations**

For Stirling and pulse tube coolers, military and space applications have dominated much of the market focus and have led to an emphasis on high reliability electronics, with broad operational temperature ranges, broad input voltage ranges, and use of high reliability electronics parts with conservative parts stress derating criteria. Many have also been designed and qualified for relatively severe particle radiation and launch vibration environments. However, the reliability and cost of cryocooler electronics is invariably an issue, and the drive electronics often cost two-thirds of the total cryocooler cost.

The key point is to be aware of the cost and reliability sensitivities in this area and to do diligence in terms of exploring electronics options and maturity prior to finalizing the cryocooler selection and the application's system design. Even with proven electronics designs, electronic parts selection and acquisition seems to always be an issue because of parts obsolescence issues and application-specific requirements.

## **6.5.4 Measuring Cryocooler Refrigeration Performance**

The ability to cool a refrigeration load to a particular temperature is the most fundamental performance attribute of a cryocooler. Depending on the type of cryocooler, its performance generally depends on a wide variety of performance variables such as cold-load temperature, expander heatsink temperature, compressor heatsink temperature, compressor input power, compressor stroke, compressor drive frequency or speed (rpm), expander stroke and phase, and working-fluid fill pressure. As a result, understanding and predicting cryocooler performance in a given application can require an extensive set of performance data, together with a knowledge of how to interpolate and extrapolate the data trends for the type of cooler being examined.

Over the years, Oxford-type Stirling and pulse tube coolers have received great attention, and means of generating and displaying thermal performance data for this class of coolers have been highly refined. For example, an entire chapter is devoted to this topic in the *Spacecraft Thermal Control Handbook, Vol. II: Cryogenics* [Ross, 2003d].

However, many times, the performance of a specific cooler model is only specified in the product literature for a single operating point (e.g., 1 W at 80 K with a 20°C heatsink temperature) even though the same cooler will perform usefully over a broad range of refrigeration temperatures, cooling loads, and operating conditions. The goal of refrigeration performance characterization is to map out this complete operating space of a cryocooler.

#### **6.5.4.1 Measurement Procedures and Equipment**

Accurately measuring the performance of a cryocooler requires careful control of the key performance-determining parameters, particularly the heatsink temperature. For space applications, where cooling by convective heat transfer is generally not feasible, duplicating the expected conductive heat transfer paths and their associated thermal gradients is critically important. During measurements, it is necessary to insure that equilibrium conditions have been reached for a given cooling load prior to acquiring the cooler electrical input power data and the achieved coldend temperature. Also, it is necessary to protect the coldend from parasitic radiation or conduction loads. This is achieved by shielding the cold end with multilayer insulation (MLI) and by using low conductivity wiring for the coldend thermometry and heater leads.

To prevent significant gaseous conduction loads, tests need to be conducted in a vacuum that is kept well below  $10^{-4}$  torr. Fig. 28, presented earlier in Section 6.4.3, presents a handy means of roughly estimating gaseous conduction loads as a function of vacuum level and hardware surface area. However, much lower vacuum levels are required to prevent long-term buildup of contaminants that degrade the emittance of low-e surfaces and MLI. Minimizing parasitic load buildup during multi-month life tests can easily demand vacuum levels of  $10^{-8}$  torr. Detailed calculational procedures for estimating contaminant buildup versus residual gas pressure levels and the corresponding emittance changes that will occur are presented by [Ross, 2003a].

An effective means of achieving the low-contaminant environments needed for long-term tests is to envelope the cryogenic hardware under test with a separate cryogenically-cooled shield that is maintained well below the dew point of gases that could condense on the test hardware's surfaces. A common means of doing this is to use a separate GM cryocooler that is running at temperatures near 10 K to cool the shields. This prevents degrading contaminants from building up on the cryogenic surfaces of the test hardware.

#### **6.5.4.2 Data Presentation Formats and Examples**

A common means of displaying the refrigeration performance of regenerative cryocoolers such as Stirling, pulse tube and GM coolers, is a load-line plot. Such plots display the cryogenic load-carrying capability of a cryocooler as a function of its refrigeration temperature. The plot may include a second parameter such as stroke, input power, or heatsink temperature. Since the heatsink temperature has a strong effect, it is important to indicate on the plot the value of the heatsink temperature used for the measurements. Figure 36 shows an example load-line plot for a Stirling cooler with a heatsink temperature of 20°C and with the compressor piston stroke amplitude as a parameter.

As noted in Fig. 36, cooling load versus temperature lines are generally quite linear, and this allows easy interpolation and extrapolation to additional conditions of interest from only a few measurements. A key attribute of each of the load lines is their slope and the temperature corresponding to zero refrigeration load (the 'no-load' temperature). However, a weakness of this type of plot is that it doesn't provide information to conveniently understand the dependence of the measured cooling performance on input power or information on thermodynamic efficiency.

#### **6.5.4.3 Multiparameter Plots**

To expand the ability to view a cryocooler's efficiency performance dependencies simultaneously with its cooling capacity, refrigeration performance can be presented as input power versus cooling power as shown in Fig. 37. Radial lines from the origin are then lines of constant specific power, i.e. watts of cooling power generated per watt of input power — a measure of efficiency. Refrigeration temperature is then displayed as a family of isotherms to allow easy determination of

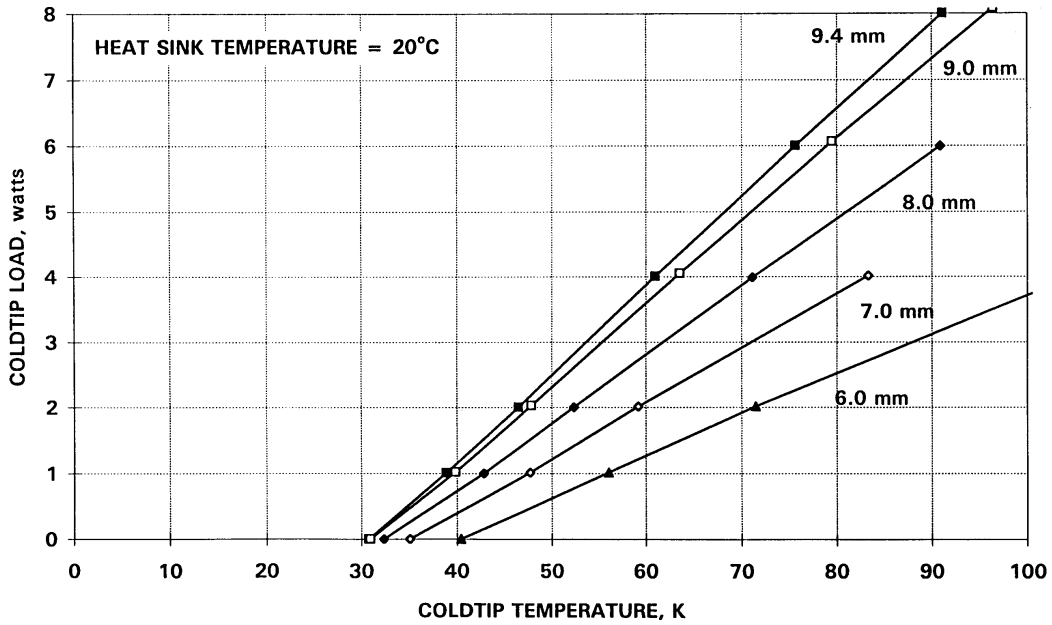


**Figure 36.** Example Stirling cooler load-line plot with piston stroke as a parameter.

information over a broad range of temperatures. Since the input voltage and compressor stroke generally have a smooth dependency on the input power, these curves are often added as was done in Fig. 37.

As shown, the multiparameter-plot format can easily display five parameters simultaneously on a single two-dimensional plot; this greatly aids in understanding the strong interrelationships among many cryocooler performance variables. Such plots also allow documenting cryocooler performance dependence on other key operational variables, such as drive frequency, heatsink temperature, and fill pressure [Johnson, et al., 1997]. Even though it requires a bit more effort to generate such plots, building on the well-behaved load-line characteristics, only three to four measurement points are needed per stroke load-line. Means of efficiently generating such plots are presented in Appendix A of the *Spacecraft Thermal Control Handbook, Vol. II: Cryogenics* [Ross, 2003g].

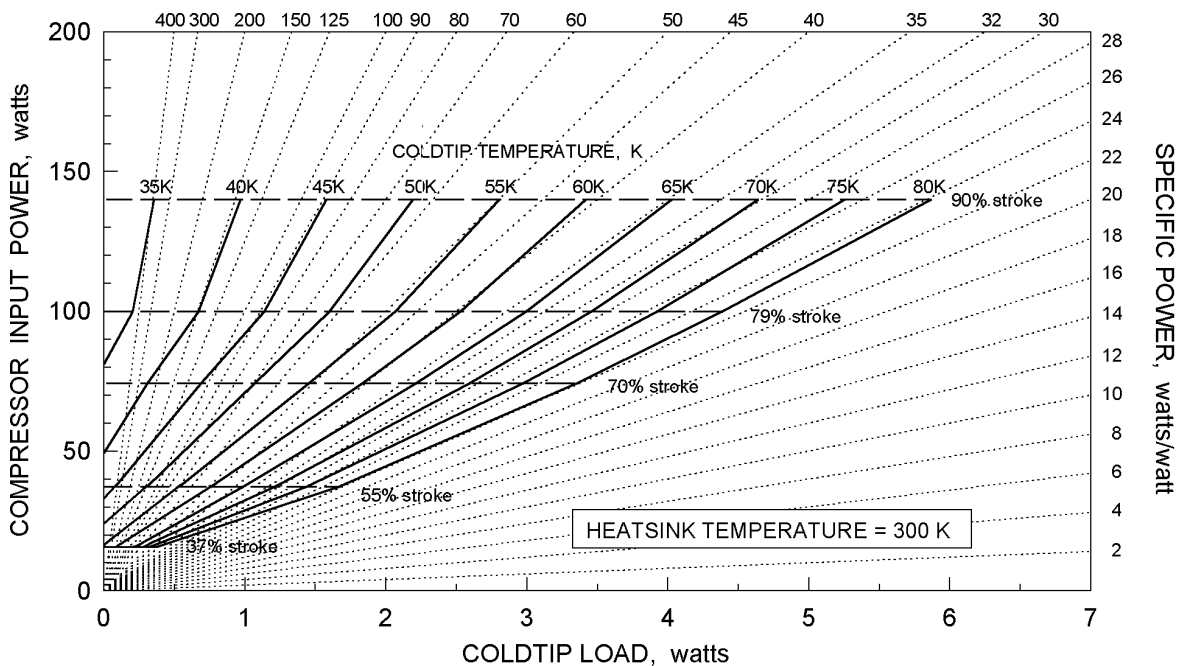


**Figure 37.** Multiparameter plot for the AIRS pulse tube cryocooler with piston stroke as a parameter.

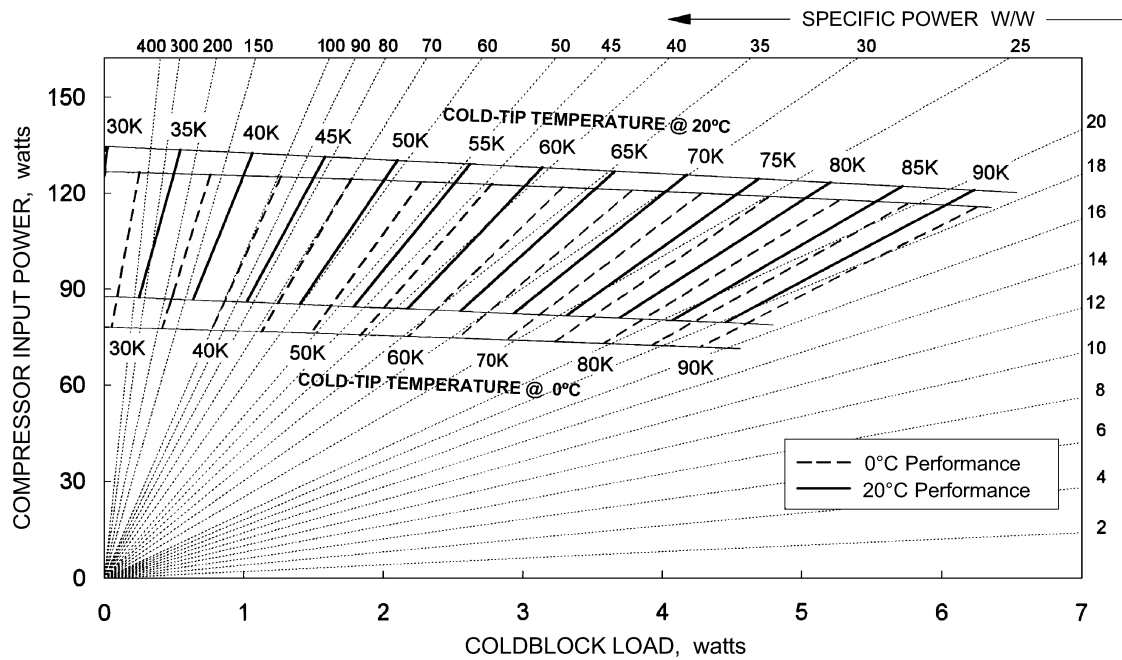


**Figure 38.** Multiparameter plot generated with data taken at two heatsink temperatures.

**Displaying the Effect of Heat Sink Temperature.** Drawing from the Carnot relationship presented earlier as Eq. (2) in Section 6.3.1.2, heatsink temperature has a large influence on cryocooler performance. Using the multiparameter plot, one can plot this dependence for a measured cryocooler and develop a useful algorithm for computing the refrigeration performance dependence on heatsink temperature.

Figure 38 displays the heat sink temperature dependency for a representative pulse tube cryocooler by displaying the shift in the cooler performance caused by lowering the heatsink temperature from 20°C to 0°C. Note that the new isotherms (lines of constant refrigeration temperature) for a 0°C heatsink temperature are positioned on top of similar 20°C-isotherms corresponding to refrigeration temperatures approximately 3 K warmer; i.e. the performance at 55 K with a 0°C heatsink temperature is the same as the performance at 58 K with a 20°C heatsink temperature. Note that this shift is also quite constant over the complete range of refrigeration temperatures plotted.

For this particular cooler the proportionality constant ( $\mathfrak{R}$ ) between heatsink temperature and coldend temperature is  $20^\circ\text{C} / 3 \text{ K} \approx 7$ . This fixed relationship between coldtip temperature and change in heatsink temperature has been found to be approximately true for a wide variety of cryocoolers, not just the pulse tube cooler shown here. However, the actual value of the proportionality ( $\mathfrak{R}$ ) is found to vary somewhat between cooler models from a low value of around  $2^\circ\text{C}/\text{K}$  to a high value of around  $10^\circ\text{C}/\text{K}$  [Ross and Johnson, 1998]. If measured values don't exist for a refrigerator of interest, a good mean value for estimating purposes is around  $5^\circ\text{C}/\text{K}$ .

Based on this empirically derived finding between coldtip temperature ( $\Theta$ ) and heatsink temperature ( $T$ ), one can derive the cooling power  $P(\Theta_A, T_A)$  at coldend temperature  $\Theta_A$  and heatsink temperature  $T_A$  as equal to the cooling power  $P(\Theta_B, T_0)$  at coldend temperature  $\Theta_B$  at the baseline heatsink temperature  $T_0$ , i.e.

$$P(\Theta_A, T_A) = P(\Theta_B, T_0); \quad \text{where } \Theta_B = \Theta_A - (T_A - T_0)/\mathfrak{R} \quad (8)$$

where  $\mathfrak{R}$  is the measured change in heatsink temperature required to shift the coldend performance by 1 K. Equation (8) allows a performance plot such as Fig. 37 to be used to determine refrigeration performance for a broad range of heatsink temperatures.

## 6.6 Summary

This chapter has provided an overview of the common means of achieving cryogenic temperatures, including both passive systems involving the use of liquid and frozen cryogenes, as well as

active cryocoolers. In addition, the critical aspects of cryogenic cooling system design and sizing—including load estimation and margin management—and cryocooler application and integration considerations have been reviewed. Because this field is very extensive, a single chapter precludes delving into specific details and must by necessity be limited to providing an introductory description of the available technologies and to summarizing the key decision factors and engineering considerations in the acquisition and use of cryogenic cooling systems.

For the process of pursuing this topic in more detail, the reader is directed to the many references in the References section of this chapter, but even more important, to the prominent journals and proceedings that they are published in. Within the cryogenics community there is a relatively finite number of prominent conferences and journals covering the field. Within the U.S. there are two primary conferences held every two years on staggered years: The Cryogenic Engineering Conference/International Cryogenic Materials Conference (CEC/ICMC), which publishes the *Advances in Cryogenic Engineering* proceedings, and the International Cryocooler Conference, which publishes the *Cryocoolers X* proceedings. Both of these conferences have been active for more than 30 years and contain a wealth of knowledge in their past proceedings. Complementing these conference proceedings is the monthly journal *Cryogenics*, which publishes a wealth of cryogenics related articles, including the proceedings of the Space Cryogenics Workshop, which is held every two years with a specific focus on cryogenics applications in space.

Also available, but somewhat less accessible, are the proceedings of the International Cryogenic Engineering Conference/International Cryogenic Materials Conference (ICEC/ICMC) that is held every two years, typically in Europe or Asia

In terms of texts, the *Spacecraft Thermal Control Handbook, Vol II: Cryogenics* provide an extensive review of cryogenics technologies associated with space missions [Donabedian, 2003a]. The key drawback here is the absence of data on ground-based technologies such as Gifford-McMahon cryocoolers.

## 6.7 Acknowledgment

Some of the research reported in this Chapter was conducted at the Jet Propulsion Laboratory (JPL), California Institute of Technology, under a contract with the National Aeronautics and Space Administration. The author would like to express his appreciation of the many scientists and engineers who contributed to the reported technologies and would like to express a special thanks to Dr. Dean Johnson, Jet Propulsion Laboratory, Saul Miller, The Aerospace Corp., Jeff Raab, Northrup Grumman AS, and Dr. Chao Wang, Cryomech, for reviewing this chapter and providing valuable technical comments and suggestions.

## 6.8 References

- Arentz, R.F., et al., "Design and Verification of Stirling Cooler Interfaces Suitable for Long-lifetime, Spaceborne Sensor Systems," *Cryocoolers 8*, Plenum Publishing Corp., New York (1995), pp. 855-867.
- Arkipov, V.T., et al., "Multicomponent Gas Mixtures for J-T Cryocoolers," *Cryocoolers 10*, R. Ross Jr., ed., Kluwer Academic/Plenum Publishers, New York (1999), pp. 487-495.
- Boiarski, M.J., Brodianski, V.M. and Longworth, R.C., "Retrospective of Mixed Refrigerant Technology and Modern Status of Cryocoolers Based on One-Stage, Oil-lubricated Compressors," *Advances in Cryogenic Engineering*, Vol. 43, Plenum Press, NY (1998), pp. 1701-1708.
- Bonney, G.E. and Longworth, R.C., "Considerations in Using Joule-Thomson Coolers," *Proceedings of the Sixth International Cryocoolers Conference*, Vol. 1, David Taylor Research Center, Bethesda, MD (1990), pp. 231-244.
- Bradley, P., Radebaugh, R., Huber, M., Lin, M. and Lee, Y., "Development of a Mixed-Refrigerant Joule-Thomson Microcryocooler," *Cryocoolers 15*, ICC Press, Boulder, CO (2009), pp. 425-432.
- Bradshaw, T.W., Delderfield, J., Werrett, S.T. and Davey, G., "Performance of the Oxford Miniature Stirling Cycle Refrigerator," *Advances in Cryogenic Engineering*, Vol. 31, Plenum Press, NY (1986), pp. 801-809.
- Bradshaw, T.W. and Orlowska, A.H., "A Closed-Cycle 4K Mechanical Cooler for Space Applications," *Proc. of 9th European Symposium on Space Environmental Control Systems*, Florence, Italy (1991).

- Bradshaw, T.W., Orłowska, A.H. and Jewell, C., Life Test and Performance Testing of a 4K Cooler for Space Applications, *Cryocoolers 10*, Kluwer Academic, New York (1999), pp. 521-528.
- Clappier, R.R. and Kline-Schoder, R.J., "Precision Temperature Control of Stirling-cycle Cryocoolers," *Advances in Cryogenic Engineering*, Vol. 39, Plenum Press, NY (1994), pp. 1177-1184.
- Collins, S.A., Johnson, D.L., Smedley, G.T. and Ross, R.G., Jr., "Performance Characterization of the TRW 35K Pulse Tube Cooler," *Advances in Cryogenic Engineering*, Vol. 41B, Plenum Publishing Corp., New York (1995), pp. 1471-1478.
- Crawford, L., "Radiant Coolers," *Spacecraft Thermal Control Handbook, Vol. II: Cryogenics*, M. Donabedian Editor, The Aerospace Press, El Segundo, CA (2003), pp. 55-90.
- Dobak, J., Yu, X. and Ghaerzadeh, K., "A Novel Closed-Loop Cryosurgical Device," *Advances in Cryogenic Engineering*, Vol. 43, Plenum Press, NY (1998), pp. 897-902.
- Dolan, E.X., Swift, W.L., Tomliison, B.J., Gilbert, A. and Bruning, J., "A Single Stage Reverse Brayton Cryocooler: Performance and Endurance Tests on the Engineering Model," *Cryocoolers 9*, R. Ross Jr., ed., Plenum Press, New York (1997), pp. 465-474.
- Donabedian, M., "Chapter 15: Cooling Systems," *The Infrared Handbook*, revised edition, IRIA Series in Infrared & Electro-Optics, George J. Zissis (Editor), William L Wolfe (Editor) (1993), pp. 15-1 to 15-85.
- Donabedian, M., *Spacecraft Thermal Control Handbook, Vol. II: Cryogenics*, The Aerospace Press, El Segundo, CA (2003a).
- Donabedian, M., "Chapter 2: Cryogenic Fluid Storage," *Spacecraft Thermal Control Handbook, Vol. II: Cryogenics*, The Aerospace Press, El Segundo, CA (2003b), pp. 13-29.
- Donabedian, M., "Chapter 6: Cryogenic Radiator Design and Comparative Performance," *Spacecraft Thermal Control Handbook, Vol. II: Cryogenics*, M. Donabedian Editor, The Aerospace Press, El Segundo, CA (2003c), pp. 91-117.
- Fowler, B.L., Flinta, E.M., Olson, S.E., "Design Methodology for Particle Damping," Proc. SPIE 4331, Smart Structures and Materials 2001: Damping and Isolation, 186, July (2001).
- Gifford, W.E. and Longworth, R.C., "Pulse Tube Refrigeration Progress," *Advances in Cryogenic Engineering*, Vol. 10B, Plenum Press, NY (1965), pp. 69-79.
- Harris, R., Chenoweth, J., and White, R., "Cryocooler Development for Space Flight Applications," SPIE Technical Symposium Paper 280-10, Washington, DC, April (1981).
- Harvey, D., et al., "Advanced Cryocooler Electronics for Space," *Cryogenics*, Vol. 44, Issues 6-8, June-August (2004), pp. 589-593.
- Johnson, D.L. and Ross, R.G., Jr., "Spacecraft Cryocooler Thermal Integration," *Proceedings of the Spacecraft Thermal Control Symposium*, Albuquerque, NM, November (1994).
- Johnson, D.L., Smedley, G.T., Mon, G.R., Ross, R.G., Jr. and Narvaez, P., "Cryocooler Electromagnetic Compatibility," *Cryocoolers 8*, Plenum Publishing Corp., New York (1995), pp. 209-220.
- Johnson, D.L., Collins, S.A., Heun, M.K. and Ross, R.G., Jr., "Performance Characterization of the TRW 3503 and 6020 Pulse Tube Coolers," *Cryocoolers 9*, Plenum Publishing Corp., New York (1997), pp. 183-193.
- Johnson, D.L., Collins, S.A. and Ross, R.G., Jr., "EMI Performance of the AIRS Cooler and Electronics," *Cryocoolers 10*, Plenum Publishing Corp., New York (1999), pp. 771-780.
- Johnson, W.R., *Final Report, Thermal Performance of Multilayer Insulations*, NASA CR-134477, LMSC-D349866, prepared for NASA LeRC by Lockheed Missiles and Space Co., 5 April (1974).
- Kawecki, T., "High Temperature Superconducting Space Experiment II (HTSSE II) Overview and Preliminary Cryocooler Integration Experience," *Cryocoolers 8*, Plenum Publishing Corp., New York (1995), pp. 893-900.
- Konkel, C. and Bradley, W., "Design and Qualification of Flight Electronics for the HST NICMOS Reverse Brayton Cryocooler," *Cryocoolers 10*, R.G. Ross Jr., ed., Kluwer Academic Plenum Publishers, New York (1999), pp. 439-448.
- Kotsubo, V., Johnson, D.L. and Ross, R.G., Jr., "Cold-tip Off-state Conduction Loss of Miniature Stirling Cycle Cryocoolers," *Advances in Cryogenic Engineering*, Vol. 37B, Plenum Press, NY (1991), pp. 1037-1043.
- Kotsubo, V.Y., Johnson, D.L., and Ross, R.G., Jr., "Calorimetric Thermal-Vacuum Performance Characterization of the BAe 80 K Space Cryocooler," SAE Paper No. 929037, *Proceedings of the 27th Intersociety Energy Conversion Engineering Conference*, P-259, Vol. 5, San Diego, California, August 3-7, (1992), pp. 5.101-5.107.

- Kutzner, K., Schmidt, F. and Wietzke, “Radiative and Conductive Heat Transmission through Superinsulations—Experimental Results for Aluminum Coated Plastic Films,” *Cryogenics*, July (1973), pp. 396-404.
- Lin, E.I., Stultz, J.W., and Reeve, R.T., “Test-derived Effective Emittance for Cassini MLI Blankets and Heat Loss Characteristics in the Vicinity of Seams,” AIAA paper 95-2015, 30th AIAA Thermophysics Conference, San Diego, CA, June 19-22, (1995).
- Longworth, R.C. and Steyert, W.A., “JT Refrigerators for Fast Cooldown to  $< 100$  K and  $< 80$  K,” *Proceedings of the Third Interagency Meeting on Cryocoolers*, David Taylor Research Center, Bethesda, MD (1988), pp. 133-148.
- Longworth, R.C., Boiarski, M.J., and Klusmier, L.A., “Closed Cycle Throttle Refrigerator,” *Cryocoolers 8*, Plenum, New York (1995), pp. 537-541.
- Longworth, R.C., “80K Throttle-Cycle Refrigerator Cost Reduction,” *Cryocoolers 9*, Plenum, New York (1997), pp. 521-528.
- Longworth, R.C., “Considerations in Applying Open Cycle JT Cryostats to Cryosurgery,” *Cryocoolers 11*, Kluwer Academic Plenum Press, NY (2001), pp. 783-792.
- Marquardt, E.D., Radebaugh, R. and Dobak, J., “A Cryogenic Catheter for Treating Heart Arrhythmia,” *Advances in Cryogenic Engineering*, Vol. 43, Plenum Press, NY (1998), pp. 903-910.
- Maytal, B-Z. and Pfothner, J.M., *Miniature Joule-Thomson Cryocooling: Principles and Practice*, Springer (2012).
- Miller, C.D., “Development of the Long-Lifetime Solid Nitrogen Dewar for NICMOS,” *Adv. in Cryogenic Engin.*, Vol. 43, Plenum Press, NY, (1998a), pp. 927-933.
- Miller, C.D., “Pre- and Post-Launch Performance of the NICMOS Dewar,” *Advances in Cryogenic Engineering*, Vol. 43, Plenum Press, NY, (1998b), pp. 935-940.
- Mon, G.R., Smedley, G.T., Johnson, D.L. and Ross, R.G., Jr., “Vibration Characteristics of Stirling-Cycle Cryocoolers for Space Application,” *Cryocoolers 8*, Plenum Publishing Corp., New York (1995), pp. 197-208.
- Nast, T.C. and Murray, D.O., “Orbital Cryogenic Cooling of Sensor Systems,” AIAA Paper 76-979, *Proceedings of the Systems Designs Driven by Sensors, AIAA Technical Specialists Conference*, Pasadena, CA, October 19-20 (1976).
- Nast, T.C., “A Review of Multilayer Insulation Theory, Calorimeter Measurements, and Applications,” *Recent Advances in Cryogenic Engineering - 1993*, ASME HTD-Vol. 267, J.P. Kelley and J. Goodman, eds., American Society of Mechanical Engineers, New York (1993), p. 29-43.
- Orlowska, A.H. and Davey, G., “Measurement of Losses in a Stirling-cycle Cooler,” *Cryogenics*, vol. 27 (1987), p. 645-651.
- Petach, M. and Michaelian, M., “Mid InfraRed Instrument (MIRI) Cooler Cold Head Assembly Acceptance Testing and Characterization,” *Cryocoolers 18*, ICC Press, Boulder, CO (2014), pp. 11-17.
- Raab, J. and Tward, M., “Northrop Grumman Aerospace Systems Cryocooler Overview,” *Cryogenics*, Vol. 50, Issue 9, September (2010), pp. 572-581.
- Radebaugh, R., Zimmerman, J. and Smith, D.R., “A Comparison of Three Types of Pulse Tube Refrigerators: New Methods for Reaching 60 K,” *Advances in Cryogenic Engineering*, Vol. 31, Plenum Press, NY (1986), pp. 779-789.
- Radebaugh, R. “Refrigeration for Superconductors,” *Proc. IEEE, Special Issue on Applications of Superconductivity*, vol. 92, October (2004), pp. 1719-1734.
- Ravex, A., Trollier, T., Sentis, L., Durand, F., Crespi, P., “Cryocoolers Development and Integration for Space Applications at Air Liquide,” *Proceedings of the Twentieth International Cryogenic Engineering Conference (ICEC 20)*, Elsevier (2005), pp. 427-436.
- Ross, R.G., Jr. and Green, K.E., “AIRS Cryocooler System Design and Development,” *Cryocoolers 9*, Plenum Publishing Corp., New York (1997), pp. 885-894.
- Ross, R.G., Jr. and Johnson, D.L., “Effect of Heat Rejection Conditions on Cryocooler Operational Stability,” *Advances in Cryogenic Engineering*, Vol. 43B (1998), pp. 1745-1752.
- Ross, R.G., Jr., “Cryocooler Load Increase due to External Contamination of Low- $\epsilon$  Cryogenic Surfaces,” *Cryocoolers 12*, Kluwer Academic/Plenum Publishers, New York (2003a), pp. 727-736.
- Ross, R.G., Jr., “AIRS Pulse Tube Cooler System Level Performance and In-Space Performance Comparison,” *Cryocoolers 12*, Kluwer Academic/Plenum Publishers, New York (2003b), pp. 747-754.

- Ross, R.G., Jr., "Vibration Suppression of Advanced Space Cryocoolers — An Overview," *Proceedings of the International Society of Optical Engineering (SPIE) Conference*, San Diego, CA, March 2-6, (2003c).
- Ross, R.G., Jr., "Chapter 11: Cryocooler Performance Characterization," *Spacecraft Thermal Control Handbook, Vol. II: Cryogenics*, The Aerospace Press, El Segundo, CA (2003d), pp. 217-261.
- Ross, R.G., Jr., "Chapter 12: Cryocooler Reliability and Redundancy Considerations," *Spacecraft Thermal Control Handbook, Vol. II: Cryogenics*, The Aerospace Press, El Segundo, CA (2003e), pp. 263-284.
- Ross, R.G., Jr., "Chapter 13: Cryocooler Integration Considerations," *Spacecraft Thermal Control Handbook, Vol. II: Cryogenics*, The Aerospace Press, El Segundo, CA (2003f), pp. 285-324.
- Ross, R.G., Jr., "Appendix A: Constructing a Cryocooler Multiparameter Plot," *Spacecraft Thermal Control Handbook, Vol. II: Cryogenics*, The Aerospace Press, El Segundo, CA, (2003g), pp. 605-608.
- Ross, R.G., Jr., Johnson, D.L. and Rodriguez, J.I., "Effect of Gravity Orientation on the Thermal Performance of Stirling-type Pulse Tube Cryocoolers," *Cryogenics*, Vol. 44, Issue: 6-8, June - August (2004), pp. 403-408.
- Ross, R.G., Jr., "Estimation of Thermal Conduction Loads for Structural Supports of Cryogenic Spacecraft Assemblies," *Cryogenics*, Vol. 44, Issue: 6-8, June - August, (2004), pp. 421-424.
- Ross, R.G., Jr., "Chapter 11: Aerospace Coolers: a 50-Year Quest for Long-life Cryogenic Cooling in Space," *Cryogenic Engineering: Fifty Years of Progress*, Ed. by K. Timmerhaus and R. Reed, Springer Publishers, New York (2007), pp. 225-284.
- Ross, R.G., Jr., Johnson, D.L., Elliott, D. "AIRS Pulse Tube Coolers Performance Update –Twelve Years in Space," *Cryocoolers 18*, ICC Press, Boulder, CO (2014), pp. 87-95.
- Saes, *St 171 and St 172 - Sintered Porous Getters*, SAES Getters Group (2007).
- Scott, Russell B., *Cryogenic Engineering*, Met-Chem Research, Inc., Boulder, CO (1988), pp. 146-147.
- Selzer, P.M., Fairbank, W.M. and Everitt, C.W.F., "A Superfluid Plug for Space," *Advances in Cryogenic Engineering*, Vol. 16, Plenum Press, NY (1971), pp. 277-281.
- Sixsmith, H., "Miniature Cryogenic Expansion Turbines—a Review," *Advances in Cryogenic Engineering*, Vol. 29, Plenum Press, NY (1984), pp. 511-523.
- Sherman, A., "History, Status and Future Applications of Spaceborne Cryogenic Systems," *Advances in Cryogenic Engineering*, Vol. 27, Plenum Press, NY (1982), pp. 1007-1029.
- Sugimura, R.S., Russo, S.C. and Gilman, D.C., "Lessons Learned During the Integration Phase of the NASA IN-STEP Cryo System Experiment," *Cryocoolers 8*, Plenum Publishing Corp., New York (1995), pp. 869-882.
- Swift, W. and Sixsmith, H. "Performance of a Long Life Reverse Brayton Cryocooler," *7th International Cryocooler Conference Proceedings*, Air Force Phillips Laboratory Report PL-CP--93-1001, Kirtland Air Force Base, NM, April (1993), pp. 84-97.
- Swift, W.L., Dolan, F.X. and Zagarola, M.V., "The NICMOS Cooling System—5 Years of Successful On-Orbit Operation," *Advances in Cryogenic Engineering*, Vol. 53, Amer. Institute of Physics, Melville, NY (2008), pp. 799-806.
- ter Brake, H.J.M., et al., "14.5 K Hydrogen Sorption Cooler: Design and Breadboard Tests," *Cryocoolers 16*, ICC Press, Boulder, CO (2011), pp. 445-454.
- Viehmann, W. and Eubanks, A.G., *Effects of Surface Contamination on the Infrared Emissivity and Visible-Light Scattering of Highly Reflective Surfaces at Cryogenic Temperatures*, NASA Technical Note TN D6585, NASA Goddard Space Flight Center, February (1972).
- Wade, L.A., et al., "Hydrogen Sorption Cryocoolers for the Planck Mission," *Advances in Cryogenic Engineering*, Vol. 45, Plenum Press, New York (2000), pp. 499-506.
- Wang, C. and Gifford, P.E., "Two-Stage Pulse Tube Cryocoolers for 4 K and 10 K Operation," *Cryocoolers 12*, Kluwer Academic/Plenum Press, NY (2003), pp. 293-300.
- Wang, C., "Characteristics of 4 K Pulse Tube Cryocoolers in Applications," *Proceedings of the Twentieth International Cryogenic Engineering Conference (ICEC 20)*, Beijing, China, Elsevier, Ltd. (2005), pp. 265-268.
- Werrett, S.T., Peskett, G.D., Davey, G., Bradshaw, T.W. and Delderfield, J., "Development of a Small Stirling Cycle Cooler for Space Applications," *Advances in Cryogenic Engineering*, Vol. 31 (1986), pp. 791-799.
- Williams, B., Jensen, S., and Batty, J.C., "An Advanced Solderless Flexible Thermal Link," *Cryocoolers 9*, Plenum Publishing Corp., New York (1997), pp. 807-812.

- Xu, M.Y., Yan, P.D., Koyama, T., Ogura, T., and Li, R., "Development of a 4K Two-Stage Pulse Tube Cryocooler," *Cryocoolers 12*, Kluwer Academic/Plenum Press, NY (2003), pp. 301-307.
- Zagarola, M., McCormick, J., Cragin, K., "Demonstration of an Ultra-Miniature Turboalternator for Space-Borne Turbo-Brayton Cryocooler," *Cryocoolers 17*, ICC Press, Boulder, CO (2012), pp. 453-460.